National Library of Canada

Acquisitions and Bibliographic Services Branch

395 Wellington Street
Ottawa, Ontario
K1A 0N4

Bibliothèque nationale du Canada

Direction des acquisitions et des services bibliographiques

395, rue Wellington
Ottawa (Ontario)
K1A 0N4

Your file Votre référence

Our file Notre référence

NOTICE

The quality of this microform is heavily dependent upon the quality of the original thesis submitted for microfilming. Every effort has been made to ensure the highest quality of reproduction possible.

If pages are missing, contact the university which granted the degree.

Some pages may have indistinct print especially if the original pages were typed with a poor typewriter ribbon or if the university sent us an inferior photocopy.

Reproduction in full or in part of this microform is governed by the Canadian Copyright Act, R.S.C. 1970, c. C-30, and subsequent amendments.

AVIS

La qualité de cette microforme dépend grandement de la qualité de la thèse soumise au microfilmage. Nous avons tout fait pour assurer une qualité supérieure de reproduction.

S'il manque des pages, veuillez communiquer avec l'université qui a conféré le grade.

La qualité d'impression de certaines pages peut laisser à désirer, surtout si les pages originales ont été dactylographiées à l'aide d'un ruban usé ou si l'université nous a fait parvenir une photocopie de qualité inférieure.

La reproduction, même partielle, de cette microforme est soumise à la Loi canadienne sur le droit d'auteur, SRC 1970, c. C-30, et ses amendements subséquents.

Canada

UNIVERSITY OF ALBERTA

CARBONATE SEDIMENTOLOGY AND CYCLOSTRATIGRAPHY OF THE UPPER PERMIAN GRAYBURG FORMATION AT NORTH McELROY FIELD (TEXAS)

By

Leonardo Piccoli ©

A thesis submitted to the Faculty of Graduate Studies and Research in partial fulfillment of the requirements for the degree of MASTER OF SCIENCE

DEPARTMENT OF GEOLOGY

EDMONTON, ALBERTA

FALL 1995

National Library of Canada
Acquisitions and Bibliographic Services Branch
395 Wellington Street
Ottawa, Ontario
K1A 0N4

Bibliothèque nationale du Canada
Direction des acquisitions et des services bibliographiques
395, rue Wellington
Ottawa (Ontario)
K1A 0N4

Your file *Votre référence*

Our file *Notre référence*

THE AUTHOR HAS GRANTED AN IRREVOCABLE NON-EXCLUSIVE LICENCE ALLOWING THE NATIONAL LIBRARY OF CANADA TO REPRODUCE, LOAN, DISTRIBUTE OR SELL COPIES OF HIS/HER THESIS BY ANY MEANS AND IN ANY FORM OR FORMAT, MAKING THIS THESIS AVAILABLE TO INTERESTED PERSONS.

L'AUTEUR A ACCORDE UNE LICENCE IRREVOCABLE ET NON EXCLUSIVE PERMETTANT A LA BIBLIOTHEQUE NATIONALE DU CANADA DE REPRODUIRE, PRETER, DISTRIBUER OU VENDRE DES COPIES DE SA THESE DE QUELQUE MANIERE ET SOUS QUELQUE FORME QUE CE SOIT POUR METTRE DES EXEMPLAIRES DE CETTE THESE A LA DISPOSITION DES PERSONNE INTERESSEES.

THE AUTHOR RETAINS OWNERSHIP OF THE COPYRIGHT IN HIS/HER THESIS. NEITHER THE THESIS NOR SUBSTANTIAL EXTRACTS FROM IT MAY BE PRINTED OR OTHERWISE REPRODUCED WITHOUT HIS/HER PERMISSION.

L'AUTEUR CONSERVE LA PROPRIETE DU DROIT D'AUTEUR QUI PROTEGE SA THESE. NI LA THESE NI DES EXTRAITS SUBSTANTIELS DE CELLE-CI NE DOIVENT ETRE IMPRIMES OU AUTREMENT REPRODUITS SANS SON AUTORISATION.

ISBN 0-612-06522-7

Canada

UNIVERSITY OF ALBERTA

RELEASE FORM

NAME OF AUTHOR: **LEONARDO PICCOLI**

TITLE OF THESIS: **CARBONATE SEDIMENTOLOGY AND CYCLOSTRATIGRAPHY OF THE UPPER PERMIAN GRAYBURG FORMATION AT NORTH McELROY FIELD (TEXAS)**

DEGREE: **MASTER OF SCIENCE**

YEAR THIS DEGREE GRANTED: **1995**

Permission is hereby granted to the University of Alberta Library to reproduce single copies of this thesis and to lend or sell such copies for private, scholarly, or scientific research purposes only.

The author reserves all other publication and other rights in association with the copyright in the thesis, and except as hereinbefore provided neither the thesis nor any substantial portion thereof may be printed or otherwise reproduced in any material form whatever without the author's prior written permission.

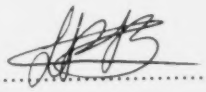

MARAVEN S.A.
Gerencia de Exploracion y Produccion
Apartado 829
Caracas, Venezuela

July 17, 1995

UNIVERSITY OF ALBERTA

FACULTY OF GRADUATE STUDIES AND RESEARCH

The undersigned certify that they have read, and recommended to the Faculty of Graduate Studies and Research for acceptance, a thesis entitled CARBONATE SEDIMENTOLOGY AND CYCLOSTRATIGRAPHY OF THE UPPER PERMIAN GRAYBURG FORMATION AT NORTH McELROY FIELD (TEXAS) submitted by LEONARDO PICCOLI in partial fulfillment of the requirements for the degree of MASTER OF SCIENCE.

.....

Dr. B. Jones (Supervisor)

.....

Dr. K. Muehlenbachs

.....

Dr. C.R. Stelck

.....

Dr. W.G. Evans

July 13, 1995

Dedicated to Selena for all her love, understanding and unique way to look at life and to Dr. Franklin Yoris who has been my role model in science

ABSTRACT

The Upper Permian Grayburg Formation in the North McElroy Field (West Texas) encompasses seventeen depositional facies that belong to six facies associations which formed on shelves that were up to 3 km wide. The slope facies association is composed of muddy sediments deposited at or below storm wave action. The shelf margin was the site of submerged bioherm, bioclastic bank, and fusulinid bank formation. The outer shelf was dominated by sediments rich in fusulinids, bioclasts, and peloids that were deposited at depths between fairweather and storm wave action. Ooid shoals formed in agitated shallow-waters along the shelf crest. The inner shelf was a protected, shallow subtidal to supratidal setting on the leeward side of the shelf crest. During sea-level lowstands the entire platform was exposed and deposition was restricted to a mixed carbonate-siliciclastic shoreface.

The Grayburg Formation is composed of a third-order depositional sequence (1.3 m.y.) bounded by two major unconformities. Internal unconformities and discontinuities define sixth-order (~18,000 years), fifth-order (~86,000 years), and fourth-order cycles (~516,000 years). Each sequence or cycle contains similar internal transgressive-regressive successions that are the record of retrogradational, aggradational, and progradational settings which formed in response to sea-level fluctuations. Sixth- and fifth-order cycles were probably controlled by precession and short-eccentricity Milankovitch orbital perturbations that were locally overprinted by non-periodic events. Lower-frequency cyclicity (fourth- to third-order) was controlled by a complex interplay of glacio-eustatic and tectono-eustatic (flexural subsidence and viscoelastic relaxation) driven mechanisms.

The North McElroy Field is one of the largest oil producers from the Grayburg Formation in the Central Basin Platform. The reservoir quality is related to the early dolomitization and fabric selective dissolution that enhanced the porosity and permeability. These diagenetic processes were probably related to exposure of the platfom that occurred during fourth-order relative sea-level falls.

ACKNOWLEDGMENTS

I am deeply grateful to Maraven S.A. (Filial de Petroleos de Venezuela) who made this Master's degree possible from the first to the last day, through generous financial and personal support. They always tried to help me and solve my different problems. Thank you again.

I particularly acknowledge Dr. Susan Longacre and Texaco for allowing me to gather information from the North McElroy Field which formed the data base for this project. Many thanks to Dr. Hans Machel who made initial arrangements with Texaco to get support and technical help during my stay in Houston. I am indebted to Dr. Frank Wind, William Lawrence, Greg Vardilos, Gary Hare, and Richard Arnold from Texaco for their friendship and technical support. I swear that I am not going to ask you to get a core box again or to fix the powerbook!!!.

I thank the mighty pseudo-doctors Richard " Ricardo" Evoy, Paul "Smelly" Blanchon, Harald "Gerhard" Huebscher, and Chun " Gung Kai" Li for their honest friendships and ability to bear all my "never ending" monologues of fusulinids, Permian carbonates, Milankovitch dreams, and so on. They were always available for any technical question, from thesis format to computer troubles. In particular many thanks to Paul because he guided me through the "Universe of Macintosh" to the very end (actually I am dictating and he is typing the acknowledgments, ja, ja!!).

To my dear friends Kim "Trini" Manzano, Mark "Freak" Hearn, William "Bodyguard" Kalbfleisch, Jason "G#@son" Monpetit, Dave "Duracell" Hills, Jen "Spinach-Popeye" Vezina, and Brent "Brent-himself" Wignall for the good time that we had. Special thanks to Evoy's and Moslow's families for the hospitality that they offered to Selena and I during our staying in Canada. I would like also to thank Dr. Karlis Muehlenbachs "the spiritual supervisor" from whom I learned a lot of stable isotopes in the different projects that I carried under his supervision, and for his advice and wisdom.

Finally, I wish to express my sincere thanks to Dr. Brian Jones who accepted me under his supervision in a very difficult situation. His main objective, to see me succesfully finished, was accomplished. I really appreciate all his technical advice and the time that he spent "reading and digesting the complicated way I express my ideas". He made a great difference to this work.

TABLE OF CONTENTS

Chapter	Page
1. INTRODUCTION	**1**
General Overview	1
Objectives	2
The Grayburg Formation	2
Study Area	2
Regional Setting	5
Methods	7
2. LITHOFACIES AND FACIES ASSOCIATIONS	**9**
Introduction	9
Depositional Facies in the Grayburg Formation	10
Facies 1: Peloid-fine skeletal debris mudstone	10
Facies 2: Bioturbated peloid-bioclastic wackestone	13
Facies 3: Structureless bioclastic-peloid packstone/grainstone	13
Facies 4: Calcareous sponge bafflestone/floatstone	15
Facies 5: Bedded "*Archaeolithoporella*" bindstone	17
Facies 6: "*Archaeolithoporella*"-sponge-bryozoa framestone	18
Facies 7: Peloid-fusulinid mudstone	19
Facies 8: Bioturbated fusulinid-peloid wackestone	19
Facies 9: Fusulinid packstone/grainstone	21
Facies 10: Peloid-pellet packstone/grainstone	22
Facies 11: Vertically burrowed peloid-bivalve-crinoid wackestone	23
Facies 12: Ooid-peloid grainstone	24
Facies 13: Pisoid-peloid-ooid-intraclast packstone/grainstone	26
Facies 14: Laminated peloidal mudstone/wackestone	27

Facies 15: Massive fine quartzarenite/sandy wackestone 27

Facies 16: Cross-bedded sandy fusulinid-peloid wackestone/packstone 29

Facies 17: Sandy burrowed bryozoa-brachiopod wackestone 30

Facies Associations and Depositional Settings 31

Slope Facies Associations 31

Lower Slope (Bioclastic Dominated) 31

Upper Slope (Bioclastic Dominated) 33

Upper Slope (Fusulinid Dominated) 33

Shelf Margin Facies Associations 33

Bioclastic Bank 34

Bioherm 34

Fusulinid Bank 37

Outer Shelf Facies Associations 38

Fusulinid-Dominated Outer Shelf 38

Peloid-Dominated Outer Shelf 38

Shelf Crest Facies Association 39

Inner Shelf Facies Assciation 39

Shoreface Facies Association 40

Regional Unconformities and Discontinuities 40

Unconformity A 40

Discontinuity B 42

Unconformity C 42

Unconformity D 42

Unconformity E 43

Platform Evolution 43

Stage 1: Narrow Shelf with Shelf-Edge Reef and Fusulinid Shoals 43

Stage 2: Aggradational Shelf with a Fusulinid-Bank Shelf Margin 47

Stage 3: Shelf with a Bioclastic-Bank Shelf Margin 47

Stage 4: Progradational Shelf with a Fusulinid-Bank Shelf Margin 47

Synopsis 48

3. SEQUENCE STRATIGRAPHY AND CYCLOSTRATIGRAPHY **50**

Introduction 50

Sequence Stratigraphy and description of Systems Tracts 51

Lowstand/Transgressive Systems Tract (LTST) 54

Highstand Systems Tract (HST) 55

Early Highstand Systems Tract (EHST) 55

Middle Highstand Systems Tract (MHST) 56

Late Highstand Systems Tract (LHST) 57

Cyclostratigraphy: Internal Architecture of Fifth- to Sixth-Order Cycles 58

Cycle 19 59

Cycle 20 63

Cycle 17 67

Control Factors on Carbonate Deposition and Cyclicity 70

Water Geochemistry 70

Antecedent Topography 71

Siliciclastic Influx 71

Autocyclicity 74

Tectonics 75

Glacio-Eustatic Sea-Level Oscillations 76

Reservoir Characterization 84

Synopsis 87

4. SUMMARY AND CONCLUSIONS **89**

5. REFERENCES **92**

LIST OF TABLES

Table		Page
2.1	Summary of depositional facies	11
2.2	Summary of facies associations	32

LIST OF FIGURES

Figure		Page
1.1	Regional paleogeographic setting of the Central Platform Basin	3
1.2	Map of North McElroy Field	4
1.3	Chronostratigraphic chart of the Guadalupian (Permian) units	6
2.1	Facies 1, 2, and 3	14
2.2	Facies 4, 5, 6, and 7	16
2.3	Facies 8, 9, and 10	20
2.4	Facies 12, 13, and 14	25
2.5	Facies 15, 16, and 17	28
2.6	Key to depositional facies. Examples of facies associations	35
2.7	Dip-oriented cross section AA' showing the lateral and vertical distribution of facies associations in the Grayburg Formation	41
2.8	Schematic paleoenvironmental reconstruction of facies distribution and geometry of a cemented shelf-margin	44
2.9	Schematic diagram showing relationships and relative position of facies associations along a shelf with a shelf margin dominated by fusulinid banks	45
2.10	Schematic diagram showing relationships and relative position of facies associations along a shelf with a shelf margin dominated by bioclastic banks	46
3.1	Dip-oriented cross section AA' in North McElroy Field outlining the sequence stratigraphic framework of the Grayburg Formation	52
3.2	Interpretation of the dip-oriented cross-section AA'	53
3.3	Internal architecture of fifth-order cycle 19	60
3.4	Schematic diagram showing depositional characteristics of cycle 19	61

3.5 Internal architecture of sixth-order cycle 19C 62

3.6 Internal architecture of fifth-order cycle 20 64

3.7 Schematic diagram showing depositional characteristics at the end of cycle 20 65

3.8 Internal architecture of sixth-order cycle 20E 66

3.9 Vertical stacking pattern of sixth-order cycles in cycle 17 68

3.10 Conceptual depositional model for cycle 17 69

3.11 Location of relict breaks in slope produced during relative sea-level falls that exposed the carbonate shelf 72

3.12 Diagrammatic distribution of siliciclastic sediments in the Grayburg Fm 73

3.13 Meter-scale description of cores NMU-4123 and NMU-3713 78

3.14 Reservoir distribution superimposed on the chronostratigraphic framework 85

1. INTRODUCTION

General Overview

Following the introduction of seismic stratigraphy and sequence stratigraphy in the late 1970's-early 1980's, an unprecedented amount of research in stratigraphy and sedimentology has focused on the analysis of transgressive-regressive sequences of different orders of magnitude and the possible mechanisms that induced the stacking patterns of these sedimentary sequences. Originally developed for siliciclastic-dominated sequences, sequence stratigraphy moved into the realm of carbonate sedimentology via the pioneer works of Sarg and Lehmann (1986) and Sarg (1988). From there on, carbonate sequence stratigraphy has evolved into a separate discipline and many studies have been dedicated to this topic (Crevello et al., 1989; Tucker et al., 1990; Schlager, 1992; Loucks and Sarg, 1993).

Most of this original work in carbonate sequence stratigraphy emphasized third-order sequence (0.5-3 million years) recognition, analysis of component systems tracts, and identification of bounding discontinuities (i.e. sequence boundaries and maximum flooding surfaces). More recently, the internal architecture of these third-order sequences that are formed of higher-frequency cycles or parasequences, has been the subject of intense research. This cyclostratigraphic or high-frequency stratigraphic approach (Goldhammer et al., 1993; Schwarzacher, 1993) is mainly concerned with determining the mechanisms responsible of the formation of meter-scale, shallowing-upward cycles in the order of 10,000 to 500,000 years. These mechanisms include allocyclic glacio-eustatic phenomena (Milankovitch orbital perturbations), allocyclic tectonics, and autocyclic progradation (Goldhammer et al., 1993). The successful application of cyclostratigraphy to a carbonate sedimentary sequence largely depends on a detailed analysis of the sedimentologic features of the rocks. These are the characteristics that will be used in the interpretation of the lateral and vertical variability of cycles in a given chronostratigraphic

framework. An understanding of the cyclostratigraphic analysis also helps in the understanding of the diagenetic and reservoir characteristics of the rock packages.

Objectives

With specific reference to the Grayburg Formation in the North McElroy Field (Fig. 1.1), the main objectives of this study are to:

1) provide a meter-scale process sedimentologic description of the component depositional facies,

2) describe and interpret the depositional environment for the various assemblages of facies (facies associations),

3) establish a sequence and cyclostratigraphic template that will provide a chronostratigraphic framework for the analysis of facies associations, cycle variability, and dynamic changes of the platform, and

4) evaluate the mechanisms that controlled facies distribution and cyclicity.

By integrating all the information obtained during the course of this study, valuable insights into the distribution of the reservoir rocks can be obtained. In particular, emphasis is placed on relating the reservoir rock to the chronostratigraphic framework of the Grayburg Formation.

The Grayburg Formation Stratigraphy

Study Area

The North McElroy Field, located in West Texas, is one of the largest fields in the Permian Basin that produces oil from the Grayburg Formation (Fig. 1.1). This field occupies the northern third of the McElroy field and is operated by Texaco. The North McElroy Field comprises approximately 17 square miles of the McElroy Field (Fig. 1.2). The database available is 113 wells with wirelogs and 30 cores that penetrated the Grayburg Formation.

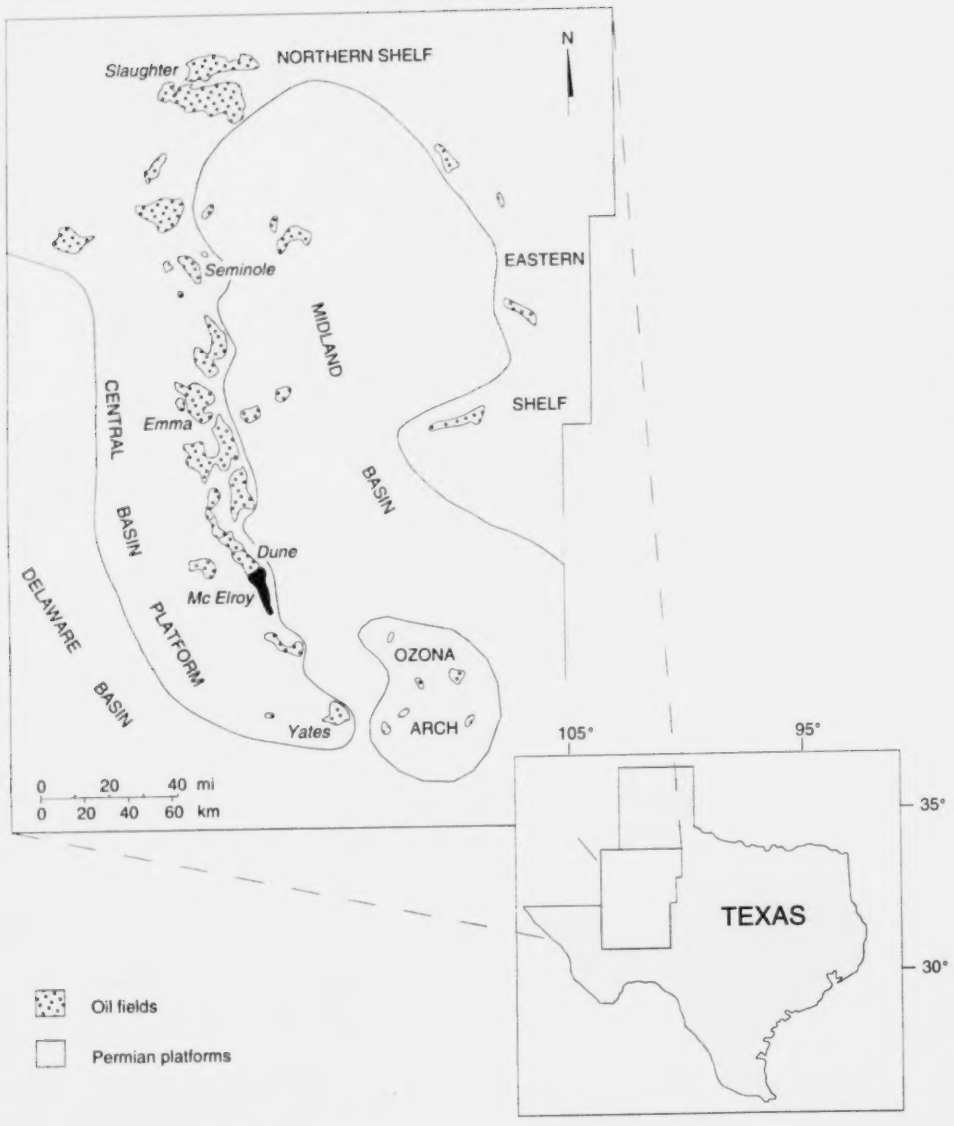

Figure 1.1: Regional paleogeographic setting of the Central Basin Platform and distribution of the major oil fields (modified from Longacre, 1990)

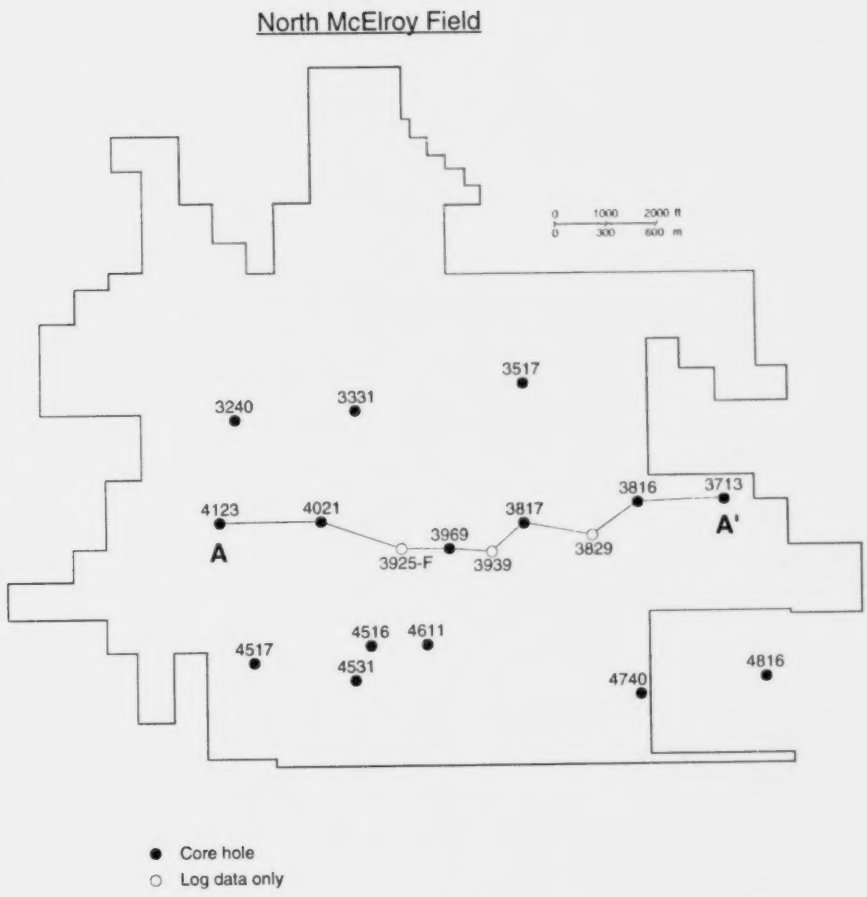

Figure 1.2: Map of North McElroy Field showing the location of cores and wells analyzed. Section AA' is a dip-oriented cross section.

The McElroy Field was discovered in the 1920's during the initial exploration of the Central Basin Platform and is currently producing by secondary recovery. Extensive geologic studies of the field began in 1972 using core analyses, wirelogs and production data, in order to define the reservoir characteristics (Longacre, 1990).

Regional Setting

The Permian basin of west Texas and southern New Mexico is located in the foreland area of the Ouachita-Marathon orogenic belt (Yang and Dorobek, 1992). This basin resulted from the development of an asymmetric structural depression in the Precambrian basement at the southern margin of the North American plate (Hills, 1985; Horak, 1985; Harris and Walker, 1988). The Central Basin Platform, which is a structural high (Fig. 1.3) that separates the Delaware Basin to the west and the Midland Basin to the east, persisted throughout most of the Pennsylvanian and Permian (Harris and Walker, 1988; Yang and Dorobek, 1992). Regional stratigraphic relationships and subsidence studies by Yang and Dorobek (1992) concluded that a complex history of deposition, subsidence, and periods of erosion were related to different stages of the Marathon Orogeny that started in the upper Mississippian to lower Pennsylvanian. Hills (1984, 1985), Horak (1985), Font (1985), and Yang and Dorobek (1992) suggested that these tectonic movements continued into the early Permian (Wolfcampian). During the late Permian, the Midland Basin was tectonically quiescent and progressively filled with carbonate banks that grew on sea-floor highs, and sands that were trapped behind the carbonate banks or reefs (Hills, 1985).

The Upper Permian (Guadalupian) sequence in the Central Basin Platform is composed, in ascending order, of the San Andres, Grayburg, Queen, Seven Rivers, Yates, and Tansill formations (Fig. 1.3). The time equivalents to these formations on the Northwest Shelf, are the Goat Seep Dolomite (= Queen Formation) and Capitan Formation (= Seven Rivers, Yates, and Tansill formations; Fig. 1.3). These formations progressively filled the Midland Basin during a regressive phase. Smaller scale transgressions, which

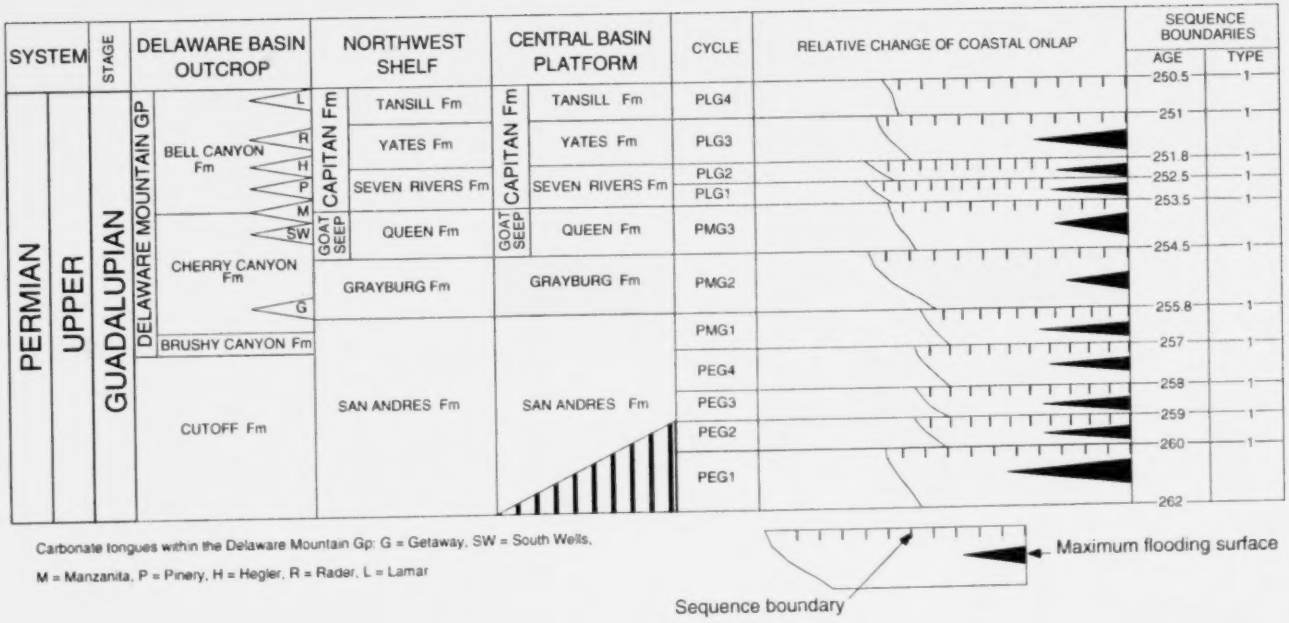

Figure 1.3: Chronostratigraphic chart of the Guadalupian (Permian) units of the Permian Basin region (modified from Kerans and Nance, 1991).

interrupted this general regression, produced an alternating sequence of siliciclastics, carbonates, and evaporites. Evaporites were especially conspicuous during the final stages of this regression (Queen to Tansill formations). The eastern windward margin of the Central Basin Platform, where North McElroy Field is located, faced northeast into prevailing winds and longshore currents that the removed fine-grained sediment (Walker et al., 1992).

The Grayburg Formation in the North McElroy field is about 200 feet thick in the most western part to at least 600 feet in the eastern part. This formation is characterized by shallow water to supratidal shelf sediments in the west that pass laterally into deeper-water marine sediments to the east. They were deposited on a gentle slope that faced into the Midland Basin. The progressive increase in the amount of siliciclastics and supratidal/evaporitic sediments toward the top of the formation was caused by a general west-to-east basinward progradation of the shoreline under arid climatic conditions. The Grayburg Formation in the North McElroy Field contains *Parafusulina lineata* in its lower part and *Parafusulina deliciasensis* in its lower and upper parts, both of middle Guadalupian age (Wilde, 1988 in Longacre, 1990). This association is found in the Cherry Canyon Formation, at its type locality in Trew Canyon, southern Delaware Mountains (Fig. 1.3), and they should be found together in the Grayburg Formation and possibly in the upper San Andres Formation.

Methods

Fifteen slabbed cores (cumulative length of about 5000 feet/1524 m) were selected from the 30 cores that are available. Cores were selected from the entire field and preference was given to the longest cores with the best recovery. Cores were logged at a scale of 1:60 using the software UNILOG ® on a portable computer. The core description template includes the following parameters: lithology, Dunham's (1962) carbonate classification, allochems, sedimentary structures, diagenetic features, sulfate types and amount, siliciclastic percentage, fusulinid preservation and percentage, grading direction,

nature of contacts, porosity and description. Gamma-ray logs were calibrated with cores for core logging and core correlations. In the homogeneous parts of the sequence, the well logs are very useful for defining bed contacts, texture changes, and cycle boundaries. About three hundred and fifty thin sections were analyzed in order to determine the composition, fabric, and textural characteristics of the constituent facies. Particular emphasis was placed on those facies with a small grain size, oil staining or a strong diagenetic overprint because they were difficult to describe in the slabbed cores. Percentage estimations of fusulinids and siliciclastics were made using the visual charts of Flugel (1982).

Each core was divided into different facies based on their lithology, texture, main allochems, and physical and biologic sedimentary structures. Vertical variability and packaging patterns between depositional facies were described (facies associations), as well as the nature of the contacts and bounding discontinuities.

Gamma-ray logs and cores at the same scale (1:60) were calibrated to exactly located textural changes, cycle boundaries and bed contacts, in particular in homogeneous intervals of the sequence. Depositional dip oriented cross-sections were constructed using cores and wirelogs in order to predict facies association distribution in a chronostratigraphic framework, vertical and lateral variability of cyclicity, geometry and reservoir distribution.

2. LITHOFACIES AND FACIES ASSOCIATIONS

Introduction

There is an extensive literature that describes the distribution and interpretation of facies in the Permian Basin of West Texas. Attention has been focused on these rocks because a) the Permian Basin is one of the most important oil-bearing basins in the world, b) there are large number of cores and well-logs available, and c) there are excellent exposures of equivalent rocks in the surrounding mountains. Facies analysis and process sedimentology have received considerable attention in recent studies on cyclicity, diagenesis, and reservoir characterization of these sequences, especially with respect to the San Andres and Grayburg formations (Bebout and Harris, 1990 ; Bebout, 1991; Kerans et al., 1992; Lindsay, 1991; Lindsay et al., 1992; Harris et al., 1993; Sonnenfeld and Cross, 1993; Kerans et al., 1994).

This report focuses on the distribution and environmental interpretation of facies in the Grayburg Formation (Guadalupian) of North McElroy Field, Central Basin Platform (Fig.). Past studies by Longacre (1980, 1983, 1986, 1990) were based on 10 interpretative facies that were later used to establish general sedimentological models for adjacent fields such as the McElroy Field (e.g. Harris et al., 1984). Bebout et al. (1987) divided the Grayburg Formation at Dune Field (inmediately north of North McElroy Field) into 9 lithofacies that are equivalent to those in the North McElroy Field. Conversely, Harris and Walker (1990) pointed out that a generalized version with only three facies is equally as useful for core and log correlations and more apt to be used by engineers during reservoir modeling. Nevertheless a more refined division is required in order to solve more specific problems, in particular those related to sedimentary processes and facies associations. This is particularly true where the original facies classification incorporated several different lithofacies facies under the same label; for example, a reef facies *sensu* Longacre (1980) may incorporate several organic structures and associated sediments that imply different ecological zonations within the buildup. Furthermore, the lithofacies

division should facilitate the interpretation of the vertical and lateral distribution of facies within a dynamic model that is based on sea level fluctuations (Walker, 1992).

Depositional Facies in the Grayburg Formation

The Grayburg Formation is formed mainly of fabric-retentive microcrystalline dolostones that can be described using Dunham's (1962) and Embry and Klovan's (1971) classifications.

This formation was divided into facies according to grain types, texture, and sedimentary structures (Table 2.1). Interpretations of the facies are based on their vertical and horizontal interrelationships, texture, sedimentary structures, and paleoecology of the biota.

Components of the different facies can be divided into: a) skeletal grains composed of fusulinids, bryozoa, red algae, brachiopods, crinoids, bivalves, corals, and green algae, b) organic structures formed by sponges, encrusting red algae, corals, bryozoa colonies, *Tubiphytes* sp., and algal/microbial mats, c) nonskeletal grains including peloids, ooids, coated grains and intraclasts of diverse origin, and d) siliciclastic grains.

Facies 1: Peloid-fine skeletal debris mudstone

Mottled to medium gray, highly burrowed mudstone with peloids and/or fecal pellets. Although small skeletal fragments (< 2 mm long) are ubiquituous, only rare crinoids and bryozoa can be clearly identified. Delicate brachiopod shells are commonly phosphatized whereas many peloids are pyritized (Fig. 2.1A). This facies, which is typically 0.6-2.4 m thick, grades upward into burrowed bioclastic wackestones (facies 2).

This lime mud-dominated facies was probably deposited in well-oxygenated deep marine environment (> 30 m) below normal storm base where bioturbation was the predominant process. Burrowing suggests an abundance of infaunal organisms. The fact that some shells are phosphatized implies a low rate of sedimentation. Rare fragments of

FACIES	COMPONENTS	STRUCTURES	THICKNESS	INTERPRETATION
Peloid-fine skeletal debris mudstone (1)	Peloids, pellets, phosphatized brachiopod shells, rare bryozoa	Massive to burrowed	0.6-2.4 m	Below storm wave base (> 30 m)
Bioturbated peloid-bioclastic wackestone (2)	Peloids, bryozoa, brachiopods, crinoids, red algae, rare corals	Burrowed	0.3-3.4 m	Between fairweather and storm wave base (10-30 m)
Structureless bioclastic-peloid packstone/grainstone (3)	Bryozoa, peloids, crinoids, brachiopods, red algae, rare corals	Massive. Rare cross-bedding. Inverse grading	0.3-4.0 m	Between fairweather and storm wave base (10-30 m)
Calcareous sponge bafflestone/floatstone (4)	Segmented-ramose calcisponges. Matrix composed of bioclastic wackestones		0.1-0.6 m	Low to moderate energy. Probably 20-30 m deep
Bedded *Archaeolithoporella* bindstone (5)	Centimeter scale, vertically stacked encrusting red algae and inorganic precipitates	Parallel or inclined bedding	0.06-1.0 m	Between fairweather and storm wave base (10-30 m)
Archaeolithoporella -sponge-bryozoa framestone (6)	Encrusting red algae, segmented calcisponges, ramose bryozoa, inorganic precipitates,*Tubiphytes*	Geopetal		Between F.W.B. and S.W.B. (10-30 m)
Peloid-fusulinid mudstone (7)	Peloid, fusulinids, rare bioclasts	Burrowed	0.05-1.0 m	Below S.W.B (> 30 m)
Bioturbated fusulinid-peloid wackestone (8)	Fusulinids, peloids, crinoids. Minor components include brachiopods, bryozoa and green algae	Burrowed. Scour surfaces	up to 1.5 m	Between F.W.B. and S.W.B. (10-30 m)
Fusulinid packstone/grainstone (9)	Fusulinids. Minor components include peloids, ooids, crinoids, brachiopods, and bryozoa	Parallel bedding, cross-bedding.	0.1-2.4 m	Between fairweather and storm wave base

Table 2.1: Summary of depositional facies

FACIES	COMPONENTS	STRUCTURES	THICKNESS	INTERPRETATION
Peloid-pellet packstone/grainstone (10)	Peloid, fecal pellets and ooids. Minor components include fusulinids, intraclasts, crinoids, and bivalves	Massive	0.3-1.8 m	Above or just below fairweather wave base
Vertically burrowed peloid-bivalve-crinoid wackestone (11)	Peloids, crinoids, bivalves, unidentified skeletal debris, and fusulinids	Vertical burrows	0.7-2.0 m	Low to moderate energy, probably above F.W.B.
Ooid-peloid grainstone (12)	Ooids. Minor components include peloids, pisoids, intraclasts, and fusulinids	Massive. Rare cross-bedding. Inverse grading	0.6-3.5 m	High energy, above fairweather wave base (< 10 m)
Pisoid-peloid-ooid-intraclast packstone/grainstone (13)	Pisoids, ooids, peloids, intraclasts, bioclasts, and siliciclastic sediments	Irregular fenestrae, chikenwire, tepee, and sheet cracks	1.0-2.7 m	High energy. Inter- to supratidal conditions (< 2 m)
Laminated peloidal mudstone/wackestone (14)	Peloids and rare bioclasts	Lamination. Spherical fenestrae	up to 2.1 m	Low energy. Shallow subtidal to intertidal (< 2 m)
Massive fine quarztarenite/sandy wackestone (15)	Peloids, pisoids, bivalves, ooids, crinoids, intraclasts, and fusulinids	Massive. Rare cross-bedding	0.3-1.4 m	Shallow subtidal (< 10-15 m)
Cross-bedded sandy fusulinid-peloid wackestone/packstone (16)	Fusulinids, peloids, and crinoids	Cross-bedding. Rare slumps.	0.3-1.0 m	Above storm wave action (< 20-30 m)
Sandy burrowed bryozoa-brachiopod wackestone (17)	Bryozoa, brachiopods. Minor components include crinoids, peloids, and rare fusulinids	Burrowed	up to 2.0 m	Below or just above storm wave base

Table 2.1 (cont.): Summary of depositional facies

crinoids, bryozoa and large brachiopods were periodically carried downslope by strong storms or by gravity flows.

Facies 2: Bioturbated peloid-bioclastic wackestone.

Burrowed, tan to medium gray, commonly mottled wackestone, composed of variable amounts of peloids, bryozoa, brachiopods, crinoids, red algae, corals, and rare green algae. The highly variable grain size depends on bioclast preservation. Large fragments (> 2 cm) of bryozoa and some corals are locally present along with entire brachiopod shells (Fig. 2.1B). Peloids and smaller skeletal fragments have an average grain size of 0.5 mm. Bioturbation patterns vary from thin horizontal burrows (< 5 mm in diameter) to large well defined vertical burrows (> 10 cm long). Transgressive lags are present locally. Facies 2, 0.3 to 3.4 m thick, grades upward into bioclastic-peloid packstones to grainstones (facies 3) or calcareous sponge bafflestones and/or floatstones (facies 4).

The fossil content of this facies suggests that it originated on bioclastic banks which accumulated at the platform edge. Sediments were deposited below fair weather wave base, but within depths affected by storm waves (10-30 m). This facies in conjunction with grainstones, packstones and rudstones of facies 3 may represent the stage stabilization of reef development (cf. James, 1984). Near the organic buildups, large fragments of branching bryozoa, corals, and articulated brachiopods suggest little or no transport. Locally, these sediments fill internal cavities in the reef.

Facies 3: Structureless bioclastic-peloid packstone/grainstone

These light gray to beige, massive grainstones, packstones, and rare rudstones are rich in skeletal fragments derived from bryozoa, crinoids, brachiopods and/or bivalves, calcareous green and red algae, and sparse coral fragments. These grains are poorly to well sorted. Nonskeletal grains include peloids. In peloid-dominated sediments, grain size is 0.25 to 0.5 mm. In skeletal-rich sediments the bioclasts are typically 0.7 to 2 mm long, but

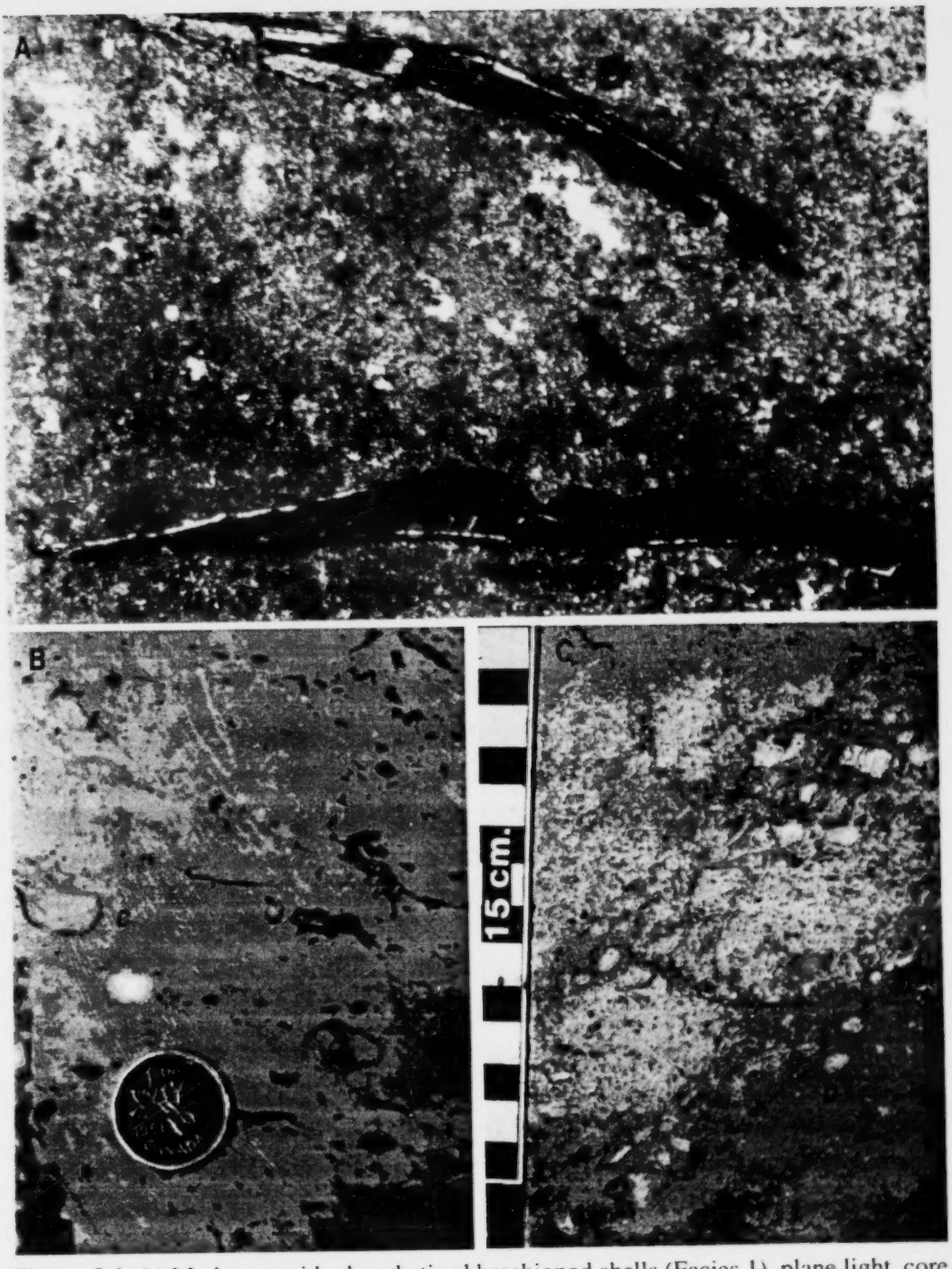

Figure 2.1: A) Mudstone with phosphatized brachiopod shells (Facies 1), plane light, core 3713-3901' (objective 12/0.06). B) Brachiopod-bioclastic wackestone (Facies 2). Notice the articulated shells (*c*). Core 3713-4142'. C) Cross-bedded bioclastic grainstone (Facies 3). Large fragments are bryozoa (*b*). Core 3713-4095'.

commonly contain fragments > 10 mm long. Although this facies is characteristically structureless, planar large-scale cross-bedding is locally present (Fig. 2.1C). Burrowing is common, particularly in the packstones. Some grainstones are rich in dark-medium gray allochems that probably originated from adjacent bindstones (facies 5). The upper contact is transitional, burrowed, stylolitic, or abrupt. Hardgrounds and "brecciated" areas with cemented bioclasts are locally present. Facies 3 is 0.3 to 4 m thick and typically underlies bedded bindstones (facies 5) and overlies bioturbated bioclastic wackestones (facies 2).

Material for this facies was provided by the breakdown of an open marine biota by physical action or bioerosion. The site of deposition was between storm wave base and at or just above fairweather wave base action (10-30 m) where bioclastic shoals accumulated along the shelf margin. Cross-bedding and bedsets indicate migration of the banks. Most of the subangular to subrounded peloids are micritized bioclasts that probably formed in a shallow water environment. Hardgrounds suggest periods of slow sedimentation. Brecciated features, evident in some rocks, were probably generated by differential compaction of soft and hard substrates during early burial.

Facies 4: Calcareous sponge bafflestone/floatstone

This boundstone is composed by segmented-ramose calcisponges (sphinctozoa) embedded in a bioclastic wackestone (Fig. 2.2A). Two genera of these sponges (*Amblysiphonella* and *Guadalupia*) were identified in these cores. These colonies, 5 to 10 mm in diameter, have a maximum measured length of 80 mm. The serially arranged chambers are filled with lime mud. The associated mottled bioclastic wackestone to mudstone contains fragments of brachiopods, bryozoa, encrusting organisms, and rare crinoids. Mottling is produced by numerous burrows that are 1-3 mm in diameter. Some sponges are encrusted by *Tubiphytes* sp. and/or red algae. This facies is 10-60 cm thick.

Delicate calcareous sponges were suspension feeders that required well oxygenated, clear waters with low to moderate energy levels at depths of ~20-30 m. These organisms, which were capable of baffling lime mud, were locally encrusted by red algae and

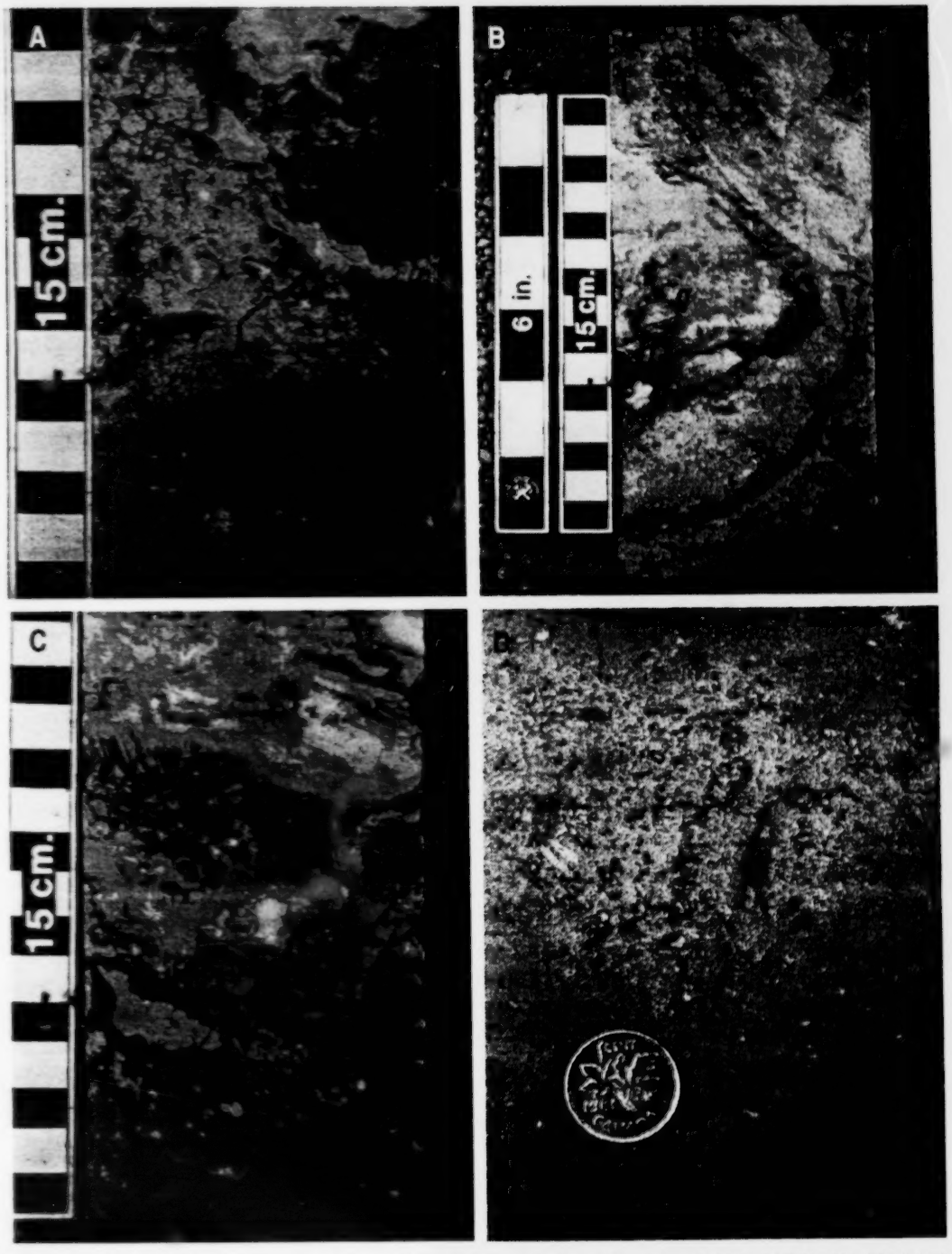

Figure 2.2: A) Calcareous sponge floatstone (Facies 4). Core 3713-4120'. B) Bedded *Archaeolithoporella* bindstone (Facies 5). This inclined bindstone ("elbow shape") is surrounding a peloidal grainstone (*g*). Core 3713-4043'. C) *Archaeolithoporella*-sponge-bryozoa framestone (Facies 6). Core 3713-4009'. D) Fusulinid mudstone (Facies 7). Core 3713-3769'.

Tubiphytes soon after the demise of the colonies. When the sponges are not in growth position, it is difficult to determine if this facies is a floatstone or a bafflestone. This facies was part of the main structure of the reef which according to James's (1984) scheme, is the diversification stage. The alternation of this facies with massive boundstones may imply lateral facies changes and/or vertical ecological changes in the reef.

Facies 5: Bedded "*Archaeolithoporella* " bindstone

This facies is formed of centimeter-scale, vertically stacked cellular structures and/or inorganic precipitates. These light gray bedded structures are ususally characterized by alternating light and dark beds (Fig. 2.2B). Crawford (1981) and Longacre (1983) suggested that these structures were the red algae *Archaeolithoporella* sp. This facies is divided into 1) parallel bindstones subfacies, that typically overlie muddy sediments with a sharp contact, and 2) inclined bindstones subfacies that commonly overlies grainstones (Fig. 2.2B). Parallel bindstones are 6-30 cm thick. On the other hand, inclined structures can cover thicker non-interrupted sections in the core (up to 1m thick).

These "bedded" structures probably represent an alternation of inorganic precipitates (finely crystalline interparticle cements) and encrusting *Archaeolithoporella.* This facies, which first appeared in the reef sequence as interbeds with the bioclastic sands during the stabilization stage, played an important role during the subsequent colonization period. Encrusting algae and inorganic precipitates stabilized the bioclastic sands preparing a suitable hard substrate for colonization by sponges and bryozoa. These inclined structures probably followed the paleotopography of the bioclastic sands. Similar laminar micrite crusts were described by Brachert and Dullo (1990, 1991) from the forereef slopes in the Red Sea of Sudan in waters deeper than 120 m. These laminar crusts produce a vertical stacking of hardgrounds, 0.5-2 cm thick, with their profile being determined by the morphology of the underlying substrate. In some slopes with inclinations of 15° to 40°, they noticed carbonate mounds (mainly grainstones) that were lithified *in situ* and provided the base for micrite crusts formation, which might be subsequently colonized by deep-

water corals. Some of these crusts occurred as hardgrounds during times of little or low sedimentation and parts of these crusts are probably biogenic in origin (cryptalgal fabrics) as indicated by calcified bacterial and/or fungal filaments (Brachert and Dullo, 1991).

Facies 6: "*Archaeolithoporella* "-sponge-bryozoa framestone

This facies is characterized by an intricate framework of binding organisms, the red algae *Archaeolithoporella*, and lesser amounts of *Tubiphytes* in combination with inorganic precipitates (Fig. 2.2C). In this framework, cavities are commonly lined with isopachous marine cements and filled with anhydrite. Dense micritic cements are apparently important and can be easily mistaken with encrusting organisms. These dense cements commonly surrounding bryozoa and sponge colonies. This facies is commonly interbedded with facies 4.

These boundstones probably formed in shallow waters with normal salinity (?) below wave action (perhaps less than 10-20 m). They form most of the reef and denotes the diversification stage (cf. James, 1984) that dominated the upper portion of a reef in a shelf margin position. Laterally discontinuous frameworks (i.e., patch reefs) with similar characteristics developed on the outer shelf. With growth these reefs eventually reached shallow water, possibly just above the fairweather wave zone. There is no evidence to suggest that these shelf margin boundstones were ever subaerially exposed. Crawford (1981) described similar facies from the Goat Seep Limestone in the Delaware Basin and suggested that the maximum water depth was about 20 m. This depth, calculated from depositional relief measured in outcrops, may also be a good estimate for this facies in the study area. The relationships between the encrusting organisms, suspension feeders (sponges and bryozoa), dense micritic cements, and isopachous cements indicate that this facies developed in a setting where early cementation was an active process. The lithified substrate provided firm attachment points for sessile suspension feeders and probably led to a less turbid environment, that was favorable for filter feeders (Crawford, 1981).

Facies 7: Peloid-fusulinid mudstone

This medium gray to beige/brown peloid-fusulinid mudstone (Fig. 2.2D), contains peloids that are < 0.5 mm in diameter. Distorted or deformed fusulinids, which form < 7% of the rock, are smaller (0.5 mm) than in those facies 8, 9 and 16. Although usually scattered through the mudstone, the fususlinids are locally concentrated in burrows. Storm layers composed of larger fusulinids are present but not common. This facies, 0.05 to 1 m thick, grades up into facies 8.

These sediments were deposited in a low energy setting below storm wave base (perhaps less than 50 m). The small fusulinids may indicate a population dominated by juvenile individuals of larger species that had been selectively removed and transported to deeper waters, where they were mixed with peloids and skeletal fragments. Most fusulinids, however, were introduced during bioturbation of overlying sediments. Changes in color suggest a variation from reducing (light gray) to better oxygenated conditions (beige/brown).

Facies 8: Bioturbated fusulinid-peloid wackestone

This facies is characterized by fusulinid foraminifera embedded in a brown to medium gray lime mud matrix that is commonly mottled (Fig. 2.3B). Peloids and/or pellets, the second most important allochem, are also common. Minor components include crinoid fragments, bivalves, dasycladaceae algae, rare brachiopods, and rare bryozoa. Large burrows (2-3 cm in diameter) are evident by the alignment of the fusulinids. Anhydrite nodules are commonly associated with the burrows. The fusulinids, which are 0.5-3.0 mm in diameter, form 5-40% of the rock. In terms of test diameter, fusulinid populations are unimodal or multimodal. They are either well preserved or fusimolds filled with anhydrite. Some fusulinids are partly replaced by anhydrite leaving the other part unaltered. This facies, which is up to 1.5 m thick, commonly overlies facies 7 and grades upward to facies 9. If facies 9 is absent, the upper contact may be sharp, stylolitic, burrowed, or defined by a hardground.

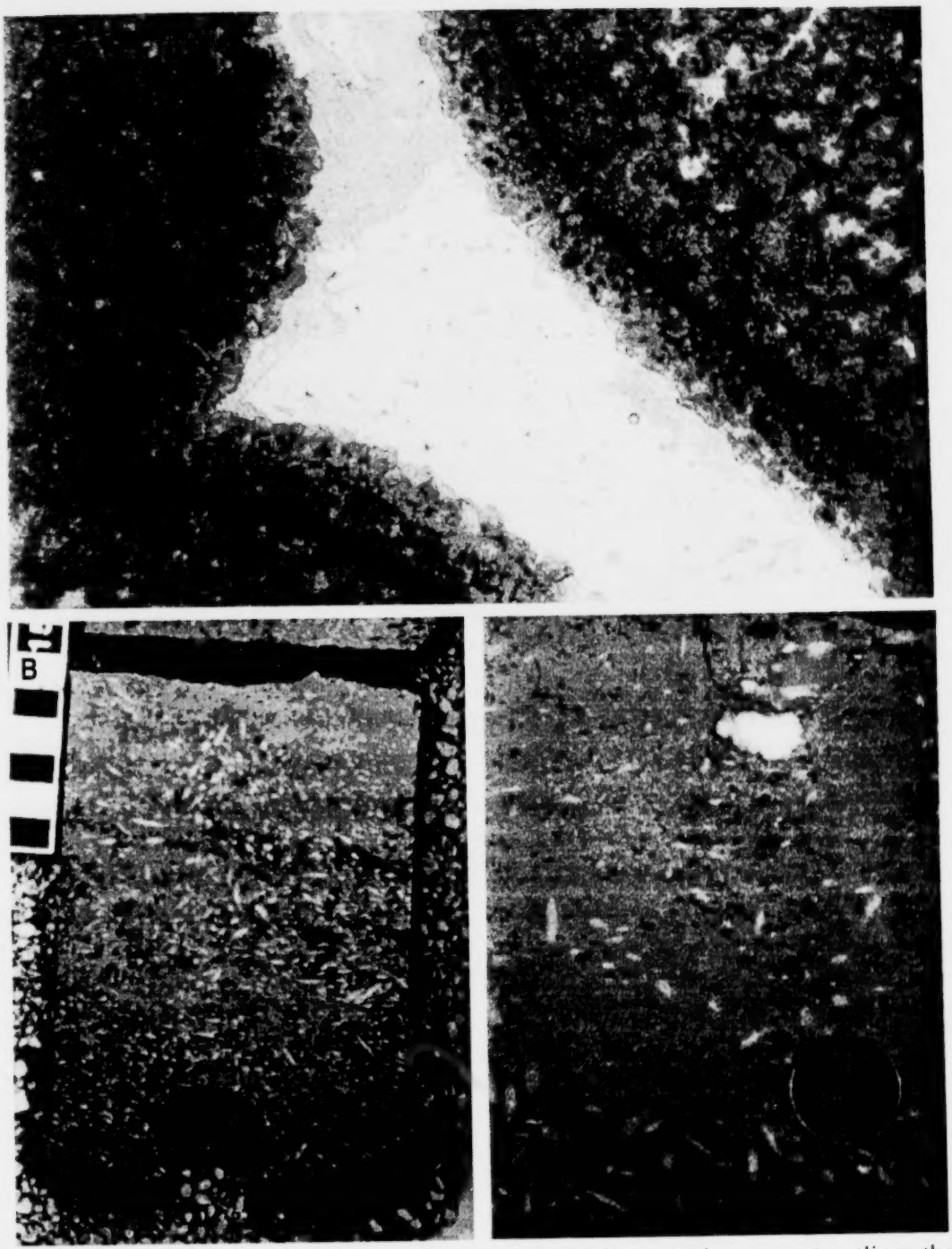

Figure 2.3: A) Fusulinid grainstone (Facies 9). Isopachous marine cement outlines the fusulinids. Plane light, core 4816-3838' (objective 12/0.06). B) Burrowed fusulinid wackestone (Facies 8). Core 3713-3778'. C) Peloid grainstone with sparse fusulinids (Facies10). Core 3713-3680'.

These sediments were deposited in a shallow subtidal environment (probably less than 20-30 m) under a low to moderate energy regime, where burrowers actively homogenized the sediments. Variability in fusulinid size may suggest a congregation of different species of mature age, juvenile/adult mixing or sexual and asexual forms of the same species. Aigner (1985), for example, explained that two different size populations of the same species may coexist because of the life cycle of large foraminifera. Eocene nummulites from Egypt, for example, commonly contain more asexually-generated (small size) than sexually-generated (large size) individuals by a factor of 10 to 1 (Aigner, 1985). Those accumulations may be ecologically similar to the fusulinid assemblages in the Permian strata of the study area. Fusulinacea, most of which probably had photosynthetic symbionts, were adapted to waters 15-20 m deep (Ross, 1983; Ross and Ross, 1988). A special niche for the foraminifera was probably created by algal mats and other non-calcareous marine plants that locally stabilized the substrate and baffled the fine sediment. This speculation is based on the interaction observed in modern lagoonal environments, where plants like *Thalassia* baffle waves and currents and bind fine sediments and epibionts (e.g., forams, small serpulids, melobesidae algae) in its root systems. The amount of micrite is not necessarily related to the energy of the environment but to the capability of these plants to reduce energy levels to the point where the fine sediment is deposited.

Facies 9: Fusulinid packstone/grainstone

Facies 9 is composed almost entirely of moderate- to well-sorted fusulinids (*Parafusulina* sp.) that are 1-4 mm in diameter. The fusulinids are well preserved with little evidence of breakage or abrasion. Peloids, ooids, crinoids, brachiopods, and bryozoa are locally common. Parallel bedding is common whereas cross stratification is rare or absent. The fusulinids are commonly oriented parallel to bedding. Large well defined vertical burrows are locally present. Isopachous cements are locally conspicuous in well sorted grainstones (Fig. 2.3A). The upper contact is sharp, erosive, or stylolitic. This facies, which is 0.1 to 2.4 m thick, commonly overlies facies 8 and underlies facies 10.

Fusulinid grainstones and packstones accumulated in banks on the shelf margin, between fairweather wave base and storm wave base (perhaps 10-20 m). They were probably deposited in a similar paleobathymetric position to the bioclastic sand shoals and reefs (i.e., facies 3, 5 and 6). As noted by Ross (1983), members of the family Schwagerinidae (which include *Parafusulina* sp.) were adapted to shallow to very shallow waters, such as reef edges, shallow lagoons, tidal flat channels, margins of algal shoals and banks, and other shallow nearshore areas. The cylindrical to ellipsoidal shape and low density tests of the fusulinids meant that they could easily be oriented aligned parallel to the prevalent current flow (Wilson and Jordan, 1983). Parallel bedding in these packstones and grainstones may reflect deposition at or just above wave base level. Early marine cementation in the form of isopachous cements in the very well sorted grainstones may be related to upwelling currents saturated in calcium carbonate. These cemented grainstones are laterally equivalent to shelf margin bindstones and framestones. There is no evidence that encrusting organisms played any role in the cementation of this grainstones.

Facies 10: Peloid-pellet packstone/grainstone

These massive, light gray to beige packstone/grainstones are composed mainly of moderate to very well sorted peloids and/or fecal pellets (Fig. 2.3C). Grain size is 0.25-0.7 mm with an average of 0.5 mm. Allochems are commonly well rounded. Most of the small peloids (~ 0.25 mm diameter) are fecal pellets. Other allochems in this facies include ooids, fusulinids, intraclasts, crinoids, and bivalves (up to 30 mm long). The intraclasts and bivalves are commonly most conspicuous in the packstones. Siliciclastic sediments (up to 25%) are locally important. When associated with fusulinid-rich facies, this facies may contain up to 30% of these foraminifera. Average thickness is 0.3-0.6 m, with some beds up to 1.8 m thick. This facies, which overlies fusulinid grainstones or wackestones (facies 9 and 8) and peloid-bivalve-crinoid wackestone (facies 11), commonly grades upward into ooid grainstones (facies 12).

The peloid-pellet packstones and grainstones, which were deposited in a very shallow water environment (less than 10 m), were associated with high-energy ooid shoals. Modern sediments with similar characteristics were described by Hine (1977) and Harris (1983, 1984) in the Bahamas, as deposited on stabilized bottoms seaward of ooid sands. In addition, peloid-rich sediments are in part responsible for the buildup of the ooid shoals (Harris, 1984). The presence of bivalves, fusulinids, and crinoids suggest open marine conditions on the platform.

Facies 11: Vertically burrowed peloid-bivalve-crinoid wackestone

These beige to light brown-colored wackestones are characterized by conspicuous, long vertical burrows. Allochems include peloids, crinoids, bivalves, unidentified skeletal debris, and rare fusulinids (< 5%). Vertical burrows (*Thalassinoides* sp.) are commonly 2-3 cm in diamenter (up to 5 cm), lined, and up to 20 cm long. Locally, these burrows have a pseudo-concentric internal lamination. Fractures and stylolites are commonly associated with these burrows, and locally caliche-like crusts are present along with breccias. Breccias, formed of fragments up to 10 cm long, have a composition similar to the host sediments. Anhydrite nodules are common and locally abundant, particularly near the brecciated areas. Typically, the sediments filling the burrows are darker in color and contain more bivalve fragments than the surrounding sediments. Some bivalves in the burrows are up to 5 mm long. Siliciclastic grains are locally common (up to 30%). This facies commonly grades upward to wackestones or packstones that lack vertical burrows. In some cases it is difficult to establish facies boundaries because of the homogeneity of the sediments and the strong diagenetic overprint. Facies 11 is 0.7-2 m thick.

The vertical burrows (*Thalassinoides* sp.), were formed by marine organisms that burrowed into semi-consolidated wackestones and packstones. Some burrows are filled with sediments that are unlike any others found in the succession. There are at least two explanations for this phenomenon 1) it denotes firmgrounds with open burrows that were filled by transgressive sediments during a relative sea level rise, or 2) the sediments inside

the burrow were reworked by the burrower. Concentric laminations are related with feeding activities of the burrowing organisms (Saunders, per. com., 1994). An excellent analog of open burrows in firm substrates that may be filled with concentrically laminated sediment are found in Holocene sediments from Florida and the Bahamas (Shinn, 1968). They were produced by Callianassid shrimps that intensively burrowed (with a penetration up to 1 m) sediments from intertidal to 10 m deep (at deeper water they become less abundant) in protected areas. Shinn (1968, p. 891, fig. 16) even suggested that the burrows from Florida and the Bahamas were remarkably similar to those found in the San Andres Formation (Permian). The fusulinids in this facies were probably transported into this environment from nearby areas. The caliche-like crusts indicate that these sediments may have been periodically exposed. The breccias which are commonly related to emplacement of sulfates in burrows, are probably unrelated to the exposure.

Facies 12: Ooid-peloid grainstone

This facies is composed of well-sorted ooids with a diameter of 0.25-1 mm (Fig. 2.4A). Quartz grains form the nucleus of some ooids. The internal structures of most ooids, however, was destroyed by dolomitization. Admixtures with peloids, pisoids, intraclasts, and fusulinids are common. Primary porosity was occluded by calcium sulfate. Beds are normally or inversally graded; low-angle unidirectional cross-bedding is rare. Siliciclastic sediments (very fine sand to silt) are locally important but never exceed 10%. The upper contact is transitional, abrupt (hardgrounds with scattered *Gastrochaenolites*), stylolitic, or erosive. Vertical fractures filled with siliciclastics, breccias, silty layers, and large pelecypods are commonly observed in the upper boundary of this facies. Facies 12, which is 0.6-3.5 m thick, overlies peloid packstones (facies 10), quartzarenites (facies 15), or vertically burrowed wackestones (facies 11). This facies underlies quartzarenites (facies 15) and pisoids-peloid-ooid-intraclast packstone/grainstones (facies 13).

Good sorting and the lack of fine-grained sediments in the ooid-peloid grainstone facies suggests a high-energy, shallow subtidal environment (perhaps < 5m). Submarine

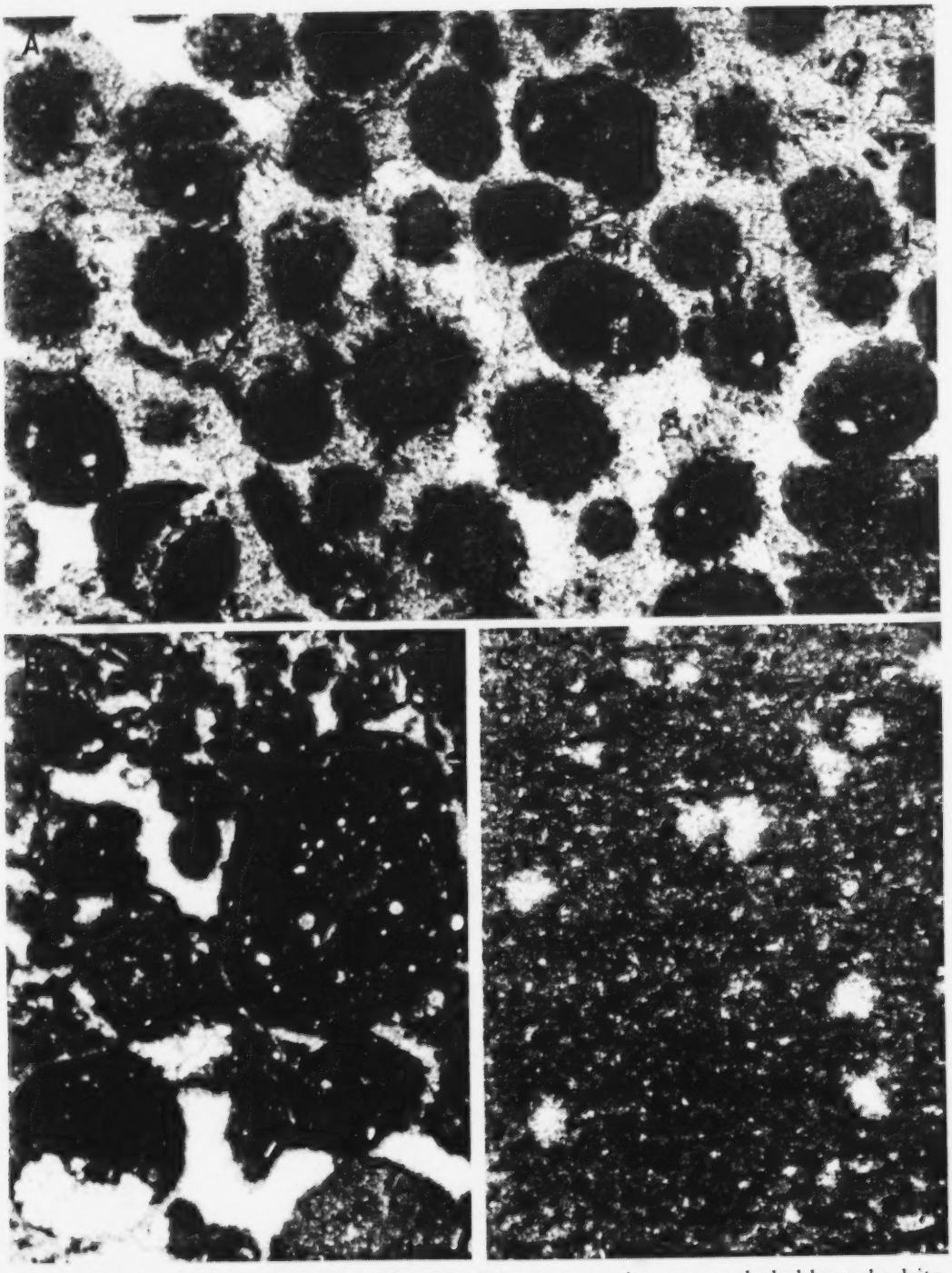

Figure 2.4: A) Ooid grainstone (Facies 12). Primary porosity was occluded by anhydrite. Plane light, core 4123-2954' (objective 12/0.06). B) Intraclast-pisoid-peloid grainstone (Facies 13). Plane light, core 4123-2904' (objective 12/0.06). C) Mudstone with spherical fenestrae filled with anhydrite (Facies 14). Plane light, core 4123-2909' (objective 12/0.06).

hardgrounds and normal gradation (deepening upward) are common and suggest a lateral migration of the banks or a relative sea level rise. Similar ooid shoals deposited in shallow water (< 10 m) are well known from the Bahamas (e.g. Hine, 1977; Halley et al., 1983; Harris, 1984)). Some of these sediments, however, accumulated in very shallow conditions possibly in the inter-supratidal zone where they were exposed for relatively short periods of time. Drying of the sediments caused local brecciation and/or fracturing. The fractures were subsequently filled with siliciclastics.

Facies 13: Pisoid-peloid-ooid-intraclast packstone/grainstone

This facies is dominated by coated grains (pisoids and ooids) and intraclasts up to 10 mm long (Fig. 2.4B). Intraclast composition is similar to the host sediments. Some grains have a reddish hue that may reflect the presence of iron oxides. This facies is mainly structureless. If bedded, the amount of pisoids and intraclast commonly increase toward the top. Irregular fenestrae, chikenwire structures, tepee structures, sheet cracks, and sparse caliche crusts are common. Siliciclastic sediments are commonly mixed with lime mud or in sheet cracks, tepees, and intergranular pores. This facies, which is 1.0-2.7 m thick, transitionally overlies facies 12 (ooid-peloid grainstone) and the upper contact is abrupt or erosive.

This facies was deposited in an intertidal to supratidal environment. The increase in pisoids and intraclasts, in addition to the presence of fenestral structures, sheet cracks, tepee structures, and caliche crusts indicate an increase in the degree of subaerial exposure of abandoned ooid bars. The intraclasts were probably formed by local reworking of the sediments by storms, waves and tides. Siliciclastic sediments were transported to the area by eolian or by marine processes, where they filtered into open spaces or mixed with the sediments.

Facies 14: Laminated peloidal mudstone/wackestone

This beige to dark brown, faintly laminated peloid mudstone contains scattered oval to spherical fenestrae filled with anhydrite (Fig. 2.4C). The number of fenestrae commonly increases toward the top of the beds. Scattered peloids, fusulinids, and intraclasts are the only allochems found in this facies. This facies, up to 2.1 m thick, commonly underlies peloid packstones (facies 10) and overlies fusulinid wackestones (facies 8).

The oval to spherical fenestrae that are filled with anhydrite suggest that this facies was deposited in a supratidal to upper intertidal setting. This type of fenestrae, usually in poorly laminated muds, was probably formed by air bubbles that were trapped in the sediments (Hardie and Shinn, 1986). This facies was probably deposited in a protected setting behind ooid bars. The rare allochems indicate a periodic onshore transport of open marine sediments by storms and spring tides. Increase of fenestrae toward the top of the sediments, indicates a progressive increment of exposure. The faintly defined lamination may be the result of succesives floods that were separated by non-deposition or by an incipient development of algal mats.

Facies 15: Massive fine quartzarenite/sandy wackestone

This medium gray/brownish gray very fine-grained dolomitic sandstone to siltstone is moderately- to well-sorted (Fig. 2.5A). Wispy lamination and horsetail structures are common. Parallel lamination occurs in intervals of carbonate-siliciclastic interbedding. Burrows are rare. Peloids, pisoids, bivalves, ooids, echinoids fragments, intraclasts, and fusulinids are common in this facies. This facies, 0.3-1.4 m thick, may grade transitionally upward into carbonate-rich facies.

Admixtures of these fine-grained sands with ooids, fusulinids, and peloids suggest that these sediments were probably deposited in a very shallow platform (probably less than 10-15 m). Bebout (1991) explained that the siliciclastic material in the Grayburg Formation was probably transported to shallow subaqueous settings by eolian processes or ephemeral streams (wadis) during times of lower sea level and then reworked by marine

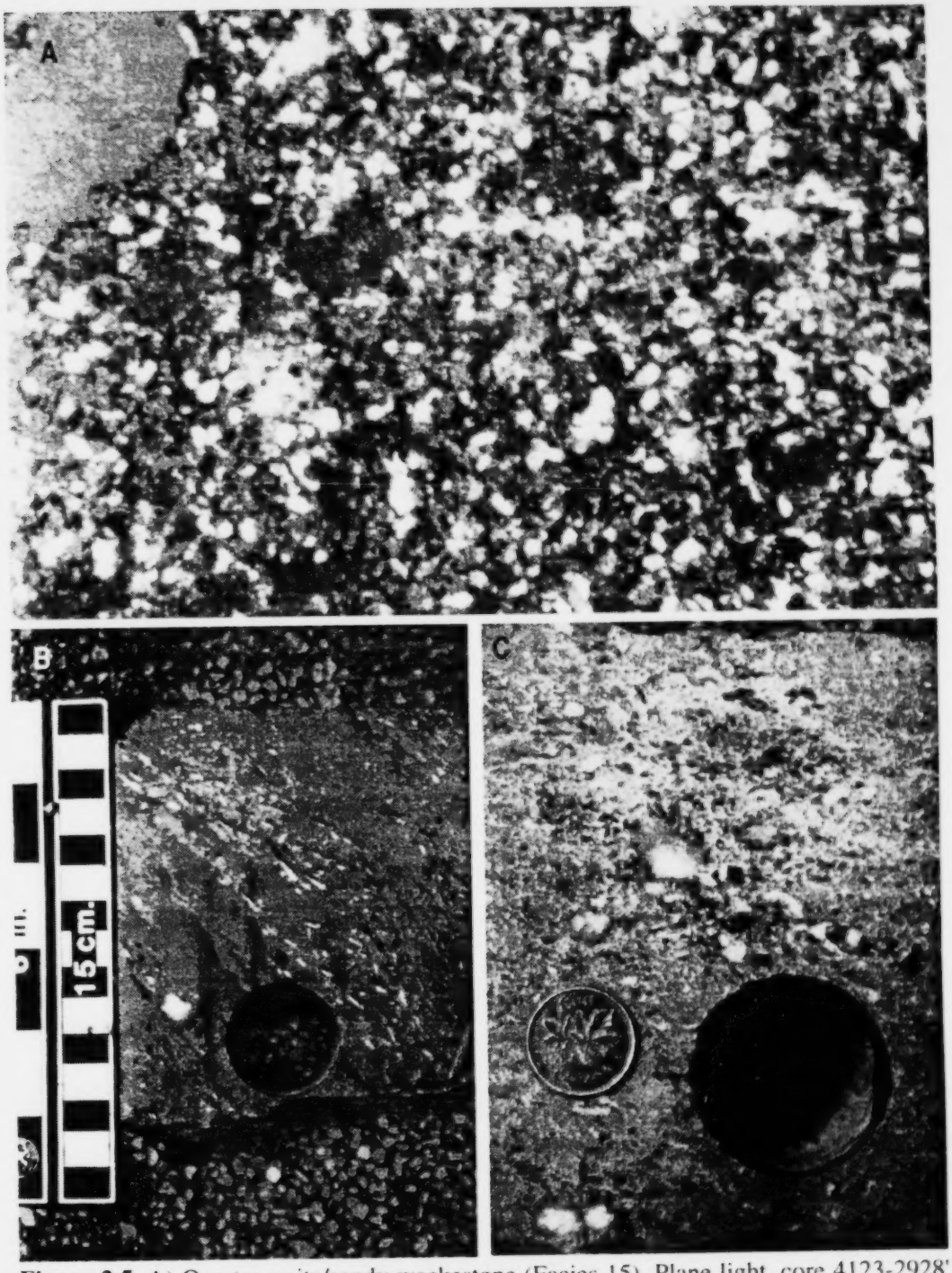

Figure 2.5: A) Quartzarenite/sandy wackestone (Facies 15). Plane light, core 4123-2928' (objective 12/0.06). B) Cross-bedded sandy fusulinid wackestone (Facies 16). Cross-bedding is defined by fusulinid orientation. Core 3713-3924'. C) Sandy burrowed bryozoa-brachiopod wackestone (Facies 17). Core 3713-3646'.

processes.The absence of burrows and other sedimentary structures is the norm and may indicate a low energy setting with restricted conditions. These sediments, however, were locally affected by waves and tide currents that produced parallel lamination and rare cross-bedding.

Facies 16: Cross-bedded sandy fusulinid-peloid wackestone/packstone

The matrix of this olive to dark gray fusulinid-peloid wackestone contains up to 40% very fine sand to silt-sized quartz grains. The fusulinids (0.5-2 mm in diameter), which form 5-20% of the rock, are mostly replaced by anhydrite. Intervals with abundant siliciclastics are characterized by high-angle bedding (30-40°; Fig. 2.5B), deformed beds, rare slump structures, and rare injection features. The inclination of the cross-beds decreases as the carbonate/siliciclastic ratio increases. Peloids, up to 1 mm in diameter, are locally abundant and in some cases are blackened. Crinoid fragments are common. When overlying an erosional surface, this facies contains floating yellow to cream, angular/subangular (larger) to rounded (smaller) intraclasts, 0.3-16 cm long, that are composed of fusulinids. This facies, 0.3 to 1 m thick, underlies facies 9 in sharp contact and is transitional with facies 10 (see peloid packstones).

These cross-bedded sediments were probably deposited above storm wave base on the lower shoreface (perhaps less than 20 m), where fusulinids, peloids, and rare crinoids were the only allochems available. Fisher and Sarnthein (1988) described the deposition of nearshore sand wedges off the Saharan west coast populated by shallow-water organisms, including the foraminifer *Amphistegina*. They directly compared this Holocene example with Permian shoal-water sand wedges where fusulinids and other skeletal grains were abundant. Large foraminifera of Eocene age (nummulites) were deposited on a mixed carbonatic-siliciclastic environment normally on the leeward side of reefs close to a shoreline dominated by siliciclastic beaches and alluvial fans (Santiesteban and Taberner, 1988). High-angle bedding, deformed beds, slumps, and injection features are probably related to hydroplastic sediments (mixtures of lime-mud and fine siliciclastics) that were

deformed a short distance below the sea bed more likely by storm-induced mechanisms, when standing waves were generated as a result of collision from different directions of waves of equal or near equal period (Johnson, 1977; Allen, 1984). Large pebbles and other lithoclasts observed in this facies were eroded from the barren-rocky sea floor and/or from subaerially exposed terraces adjacent to the shoreline. In some cases, peloid packstones (facies 10) associated with this facies contain abundant black/dark peloids mixed with light grains (salt and pepper texure). Shinn and Lidz (1988) described the occurrence of blackened peloids in Florida, similar to those described in facies 17, which were probably originated by organic matter and/or iron or manganese sulfides as blackening agents in a subtidal environment. This "blackening" effect commonly affects grains in the sand-size range (even whole foraminifera) and commonly occurs above drowned subaerial unconformities (Shinn and Lidz, 1988).

Facies 17: Sandy burrowed bryozoa-brachiopod wackestone

This facies is characterized by bryozoa fragments up to 10 mm long (Fig. 2.5C) and well- preserved brachiopod shells embedded in a medium gray siliciclastic-rich matrix. Siliciclastics (up to 40%) are composed of very fine sand and silt. Other calcareous allochems include crinoid fragments, peloids, unidentified skeletal grains, and rare fusulinids. Sediments were thoroughly burrowed. Seams and pockets of pyrite are common in the upper part of the beds. This facies, up to 2 m thick, grades upward into fusulinid wackestones (facies 8).

The absence of shallow-platform allochems, such as ooids, pisoids and only rare fusulinids, as well as, pyritized areas (reducing conditions) and intense bioturbation, suggest that these sediments were deposited below wave base probably on the slope (probably more than 15 m deep). Siliciclastic sediments bypassed the carbonate platform in large quantities and were deposited downslope. Organisms, in particular bryozoa, flourished when the rate of siliciclastic sedimentation was low. Reducing conditions (i.e.

abundance of pyrite) were probably associated with an overall decrease in sedimentation and intensification of burrowing.

Facies Associations and Depositional Settings

The variability and vertical succession of facies in the Grayburg Formation of the North McElroy Field can best be described in order of decreasing relative water depth by dividing the facies into the slope, shelf margin, outer shelf, shelf crest, inner shelf, and shoreface facies associations. These associations are defined and interpreted on the basis of their constituent facies (Table 2.2), packaging patterns, geometry, and relative position on the shelf (cf. Sami and James, 1994). One of the fundamental clues to establishing the vertical facies associations is the nature of the contacts between the facies. A gradational transition from one facies to another implies that the two facies represent environments that once were adjacent laterally whereas sharp breaks may imply fundamental changes in depositional environment and the onset of new sedimentation cycles (Walker, 1984).

Slope Facies Associations

This association, which represents the deepest water facies in the Grayburg Formation, is found in the eastern part of the field (Fig. 2.6). The association was divided into lower and upper slope according to its dominant composition, inferred paleodepth, and packaging patterns.

Lower Slope (Bioclastic Dominated)

The symmetric small-scale cycles (Fig. 2.6) characteristic of this association comprise a deepening upward succession which is formed of bioturbated peloid-bioclastic wackestones (facies 2) that is overlain by burrowed peloid-fine skeletal debris mudstone (facies 1), and capped by bioturbated bioclastic wackestone (facies 2). The amount of recognizable bryozoa fragments, brachiopods, and crinoids gradually diminished with water depth. There is a complete absence of shallower water allochems (e.g., pisoids,

FACIES ASSOCIATIONS	CONSTITUENT FACIES	INTERPRETATION
Lower Slope (bioclastic dominated)	Bioturbated peloid-bioclastic wackestone, bioturbated bioclastic wackestone (Facies 1 and 2)	Gentle slope without evidences of turbiditic flows. Deposition below storm reworking
Upper slope (bioclastic dominated)	Bioturbated peloid-bioclastic wackestone, bioclastic-peloid packstone/grainstone (Facies 2 and 3)	Section of the slope located seaward of the shelf margin and affected by storms
Upper slope (fusulinid dominated)	Peloid-fusulinid mudstone, peloid-bioclastic wackestone/mudstone, bioturbated fusulinid peloid wackestone (Facies 7, 2, and 8)	Similar to the bioclastic dominated upper slope
Shelf margin (bioclastic bank)	Bioturbated peloid-bioclastic wackestone, massive bioclastic-peloid packstone/grainstone (Facies 2 and 3)	Submerged shoal controlled by the position of the fairweather and/or storm wave base.
Shelf margin (bioherm)	Bioturbated peloid-bioclastic wackestone, bioclastic-peloid packstone or grainstone, *Archaeolithoporella* bindstone, calcareous sponge bafflestone or floatstone, *Archaeolithoporella*-sponge-bryozoa framestone (Facies 2, 3, 5, 4, and 6)	Shelf-edge reef; morphology and vertical accretion of bioherm controlled by wave and/or storm reworking. Reef biota depth sensitive
Shelf margin (fusulinid bank)	Bioturbated fusulinid-peloid wackestone, fusulinid packstone/grainstone, peloid-pellet packstone/grainstone (Facies 8, 9, and 10)	Submerged shoal that indicate large accumulations of autochthonous fusulinids below faiweather wave base
Outer shelf (fusulinid dominated)	Peloid-fusulinid mudstone, bioturbated fusulinid-peloid wackestone (Facies 7 and 8)	Partly protected by submerged shelf margin; relatively deep setting affected by storms
Outer shelf (peloid dominated)	Massive fine-grained quartzarenite, vertically burrowed peloid-bivalve-crinoid wackestone, peloid-pellet packstone/wackestone (Facies 15, 11, and 12)	Low-energy environment located between the shelf margin and the shelf crest
Shelf crest	Peloid-pellet packstone, massive fine-grained quartzarenite, ooid grainstone (Facies 10, 15, and 12)	Ooid bars deposited in agitated shallow water
Inner shelf	Fusulinid-peloid wackestone, vertically burrowed peloid-bivalve-crinoid wackestone, laminated peloid mudstone, pisoid-peloid-ooid-intraclast packstone/grainstone (Facies 8, 11, 14, and 13)	Protected, shallow subtidal to supratidal environment behind ooid bars.
Shoreface	Cross-bedded sandy fusulinid-peloid wackestone, fusulinid packstone/grainstone, peloid-pellet packstone (Facies 16, 9, and 10)	Storm and wave dominated shoreface. Mixed carbonate-siliciclastic environment

Table 2.2: Summary of facies associations

ooids). This facies association was probably deposited at or below storm wave base (> 30 m deep)

Upper Slope (Bioclastic Dominated)

This association consists of asymmetric small-scale cycles (Fig. 2.6) composed of a lower bioturbated peloid-bioclastic wackestone (facies 2) that grades up into a massive bioclastic-peloid packstone/grainstone (facies 3). The thickness of the constituent facies in each cycle is similar (Fig. 2.6). Locally, packstone/grainstone facies with hummocky cross-stratification, graded storm beds, and/or scoured surfaces, indicate that this facies association was probably deposited above storm wave base (< 30 m). The bioturbated wackestones represent the post-storm deposition where the dominant process of sedimentation was suspension.

Upper Slope (Fusulinid Dominated)

This association formed of small-scale, asymmetric cycles (< 3 m thick) that are formed of peloid-fusulinid mudstones (facies 7) or peloid-bioclastic wackestone/mudstones (facies 2) at the base of the cycles and bioturbated fusulinid-peloid wackestones at the top (facies 8) (Fig. 2.6). This association developed seaward of the fusulinid banks that formed at the shelf margin. The inferred paleodepth is above the zone of active storm-wave reworking (< 30 m).

Shelf Margin Facies Associations

Facies deposited along the shelf margin are characterized by an open marine biota (e.g., bryozoa, sponges, brachiopods, red algae, and crinoids) or fusulinids. These organisms, directly or indirectly, led to the formation of relatively deeply submerged (10-30 m deep) banks and bioherms. The shelf margin association is divided into bioclastic bank, bioherm, and fusulinid bank..

Bioclastic Bank

Asymmetric small-scale cycles (meter-scale) in this association (Fig. 2.6) consist of a relatively thin (< 0.6 m thick) bioturbated peloid-bioclastic wackestone (facies 2) that is overlain by a thick (up to 2-3 m thick) massive bioclastic-peloid packstone/grainstone (facies 3). The relative thickness of the constituent facies is the fundamental characteristic used to separate this facies association from the upper slope bioclastic dominated association (Fig. 2.6). Although the top of these cycles is commonly sharp (locally hardgrounds), stylolitic, or transitional, there is no evidence of exposure. Constant submarine erosion and redistribution of sediments probably inhibited aggradation of this facies association above the depth of fairweather base. *In situ* organic structures are absent. The scarcity of sponges and encrusting organisms indicate that water conditions were inappropriate for these organisms because of continuous storm and wave reworking that inhibited their preservation, or mobile substrates that prevented their attachment. Physical and biological destruction processes were probably important in the generation of sediments. This facies association was probably deposited between the storm wave base and the fairweather wave base.

Bioherm

This association is formed of stacked asymmetric small-scale cycles that are grouped into decameter-cycles (Fig. 2.6). The basal part of the decameter-cycles are formed of bioclastic wackestones and grainstones (facies 2 and 3; pioneer stage) that were progressively stabilized by encrusting algae and inorganic precipitates (facies 5; colonization stage). These algae and inorganic precipitates created a hard substrate on which sessile suspension feeders, such as sponges and bryozoa, attached themselves (facies 4 and 6; diversification stage). The ecological succession from the pioneer stage to the diversification stage may reflect autogenic controls, where each stage provides more favorable conditions for later communities or stages (e.g., Walker and Alberstadt, 1975; James, 1984). As suggested by Crame (1980), however, a species that prepares the

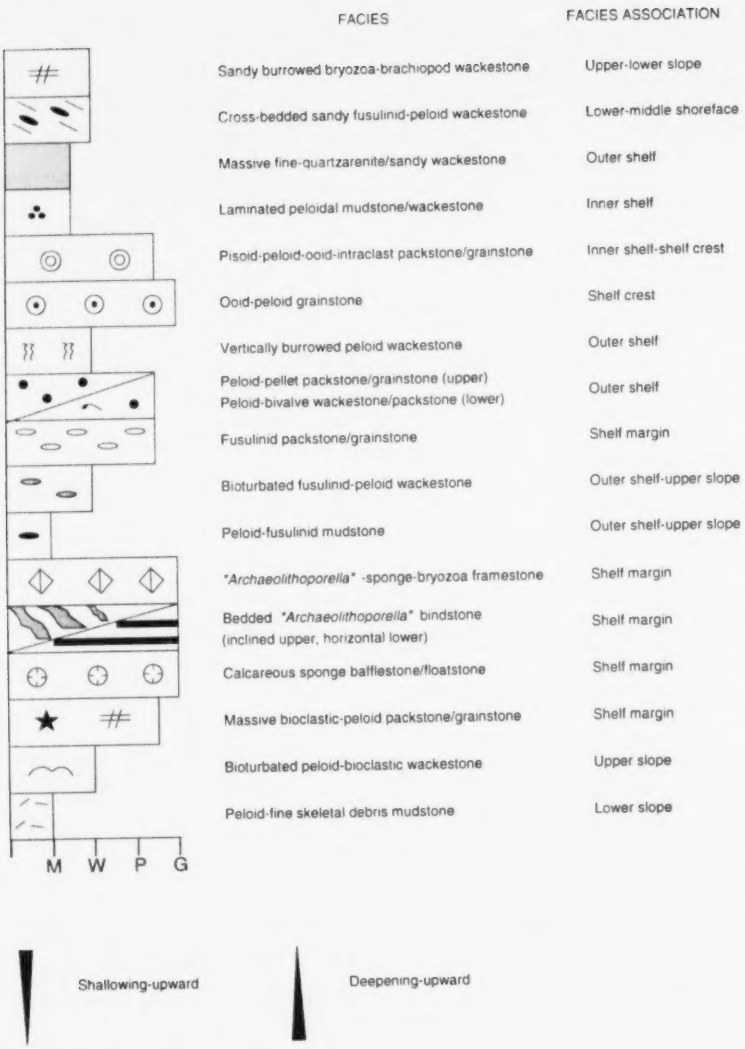

Figure 2.6: Key to depositional facies. Examples of facies associations from different sections of core.

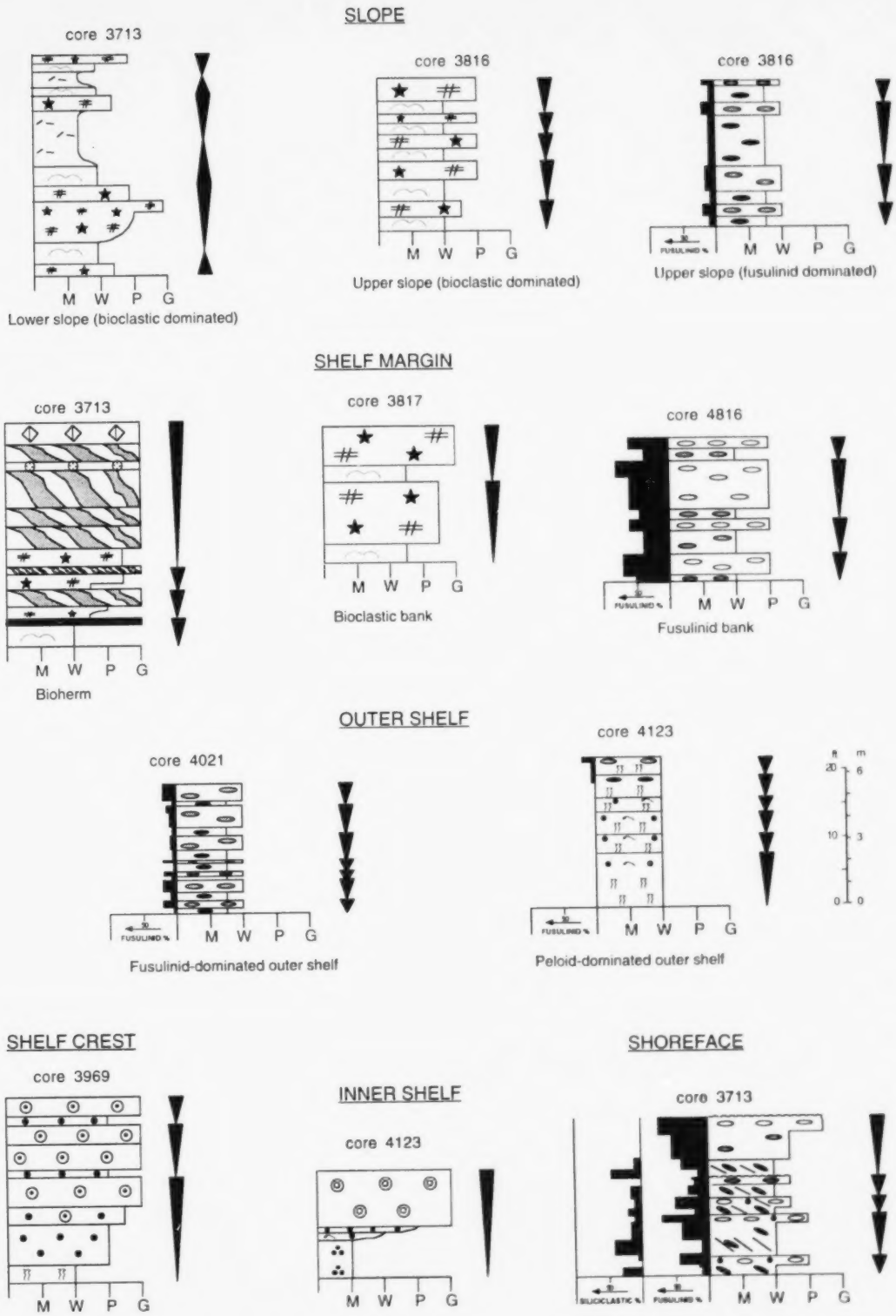

Figure 2.6: Facies associations (cont.)

ground for a later one will be creating an environment that is more favorable to the survival of another species than to itself, a process that is contrary to the principle of natural selection. Therefore, the zonation in a reef sequence is probably the product of autogenic successions (ecological) and allogenic processes such as variations in water turbulence and changes in sea level.

The stenohaline biota that characterize this facies association indicates well oxygenated, clear waters, probably about 30 m deep at the lower part of the buildups (pioneer stage) to about 20 m during the diversification stage in the upper part. The latter depth estimation is based on geometric observations made by Crawford (1981, 1989) on the Goat Seep Dolomite outcrops, a reef with similar characteristics in the Delaware Basin. This paleodepth interpretation is supported by the fact that the top of the reef during the diversification stage was dominated by delicate branching calcareous sponges and bryozoa that could only survive in low to moderate energy conditions, below fairweather base action.

Fusulinid Bank

This assemblage is composed, in ascending order, of bioturbated fusulinid-peloid wackestones (facies 8) and fusulinid packstone/grainstones (facies 9)(Fig. 2.6). Locally, however, peloid-pellet packstone/grainstones may cap this association (facies 10). Individual small-scale cycles are up to 6 m thick. This association was deposited between the fairweather wave base and the storm wave base (10-30 m deep). When capped by thin peloid-pellet grainstone/packstones, this facies association reached agitated water conditions above fairweather wave base (< 10 m). Sonnenfeld and Cross (1993) suggested that similar fusulinid packstones and grainstones in San Andres Formation were deposited at approximately 20 m (+/- 5 m) based on the 10-30 m depth range for autochthonous fusulinid growth estimated by Ross (1983).

Outer Shelf Facies Associations

The outer-shelf was characterized by muddy sediments that were rich in fusulinids and peloids. These sediments were deposited in a relatively shallow setting below fairweather wave base (up to 20-30 m deep) behind the shelf margin. The fusulinid-dominated outer shelf and peloid-dominated outer shelf associations formed on this part of the shelf.

Fusulinid-Dominated Outer Shelf

This association is formed of asymmetric small-scale cycles that are composed of peloid-fusulinid mudstones (facies 7) overlain by bioturbated fusulinid-peloid wackestones (facies 8)(Fig. 2.6). Rare scour surfaces in these sediments suggest that deposition was above storm-wave base. This vertical succession of facies is virtually identical to the upper slope fusulinid-dominated facies association and can be only distinguished from the latter because of the position of the outer shelf between the shelf margin and the shelf crest.

Peloid-Dominated Outer Shelf

This association is characterized by small-scale asymmetric cycles composed of vertically burrowed peloid-bivalve-crinoid wackestones (facies 11) that grade upward into a peloid-pellet packstone/wackestones (facies 10)(Fig. 2.6). These cycles may be capped by thin ooid-peloid grainstone beds (up to 1 m) that contain scattered bioclasts and intraclasts (facies 12). Locally, however, the lower part of the cycles are formed of massive very-fine grained quartzarenites (facies 15) or sandy peloid-bioclastic wackestones (transition between facies 10 and facies 15).

Deposition of peloid-bivalve-crinoid wackestones took place during the initial transgressive stage at relatively shallow depths (perhaps < 10-20 m). This initial transgression was followed by a progradational unit composed of peloid packstones and rare ooid grainstones that were deposited in very shallow water (< 10 m). Locally, some of the deposits were periodically exposed. The presence of terrigenous sediments at the base

of some cycles indicates that the siliciclastics were transported into the shallow shelf during lowstands of sea level and subsequently reworked during the next transgression (Bebout, 1991; Borer and Harris, 1991).

Shelf Crest Facies Association

This association represents that part of the shelf which was characterized by abundant non-skeletal grains such as ooids, peloids, intraclasts, and pisoids. Bioclasts were limited to bivalves and scattered fusulinids, crinoids, and unidentified fragments. Siliciclastic influx was common. The lack of a shallow shelf margin favored the development of shallow-water ooid-shoals ~ 2 km landward of the shelf margin.

Asymmetric, upward shallowing ooid-rich cycles, which formed bars on the shelf crest, eventually prograded over the outer-shelf sediments. The basal facies of these cycles is composed of thin intervals of peloid-pellet packstones (facies 10) or massive very fine-grained quartzarenites (facies 15) that underlie locally cross bedded ooid grainstones (facies 12)(Fig. 2.6). Ooid grainstones, up to 5-6 m thick, were probably deposited in agitated shallow waters (less than 5 m deep). Locally, however, supratidal features indicate that the ooid shoals were periodically emergent. This paleodepth interpretation is based on comparison with modern ooid-shoal deposition on the Great Bahama Bank and the Persian Gulf (e.g., Purser and Evans, 1973; Halley et al., 1983; Harris, 1984; Hardie and Shinn, 1986).

Inner Shelf Facies Association

Inner shelf sediments, present on the western part of the field, are formed of small-scale, shallowing-upward cycles that are characterized by a basal fusulinid-peloid wackestone or a vertically burrowed wackestone (facies 8 and 11 respectively) overlain by a laminated peloid mudstone with spherical fenestrae (facies 14). These cycles are capped by parallel bedded, pisoid-peloid-ooid-intraclast packstone/grainstones with supratidal features (facies 13)(Fig. 2.6). These cycles were deposited in protected, shallow subtidal to

supratidal environments on the leeward side of the ooid shoals that formed on the shelf crest.

Shoreface Facies Association

This association, found only in core 3713, consists of six asymmetrical small scale, shallowing-upward cycles (Fig. 2.6). Each cycle is composed of a cross-bedded, sandy fusulinid-peloid wackestone (facies 16) that grades upward into a slightly sandy, fusulinid packstone/grainstone or a locally cross-bedded, peloid packstone with conspicuous blackened grains (facies 9 and 10 respectively). Locally, fusulinid packstone/grainstones are brecciated (i.e. pitholes, 4-5 cm in diameter) and show oxidation traces which suggest karst development. These packstone/grainstones were probably deposited on the upper shoreface and were exposed during sea-level falls (i.e., karst evidences). Cross-bedded wackestones were probably deposited on the lower shoreface (< 20 m deep) under the action of storms. The base of this shoreface association overlies an unconformable surface and contains large pebbles eroded from this surface. Similar sharp-based shoreface associations are common in siliciclastic environments in the Cardium Formation of Alberta, and were formed by fairweather wave erosive processes during falling sea level (Plint, 1988).

Regional Unconformities and Discontinuities

The Grayburg Formation at North McElroy Field is characterized by four unconformities and one discontinuity. These bounding surfaces can be traced across the field and mark major changes in sedimentation styles.

Unconformity A

Unconformity A, the contact between the San Andres and the Grayburg formations, can be traced for about 1.5 km from wells 4123 to 3939 (Fig. 2.7). Along this surface there is evidence of subaerial erosional truncation marked by a conspicuous karst surface with breccias and fractures that locally extend more than 10 m below the surface. This

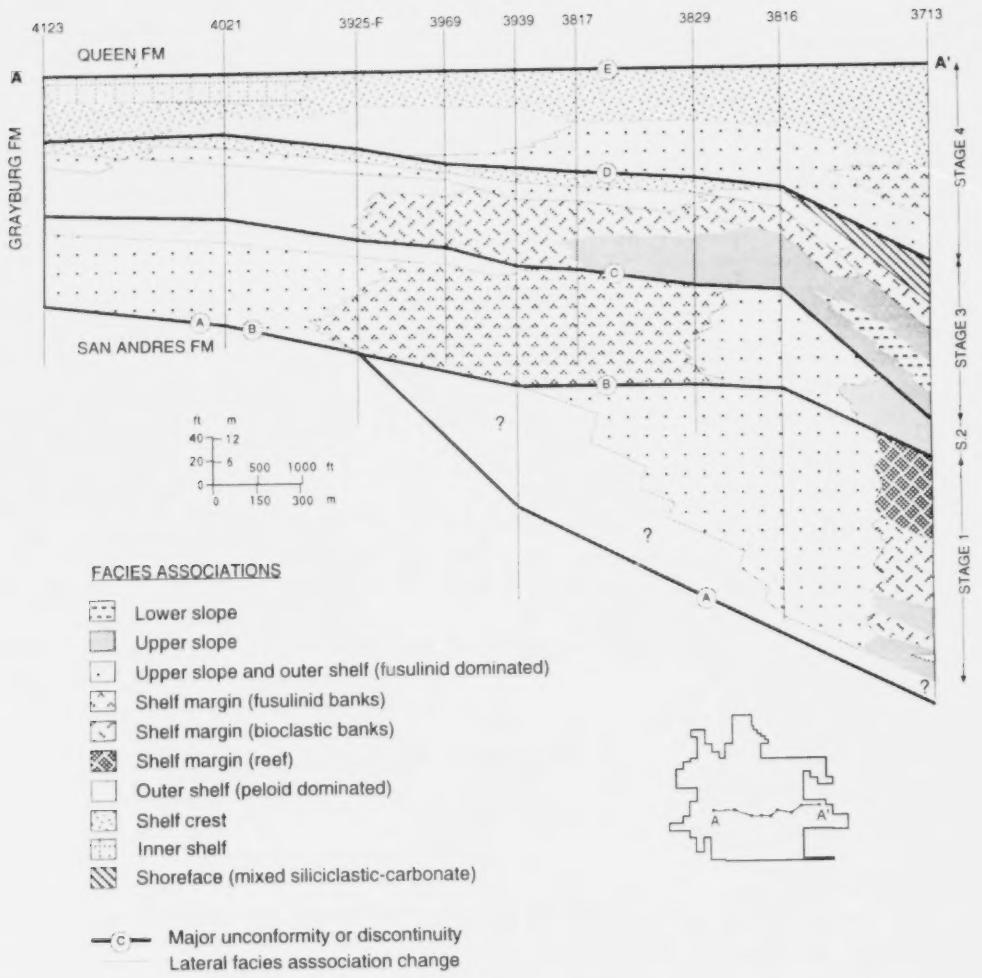

Figure 2.7: Dip-oriented cross section AA' showing the lateral and vertical distribution of facies associations in the Grayburg Formation. Platform evolution occurred in four stages marked by major unconformities and discontinuities. Unconformity E is the datum.

surface is characterized by an abrupt change in slope between wells 3925-F and 3939; the estimated relief of the unconformity between these two wells is about 30 m over a distance of 500 m.

Discontinuity B

This surface does not show any evidence of subaerial truncation. Instead, this discontinuity is marked by a distinct change in facies associations that indicate a sudden deepening. In core 3713 (Fig. 2.7), for example, the bioherm facies association is abruptly overlain by the upper slope facies association. In this core the discontinuity is represented by a hardground that indicates little or no deposition. Discontinuity B merges landward with unconformity A (Fig. 2.7).

Unconformity C

Unconformity C, which extends across the entire field, is characterized by a basinward shift in facies associations. This is particularly true between wells 3939 and 3816 (Fig. 2.7) where fusulinid-bearing facies associations are abruptly overlain by upper slope associations without fusulinids. Between wells 4123 and 3969, the unconformity is on top of outer shelf facies associations dominated by peloids deposited in shallow waters (< 10m). No clear evidences of exposure was found along this unconformity.

Unconformity D

This unconformity can be correlated across the entire field. In the past, this boundary was used as a datum line for stratigraphic correlations (Longacre, 1980). Between wells 4123 and 3816 this surface is on top of ooid-rich sediments (shelf crest) that mark a basinward shift in facies (Fig. 2.7). Between wells 3816 and 3713 the unconformity is on top of a mixed carbonate-siliciclastic shoreface facies association. This unconformity is easily recognizable because of the lateral continuity of the ooid interval, the abrupt change in facies, and the incursion of siliciclastic sediments. Moldic and vuggy

porosity occurs 15-20 m below the unconformity and is probably related with karst processes.

Unconformity E

Unconformity E, the contact between the Grayburg and the Queen formations, is at the base of a thick sandstone that can be traced across the entire field (Fig. 2.7). This sandstone overlies inner shelf and shelf crest facies associations that were deposited in a shallow subtidal to supratidal setting. Karst is only locally developed in inner shelf sediments (i.e., caliche crusts).

Platform Evolution

The regional unconformities and discontinuities in the Grayburg Formation separate carbonate platforms formed during four stages. Each stage or shelf is composed of different facies associations.

Stage 1: Narrow Shelf with Shelf-Edge Reef and Fusulinid Banks.

This shelf was characterized by the bioclastic bank, bioherm, fusulinid bank and fusulinid-dominated outer shelf facies associations (Figs. 2.7 and 2.8). This shelf, which developed above the San Andres-Grayburg unconformity during a continuous transgression, attained a maximum width of 1.5 km (Fig. 2.7). The shelf margin is marked by a vertical succession of the bioclastic bank association (lower part) and the bioherm association (upper part)(Fig. 2.7). Simultaneously to the south, the shelf margin was dominated by fusulinid banks (Fig. 2.8). The bioherm facies association represents a submerged shelf-edge reef (perhaps 20 m deep), which allowed a good water circulation across the outer shelf. Vertical accretion of the shelf-edge reef was probably controlled by the relative position of the fairweather and/or storm wave base. In a modern analog, Blanchon (1995) suggested that hurricanes have a considerable impact on the vertical accretion of modern shelf-edge reef around Grand Cayman in the Caribbean. However,

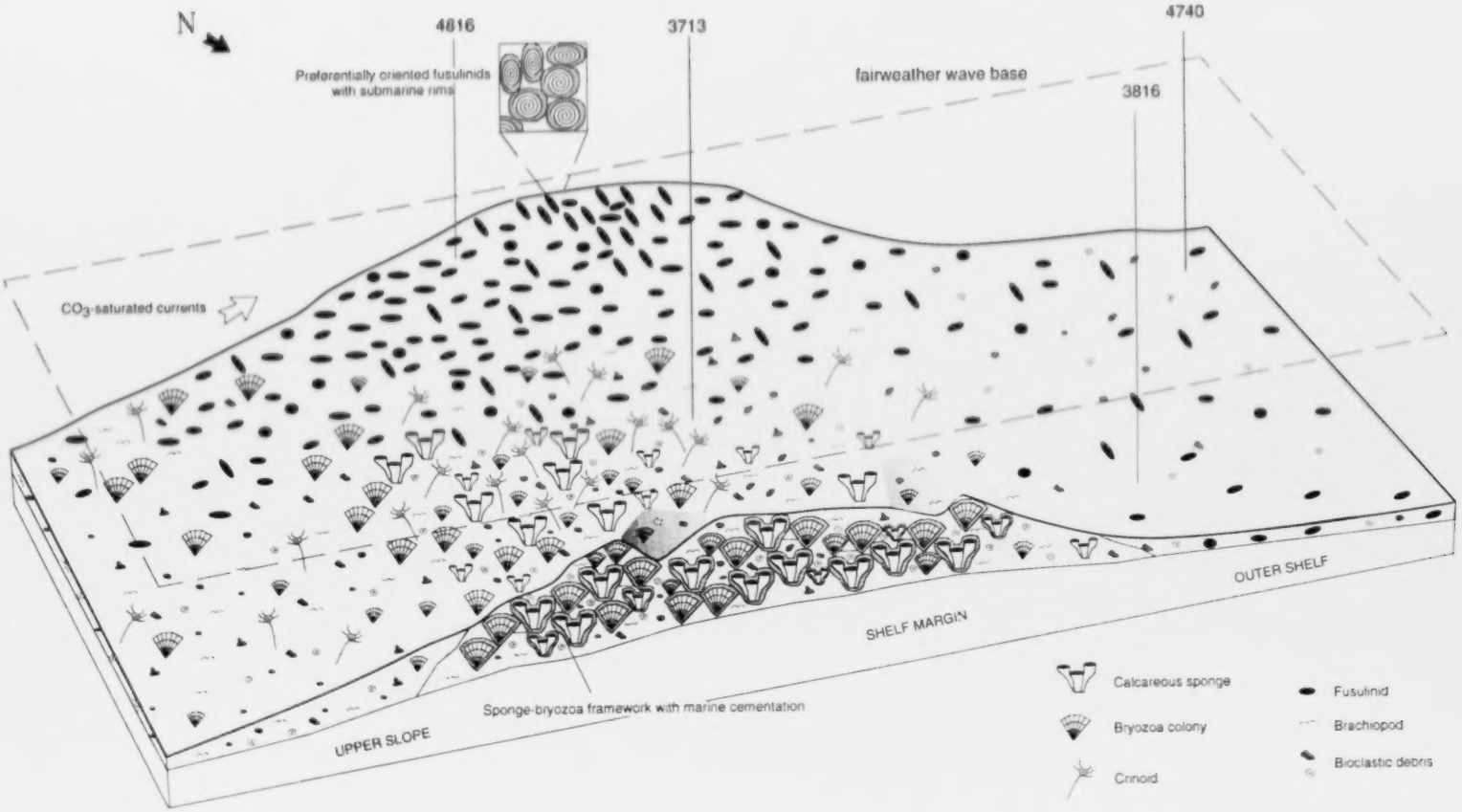

Figure 2.8: Schematic paleoenvironmental reconstruction of facies distribution and geometry of a cemented shelf-margin. The shelf margin is dominated by fusulinid banks or bioherms. Four cores indicate the relative position of the shelf in the field.

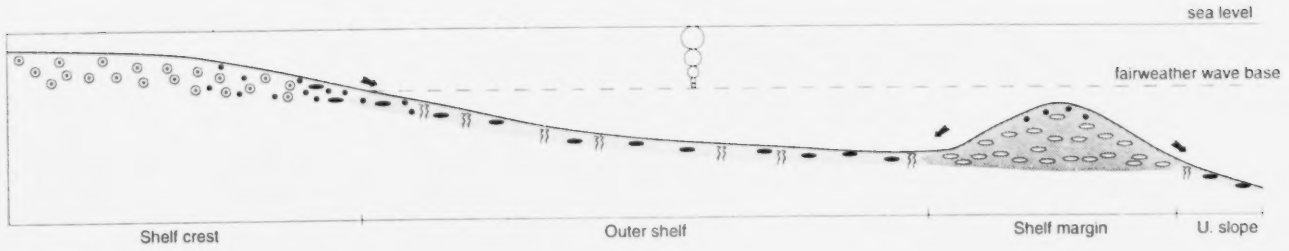

Figure 2.9: Schematic diagram showing relationships and relative position of facies associations along a shelf with a shelf margin dominated by fusulinid banks. Facies symbols in figure 2.7.

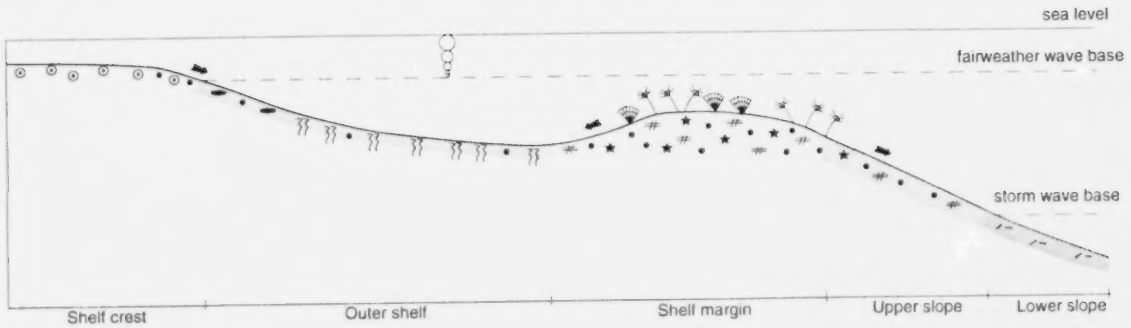

Figure 2.10: Schematic diagram showing relationships and relative position of facies associations along a shelf with a shelf margin dominated by bioclastic banks. Facies and biota symbols in figures 2.7 and 2.8.

factors like depth preferences of the reef biota and hypersaline shallow waters on the shelf may be additional factors that influenced the vertical distribution and occurrence of Permian shelf-edge reefs (Read, 1985).

Stage 2: Aggradational Shelf with a Fusulinid-Bank Shelf Margin

The carbonate shelf developed during this stage is located between discontinuity B and unconformity C (Fig. 2.8). In this aggradational shelf, the shelf margin setting is dominated exclusively by fusulinid banks, probably deposited at a similar paleobathymetry to that of the bioclastic banks and bioherms of the precedent shelves. The outer shelf was formed of fusulinid wackestones in its basinward portion and by vertically burrowed wackestones and peloid packstones upslope, close to the shelf crest (Fig. 2.9).

Stage 3: Shelf with a Bioclastic-Bank Shelf Margin

Five facies associations formed on this shelf. The shelf is bounded by two platform wide unconformities (unconformities C and D; Fig. 2.7). The lower and upper slope associations accumulated basinward of the bioclastic bank association that formed on the shelf edge (Fig. 2.10). Landward of the bioclastic banks, the outer shelf association (up to 1 km wide) was composed of vertically burrowed wackestones and peloid packstones. Thin, shallow-water ooid shoals formed on the shelf crest. The geometry shows that this type of shelf was an aggradational to progradational platform (Fig. 2.7) where the bioclastic bank at the shelf margin was probably below fairweather wave base.

Stage 4: Progradational Shelf with a Fusulinid-Bank Shelf Margin

The facies packages of this shelf are bounded by unconformity D and E. During the initial period of development, this shelf was aggradational and similar to the shelf of stage 2 (Fig. 2.7). The geometry, however, is strongly progradational during the late part of stage 4 where thick ooid shoals advanced over outer shelf sediments.

Synopsis

1) The Upper Permian Grayburg Formation, in the North McElroy Field, is composed of seventeen depositional facies that belong to six facies associations. In order of decreasing water depth these facies associations are the slope, shelf margin, outer shelf, shelf crest, inner shelf, and shoreface.

2) The slope facies associations are dominated by fusulinid-bearing or bioclastic-bearing muddy facies. This associations include burrowed peloid-fine skeletal debris mudstones and peloid-fusulinid mudstones deposited below storm wave action (> 30 m), and bioclastic wackestones to packstone/grainstones and bioturbated peloid-fusulinid wackestones deposited between fairweather and storm wave base (10-30 m).

3) The shelf margin facies association is dominated by bioclastic banks, fusulinid banks, or bioherms depending on geographic location. All these facies associations were probably deposited at similar water depths (< 30 m). Active reworking by waves and storms inhibited their vertical growth above fairweather wave base.

4) The outer shelf, which was covered by relatively deep water (< 30 m), is characterized by fusulinid-dominated and peloid-dominated facies associations. These associations are located seaward of the shelf crest facies association which comprisses ooid-rich sediments deposited in agitated, shallow waters (< 10 m). The inner shelf facies association, located behind the shelf crest, is composed of sediments that show evidences of restricted shallow-subtidal deposition and supratidal conditions.

5) Carbonate shelves in the Grayburg Formation developed during four stages and are separated by regional unconformities and discontinuities. A narrow shelf with shelf-edge reefs and fusulinid shoals developed during the first stage. During the second stage fusulinid-bearing sediments on the shelf margin, outer shelf, and slope facies associations characterized the shelf. Stage 3 is dominated by a shelf

with a bioclastic bank on the shelf margin; the outer shelf and slope facies associations are composed of bioclastic and peloid-rich sediments. During stage 4, the shelf is at first dominated by fusulinid-rich sediments that were lately substituted by ooid-shoals.

3. SEQUENCE STRATIGRAPHY AND CYCLOSTRATIGRAPHY

Introduction

Considerable attention has been focused on the origin and distribution of high-frequency cycles in carbonate platform successions (Goodwin and Anderson, 1985; Goldhammer et al., 1987; 1990; 1993; Koerschner and Read, 1989; Elrick and Read, 1991; Osleger and Read, 1991; Wright, 1992; Pomar, 1993; Sonnenfeld and Cross, 1993; Kerans et al., 1994; Pomar and Ward, 1994). Meter-scale shallowing-upward cycles (Wilson, 1975; James, 1984) or PACs (Goodwin and Anderson, 1985), the basic units in cyclostratigraphic analysis, are equivalent to siliciclastic parasequences (Van Wagoner et al., 1990) except that carbonate cycles may preserve transgressive units. These cycles are arranged into larger-scale cycles or parasequence sets (Van Wagoner et al., 1990) that commonly show similar attributes of depositional sequences. Many studies have concentrated on the stacking pattern of high-frequency cycles in order to identify third-order sequences and their component systems tracts across widely spaced outcrops on Paleozoic carbonate platforms (Elrick and Read, 1991; Osleger and Read, 1991; Goldhammer et al., 1993; Montanez and Osleger, 1993).

All the studies mentioned above are based on outcrops examples, especially in the Permian Basin (Kerans and Nance, 1991; Sonnenfeld, 1991; Sonnenfeld and Cross, 1993; Hovorka et al., 1993) where continuous outcrops permit the lateral tracing of important horizons. When cyclostratigraphy is applied to subsurface strata, as in North McElroy Field, correlation of some critical chronostratigraphic surfaces may be extremely difficult because of the lack of lateral continuity between wells. Therefore, a successful cyclostratigraphic analysis of subsurface carbonates can only be attained with a detailed description of vertical facies variability, a rigorous hierarchical system of cycles and bounding surfaces, and the use of electric logs. In addition, the strong offlapping relations observed in other Guadalupian formations in outcrops (Sonnenfeld, 1991) have to be considered in order to avoid unreal "layer-cake" correlations in the Grayburg Formation.

The objectives of this chapter are to 1) describe the lateral and vertical characteristics of depositional sequences, systems tracts and high-frequency cycles; 2) evaluate the mechanisms that controlled facies distribution and cycle formation, and 3) evaluate the relation between facies and cycles distribution, sea-level history and stratigraphic distribution of the reservoir rocks.

Sequence Stratigraphy and Description of Systems Tracts

The Grayburg Formation in the North McElroy field is composed of a single third-order sequence that accumulated over 1.3 m.y. (Ross and Ross, 1987; Fig. 1.3). This sequence is composed of a conformable succession of genetically related high-frequency cycles that are bounded by two sequence boundaries (Fig. 3.1). The lower boundary, which is the contact between the Grayburg and San Andres formation's is unconformity A which denotes a period of prolonged karst development (Figs. 2.7 and 3.1). The upper sequence boundary (unconformity E, Figs. 2.7 and 3.1), the base of the Queen Formation, is located at the base of a thick sandstone that was probably deposited during a relative fall of sea level which brought about a basinward shift of the facies.

The depositional sequence between unconformities A and E includes at least 106 sixth-order cycles (average of ~ 12,000 years), 23 fifth-order cycles (average of ~ 57,000 years) and 3 fourth-order cycles (average of ~430,000 years). These cycle orders are based on the hierarchical system of Vail et al. (1991) hierarchical system. Although the average cycle duration was obtained by dividing the duration of the formation by the number of cycles, it does not imply that each cycle was actually of the same duration. In addition, these calculations are in part restricted by the fact that the lower sequence boundary was not recognized in the thickest part of the depositional sequence (core 3713) which leaves out additional cycles deposited below cycle 1 (Fig. 3.1).

The vertical stacking patterns of high-frequency cycles (fifth-order) that are composed the third-order sequence were analyzed in order to identify internal bounding surfaces and the systems tracts that form the main depositional sequence (Fig. 3.2). As a

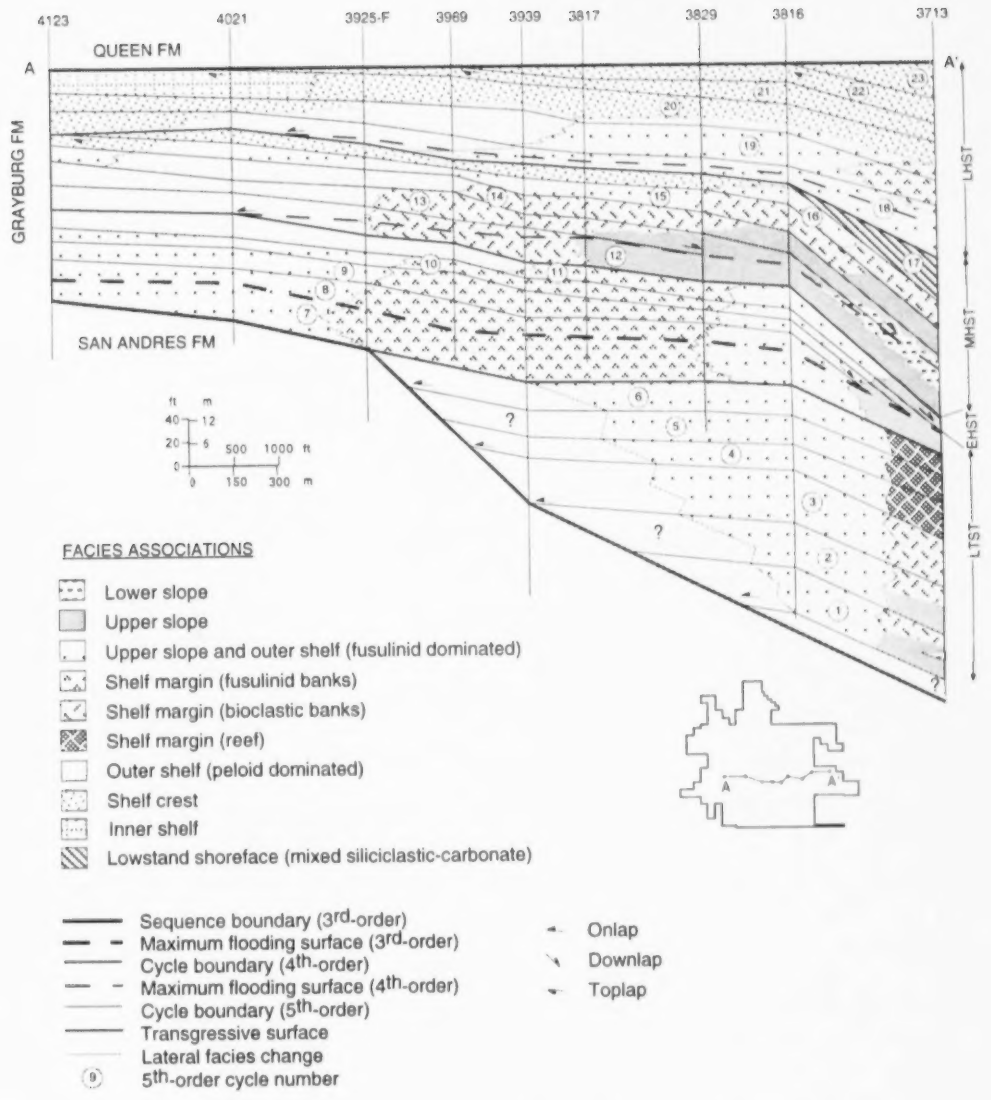

Figure 3.1: Dip-cross section AA' in North McElroy Field outlining the sequence stratigraphic framework of the Grayburg Formation. This section shows the distribution of fifth-order cycles, geometry of the constituent systems tracts, and sequence boundaries and maximum flooding surfaces of different orders. LTST= lowstand/transgressive systems tract; EHST= early highstand systems tract; MHST= middle highstand systems tract; LHST= late highstand systems tract.

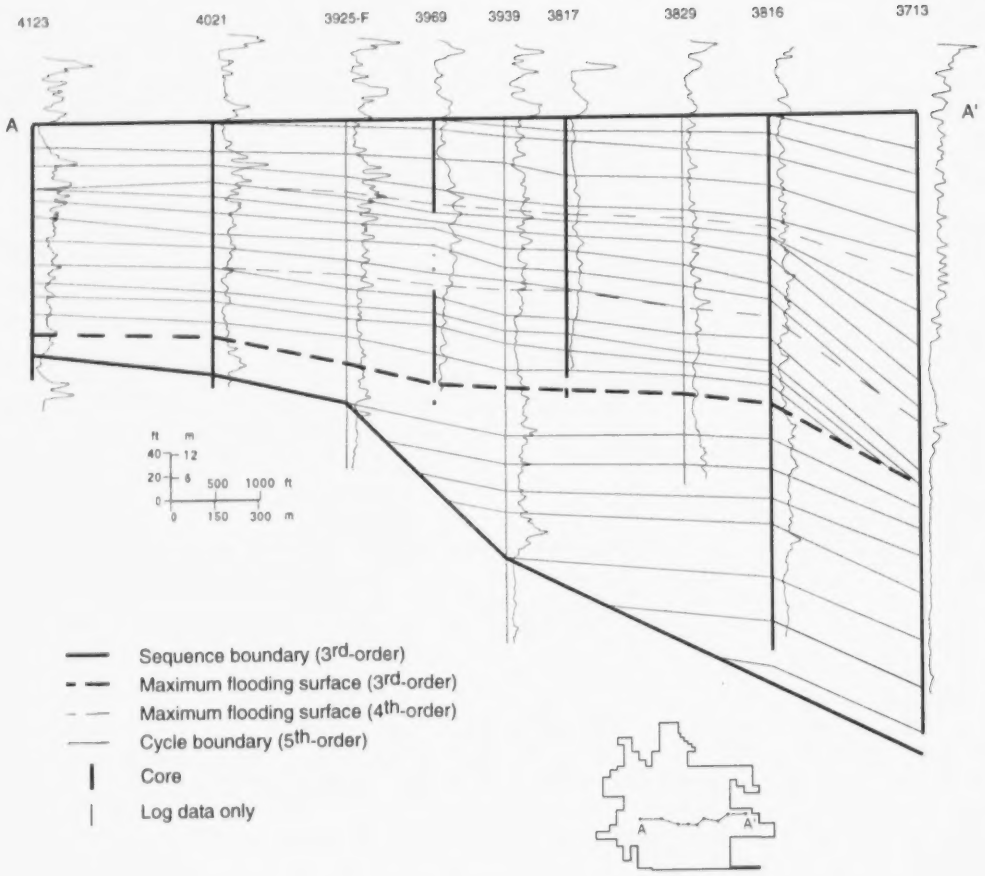

Figure 3.2: Interpretation of the dip-oriented cross-section AA'. This section displays the extend of core analyzed and the gamma-ray logs used. Discontinuities of different orders were correlated using meter-scale core logging and gamma-ray response.

result, a lowstand/transgressive systems tract and a highstand systems tract formed during specific positions of sea level were recognized.

Lowstand/Transgressive Systems Tract (LTST)

The lower boundary of this systems tract is the sequence boundary whereas its upper boundary is the maximum flooding surface (Fig. 3.1). This systems tract is composed by fifth-order cycles 1 to 7 (Figs 3.1). The sequence boundary (unconformity A, Fig. 2.7) or its correlative surface was not identified in cores on the basinward section of the system tract. Therefore, cycle 1 does not necessarily represent the first cycle of deposition following the development of unconformity A. Strata geometry is aggradational/weakly progradational (cycles 1 to 6) to retrogradational (cycle 7) and onlaps onto the sequence boundary in a landward direction (Fig. 3.1).

No distinction was made between the lowstand systems tract (LST) and the transgressive systems tract (TST) because the position of the transgressive surface (discontinuity B), which represents the upper limit of the lowstand systems tract, is uncertain. This surface, however, was tentatively placed on top of cycle 6 (Fig. 3.1). The transgressive surface on top of the sponge-bryozoa framestones (cycle 6) is a hardground or hiatal surface that is overlain by peloid-bioclastic wackestones that formed in an upper slope setting. This facies pattern records a sudden increase in water depth caused by a landward stepping of the shoreline.

The maximum flooding surface of the shelf is recorded on top of cycle 7 (Figs. 3.1 and 3.13B) where lower-slope bioturbated mudstones with peloid and fine skeletal debris (facies 1) extend landward. Cycle 7 in core 3713 (above discontinuity B) is composed of at least four sixth-order cycles that involved the enigmatic structures described as *Archaeolithoporella* bedded bindstones (facies 5). These "bindstones" may be a combination of inorganic marine lithification and organic structures (algae) that probably formed under conditions of slow sedimentation. The presence of this facies in cycle 7 may represent a succession of condensed intervals which suggest a *maximum flooding interval*

(Elrick and Read, 1991; Montanez and Osleger, 1993) rather than a single surface. For correlation purposes, however, the maximum flooding surface was placed on top of cycle 7. Landward in core 4123 (Fig. 3.1), the maximum flooding surface is on top of a 3 m-thick sixth-order cycle, which is interpreted to record the maximum of accommodation on this part of the shelf.

Highstand Systems Tract (HST)

This systems tract is formed by fifth-order cycles 8 to 23. These cycles were grouped according to their vertical stacking, facies associations, bounding surfaces and aggradation/progradation geometry into the early (stage 2), middle (stage 3) and late highstand systems tracts (stage 4)(Figs. 2.7 and 3.1). Each division in this highstand systems tract, is separated by platform-wide unconformable surfaces that represent high-frequency relative sea-level falls (unconformities C, D, and E; Fig. 2.7). These are fourth-order unconformities which bound fourth-order cycles or high-frequency depositional sequences (Mitchum and Van Wagoner, 1991).

Early Highstand Systems Tract (EHST)

The early highstand systems tract (stage 2) is composed of cycles 8 to 11 (Fig. 3.1). Cycles 8 to 10 are highly aggradational (sigmoid pattern) and downlap on the maximum flooding surface in a seaward direction. Shelf margin facies are dominated by bedded fusulinid packstones and grainstones (facies 9) that have a significant mounded topography (Fig. 3.1; cycles 8 and 9 between wells 3925-F and 3939). Upper slope sediments are composed of bioturbated fusulinid-peloid wackestones/mudstones (facies 8 and 7) whereas lower slope sediments include bryozoa-brachiopod-crinoid biostromes (facies 2 and 3). The relatively deep, wide outer shelf was characterized by the deposition of fusulinid wackestones and mudstones, and peloidal sediments.

Cycle 11, which marks the end of the EHST, is progradational and records a significant decrease in the proportions of outer-shelf fusulinid-bearing sediments relative to

peloid-rich facies. Abundant peloid-pellet packstone/grainstone facies (facies 10) suggest a shallowing of the outer shelf to, or within the realm of fairweather wave action. This upward-shallowing in cycle 11 indicates a decrease in the accommodation space produce by a fourth-order relative sea level fall superimposed on the long-term third-order decrease in accomodation. The top of cycle 11 is characterized by an abrupt change in facies from fusulinid-bearing sediments on the margin and upper slope to bioclastic-bearing deposits (unconformity C, Fig. 2.7).

Middle Highstand System Tract (MHST)

The middle highstand systems tract (stage 3) is characterized by sigmoidal (cycles 12-13) to sigmoid/oblique clinoforms (cycles 14-17). The high-frequency maximum flooding surface (fourth-order) is in cycle 12; only cycle 13 downlaps this surface between cores 3816 and 3713 (Fig. 3.1). During the aggradational stage, clinoforms on the outer shelf were composed of vertically burrowed peloid wackestones that grade upslope into peloid-bivalve packstones (facies 11 and 10 respectively). The shelf margin is dominated by massive bioclastic packstone/grainstone facies (facies 3), deposited between the faiweather and storm wave base, that grade downslope into burrowed peloid-bioclastic wackestones (facies 2; upper slope) and fine bioclastic mudstones (facies 1; lower slope). Cycles 15-17 are strongly progradational (downstepping) and were governed by a high-frequency stillstand and fall of relative sea level (fourth-order). Outer shelf facies associations in this offlapping or progradational package, are formed of burrowed fusulinid wackestones; they pass upslope into shelf-crest ooid-peloid grainstones (facies 12).

Shelf crest ooids almost reached the shelf margin position in cycle 16, when the outer shelf was reduced to a width of about 300 m because of the progressive decrease in accommodation space (Fig. 3.1). Subaerial exposure and truncation (unconformity D; toplap of cycle 15) of shelf-crest sediments took place simultaneously on the landward part of the platform as a result of a fourth-order relative sea-level fall. Siliciclastic-rich facies are

common below unconformity D and they are located at the bottom of fifth and sixth-order cycles (cycle 15, Fig. 3.13A).

By the time of deposition of cycle 17, the entire platform was completely exposed and the carbonate factory was restricted to a narrow shoreface that developed along the previous shelf margin (Fig. 3.1). Siliciclastic sands were transported onto the new shelf, either by eolian mechanisms or by sporadic floods during high-frequency lowstands (fifth and sixth-order). In this new shelf the carbonate factory fully recovered during high-frequency highstands where fusulinid grainstone/packstone facies and peloid packstones were the norm on the shoreface (Fig. 2.6). The top of cycle 17 is the continuation of the fourth-order cycle boundary (unconformity D) that is at the same time the transgressive surface of erosion of the overlying fourth-order cycle (late highstand systems tract). Cycles with similar characteristics to cycle 17 which are formed during sea-level falls, have been referred as "forced regressive wedge systems tract" (Hunt and Tucker, 1992), "forced regressive parasequences of the lowstand systems tract" (Posamentier et al., 1992) or "offlapping systems tract" (Pomar and Ward, 1994).

Late Highstand Systems Tract (LHST)

Composed of cycles 18 to 23, the late highstand systems tract (stage 4) records the end of the third-order sequence in the Grayburg Formation. These cycles display a sigmoid to sigmoid/oblique progradational pattern, that is related to a fourth-order stilltand and fall of sea level superimposed on a relative long-term sea-level fall (third-order). The fourth-order maximum flooding surface is in cycle 18; no downlapping is observed onto the maximum flooding surface (Fig. 3.1). The upper sequence boundary (unconformity E) is well defined by the presence of 1) toplap of at least three cycles (cycle 20, 21 and 22), 2) decrease in cycle thickness toward the sequence boundary as a response to the progressive decrease in accommodation space, and 3) deposition of a thick sandstone (base of the Queen Formation) in response to a third-order fall of sea level.

The facies distribution is similar to that in the early highstand systems tract, where fusulinid packstone/grainstone facies dominated the shelf margin and a wide outer shelf existed (cycles 18 and 19). Prograding ooid shoals (shelf crest), however, reached the shelf margin by the end of cycle 20 (Fig. 3.1) when the entire shelf was covered by water that was probably less than 10 m deep. Siliciclastic sediments reached the position of well 3713 during cycle 21 (Fig. 3.13B) and spilled over the slope and into deeper environments. Deposition of fusulinid-rich sediments was probably restricted to the upper slope, just downslope of the ooid shoals.

The geometrical and sedimentological characteristics of cycle 23 suggest that it may have been deposited as part of a fourth- to third-order offlapping systems tract (Pomar and Ward, 1994) similar to cycle 17 in the middle highstand systems tract. In cycle 23, siliciclastic-rich sediments interbedded with burrowed bryozoa-brachiopod wackestone/packstone facies (facies 17) grade upward into peloid packstones and grainstones. The loss of ooids is probably related to the dramatic decrease of the flooded area on the shelf within a suitable depth for the massive formation of these allochems.

Cyclostratigraphy: Internal Architecture of Fifth- to Sixth-Order Cycles

Fifth-order cycles are composed of vertically stacked small-scale shallowing-upward cycles that are herein considered to be sixth-order cycles. Fifth-order cycles show similar stratal attributes of depositional sequences, including maximum flooding surfaces and transgressive/regressive successions. The fifth-order cycles are divided into 1) asymmetrical shallowing-upward cycles, 2) symmetric cycles characterized by an initial deepening upward followed by a regressive succession of sixth-order cycles, and 3) asymmetrical deepening-upward cycles. The first two types of cycles are bounded by a fifth-order unconformity or by a marine flooding surface. The third cycle is capped by a fifth-order maximum flooding surface.

In order to show the internal geometry of sixth- and fifth-order cycles, three examples selected from the depositional sequence are described below.

Cycle 19

This cycle part of the late highstand systems tract, is composed of a vertical stacking of retrogradational to aggradational sixth-order cycles (Fig. 3.3). Retrogradational cycles 19A and 19B form the fifth-order transgressive hemicycle (high-frequency transgressive systems tract) that is capped by the maximum fifth-order flooding surface. The sixth-order cycles that formed the regressive hemicycle have a similar thickness and do not downlap the maximum flooding surface. At the shelf crest, cycle 19 is asymmetric shallowing-upward and only at the outer shelf and shelf margin is symmetrical. Due to the aggradational geometry observed, the outer shelf remained a wide and relatively deep depositional setting (1.5-2 km wide and 20-30 m deep) throughout the entire deposition of cycle 19 (Fig. 3.4).

Sixth-order cycle 19C is the basal unit of the regressive hemicycle and overlies the fifth-order cycle boundary of cycle 18 in a landward direction and the maximum flooding surface basinward (Fig. 3.5). The internal distribution of facies in cycle 19C records a characteristic asymmetric shallowing-upward across the entire platform with relatively a thick upper part only at the shelf crest (peloid packstones; core 4021) and shelf margin (fusulinid packstone/grainstones; core 3713). Massive quartzarenite deposited on the outer shelf, dominate the lower part of cycle 19C between cores 4123 and 4021 indicating a bypass of siliciclastic sediments along the exposed shelf during the preceding fifth-order sea level fall (top of cycle 18). The terrestrial signature of these siliciclastic deposits was destroyed during the subsequent rising sea level that reworked the sediments. Basinward, the lower part of cycle 19C was dominated by outer shelf facies composed of vertically burrowed wackestones and fusulinid mudstone/wackestone facies. The lower part of cycle 19C across the platform is interpreted as the early sixth-order highstand (e.g., deeper facies) whereas the upper part represents the late sixth-order highstand (e.g., shallower facies)(cf. Strasser, 1991).

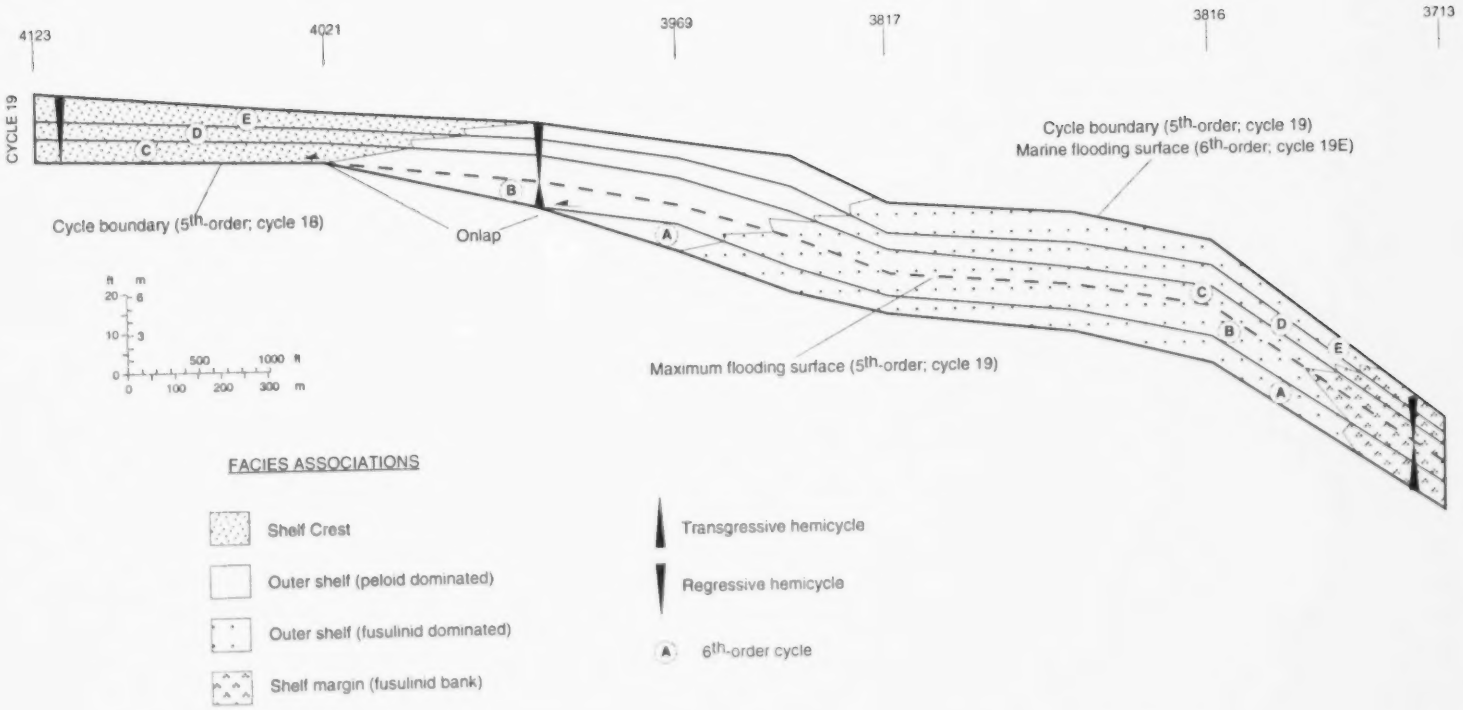

Figure 3.3: Internal architecture of fifth-order cycle 19 showing facies associations distribution, transgressive-regressive hemicycles, and discontinuities.

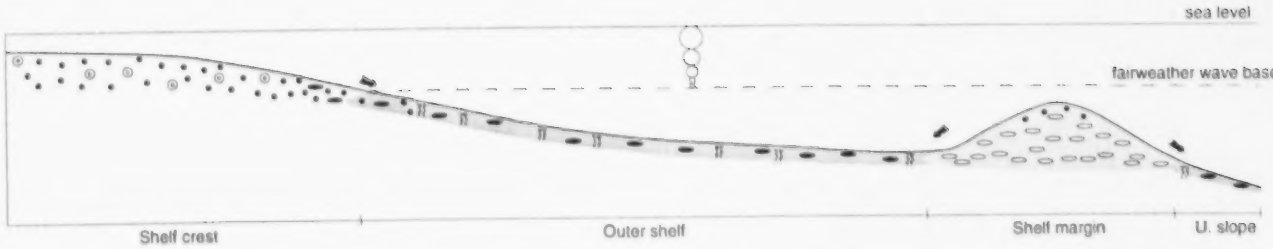

Figure 3.4: Schematic diagram showing depositional characteristics of cycle 19. The outer shelf was relatively deep and wide. Peloids were more abundant than ooids on the shelf crest which suggests relatively deep conditions or a narrow shelf crest unsuitable for ooid formation. Facies symbols in Figure 3.4.

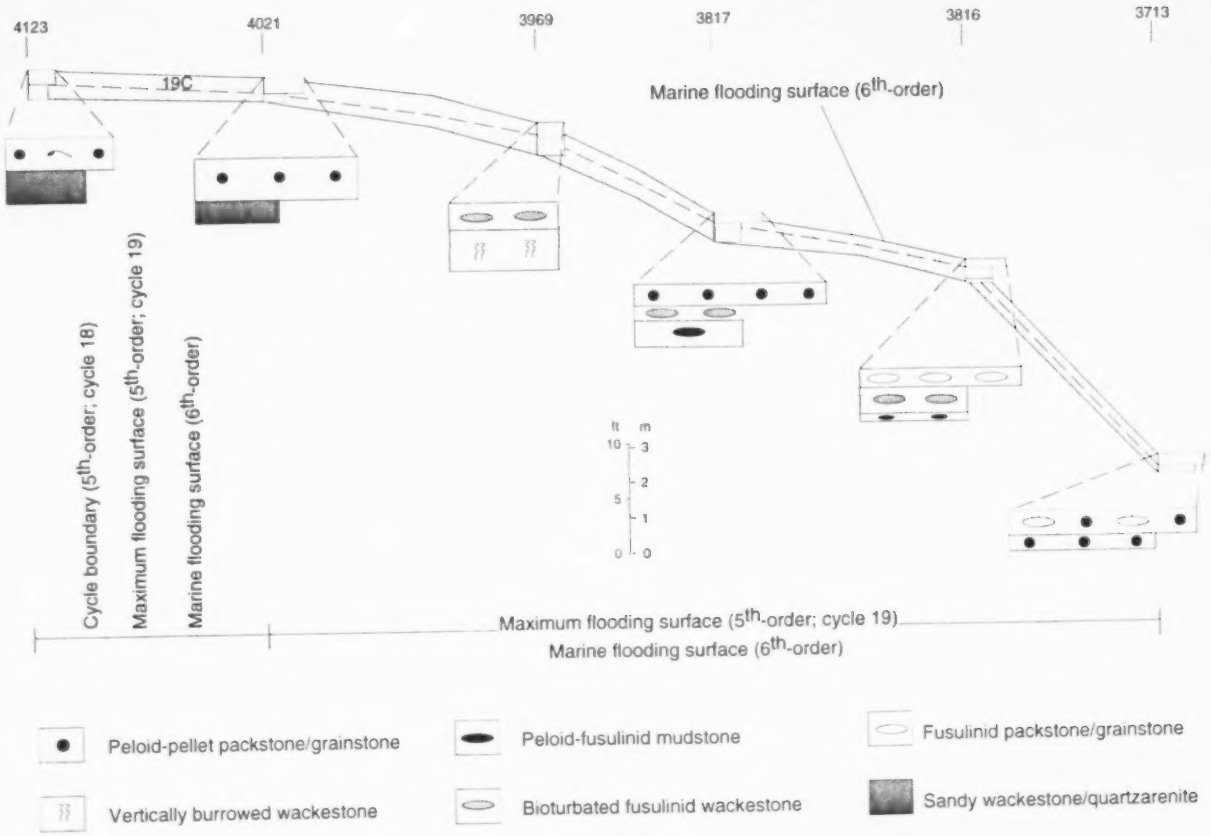

Figure 3.5: Internal architecture of sixth-order cycle 19C. The dotted line indicates the interpreted limit between the early (below) and late (above) sixth-order highstand. The cycle is asymmetric shallowing-upward along the entire clinoform.

Cycle 20

The cycle, composed by six sixth-order cycles, has a retrogradational to strongly progradational internal pattern (Fig. 3.6). The transgressive hemicycle capped by the fifth-order maximum flooding surface is composed of cycles 20A to 20C which onlap the upper boundary of the underlying cycle. Localized patch reefs grew just upslope of the shelf margin on the omission surface created during the maximum flooding. Prograding ooid shoals advanced seaward over the entire outer shelf by the time of deposition of cycle 20E, eventually reaching the position of the former shelf margin that was dominated by fusulinid-rich sediments (Fig. 3.6 and 3.7). Toplap observed in cycle 20F occurred by nondeposition and bypass of siliciclastic sediments during a relative fifth-order sea level fall, associated with formation of supratidal features. Between wells 3925F and 4123 (Fig. 3.6) in the inner shelf setting, cycles 20D and 20E are divided into two more cycles or bedsets which are difficult to correlate basinward. Deposition of cycles 20E to 20F occurred in a very shallow shelf above fairweather wave base (perhaps less than 10 m), probably similar to shelfedge sand bodies trending obliquely or normal to the bank edge in the Bahamas (Hine and Mullins, 1983).

Analysis of cycle 20E (Fig. 3.8) indicates that the clinoform reached well developed supratidal conditions associated with pisoid-peloid-ooid-intraclast packstone/grainstone facies (facies 13) with fenestrae, tepee structures, and sheet cracks in the proximity of well 4123. The shelf crest, mainly concentrated between wells 3969 and 3817, is indicated by thick parallel-bedded ooid-peloid grainstones. Between wells 3969 and 3817, sixth-order cycle 20E is formed of a relatively thin basal unit that is dominated by peloid and fusulinid packstones. This thin basal unit probably represents the deposition of early sixth-order highstand deposits. At the inner shelf, deeper conditions prevailed behind the shelf crest where laterally localized fusulinid wackestones (early sixth-order highstand) were deposited under relatively normal marine conditions. These fusulinid-bearing sediments

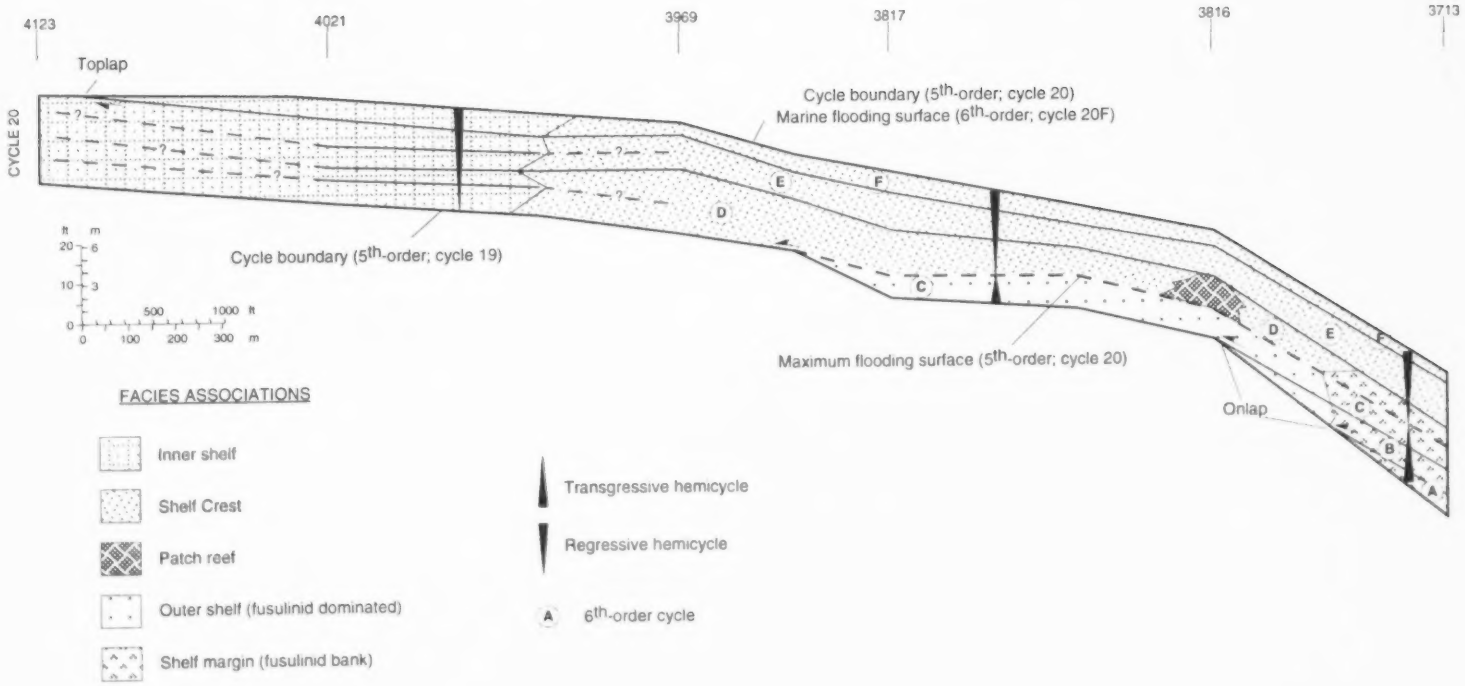

Figure 3.6: Internal architecture of fifth-order cycle 20 showing facies associations distribution, transgressive-regressive hemicycles, and discontinuities. Sixth-order cycles 20D and 20E are divided into laterally discontinuous bedsets.

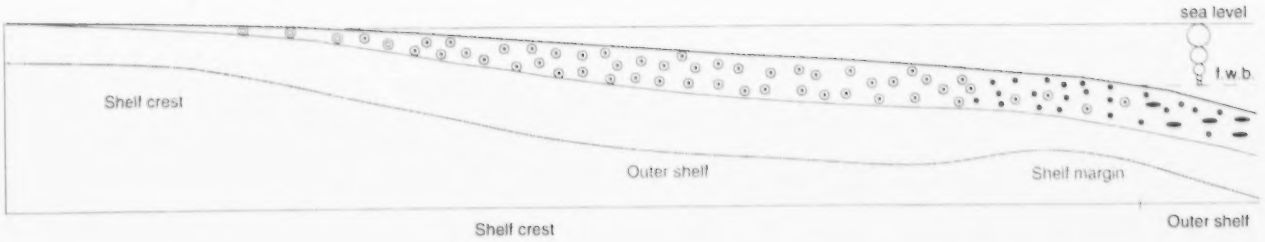

Figure 3.7: Schematic diagram showing depositional characteristics at the end of cycle 20. Ooid shoals prograded basinward until they reached the shelf margin position of the underlying cycle 19 (light letters for reference). Shallow water conditions across the shelf favored the massive formation of ooids. Facies symbols in Figure 3.4.

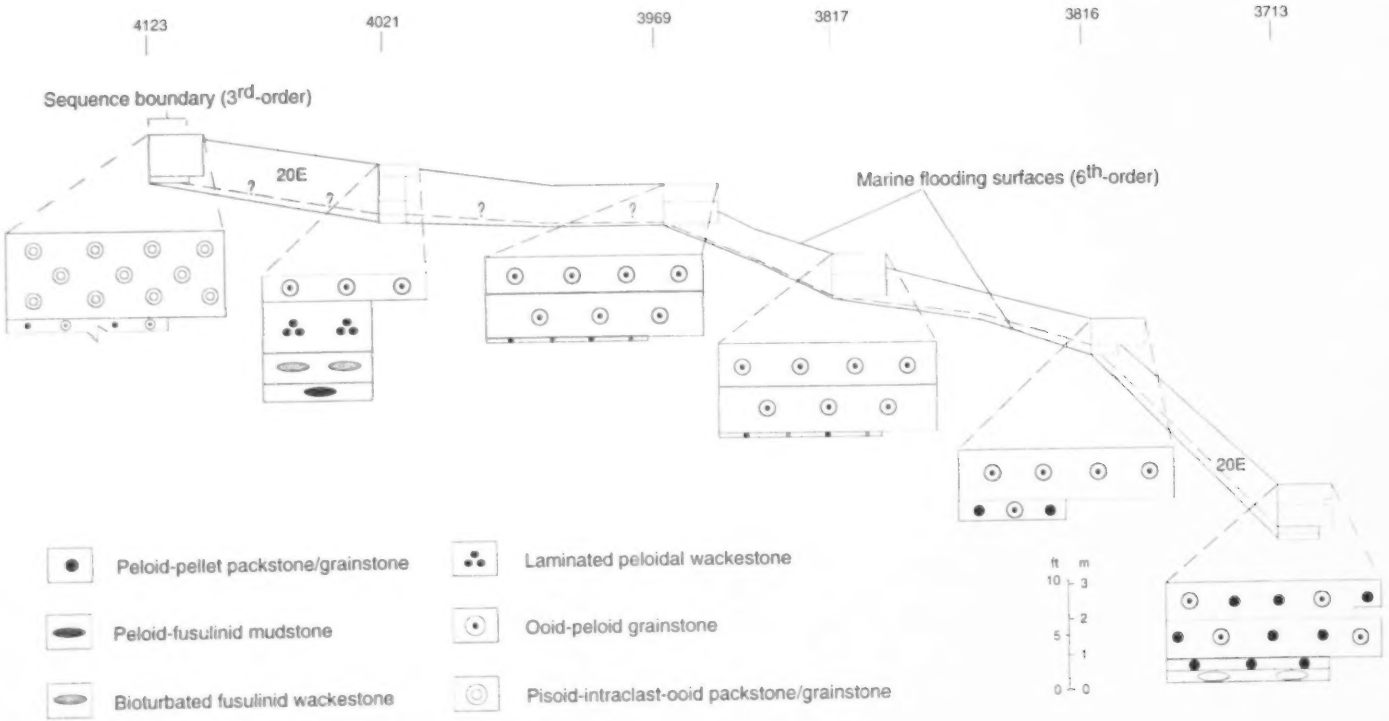

Figure 3.8: Internal architecture of sixth-order cycle 20E. The dotted line indicates the interpreted limit between the early (below) and late (above) sixth-order highstand. The early highstand is thinner where the shelf crest was best developed (between cores 3969 and 3817). The cycle is asymmetric shallowing-upward along the entire clinoform.

grade upward into laminated mudstone/wackestone facies with spherical fenestrae (facies 14) which indicates shallowing (late sixth-order highstand) and increase in restriction.

Cycle 17

Although briefly mentioned during the description of the middle highstand systems tract, cycle 17 shows unique internal characteristics that deserve a detailed description. This cycle is composed of five vertically stacked sixth-order cycles that reflect deposition on a prograding shoreface setting (Figs. 3.9 and 3.10). Two remarkable surfaces bound this package: 1) the lower boundary is a marine regressive surface of erosion produced by the lowering of the fairweather and storm-wave base during forced regressions or downstepping of the shelf; locally derived pebbles and intraclast are at or just above this surface (Fig. 3.9 and 3.10), and 2) an upper boundary that is a subaerial regressive surface of erosion (unconformity D) that formed during the lowest point of sea level fall (fourth-order cycle boundary; Fig. 3.10).

The top of cycle 17E is considered to be a fifth-order cycle boundary, based on its erosional characteristic and distinctive brecciation. The sixth-order cycle between cycle 17E and the fourth-order cycle boundary, probably records the landward pinching-out of a younger fifth-order regressive wedge that lies basinward of cycles 17A to 17E (Fig. 3.9). Figure 3.9 shows that sixth- to-fifth order cycles boundaries (subaerial surfaces of erosion) merge landward with the lower-frequency fourth-order cycle boundary. Progadation and downstepping of sixth-order clinoforms in the wedge is controlled by higher-frequency falls of sea level which allowed a periodic bypass of siliciclastics.

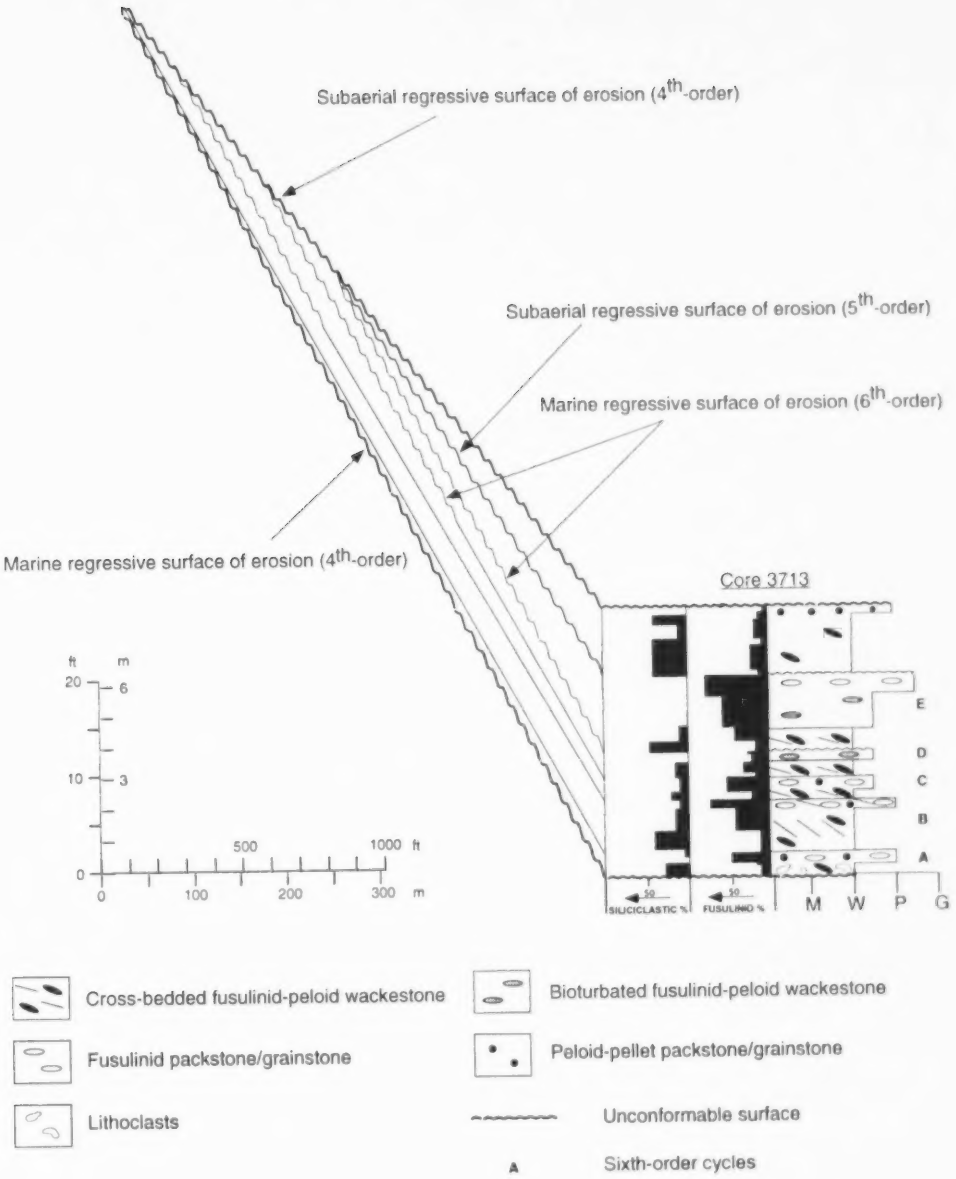

Figure 3.9: Vertical stacking pattern of sixth-order cycles in cycle 17 outlining the hierarchy of discontinuities. Cycle 17 represents a mixed carbonate-siliciclastic forced regressive wedge that pinches out landward. This wedge was formed when eustatic sea-level fall outpaced the rate of subsidence, inducing the shelf to downstep and offlap.

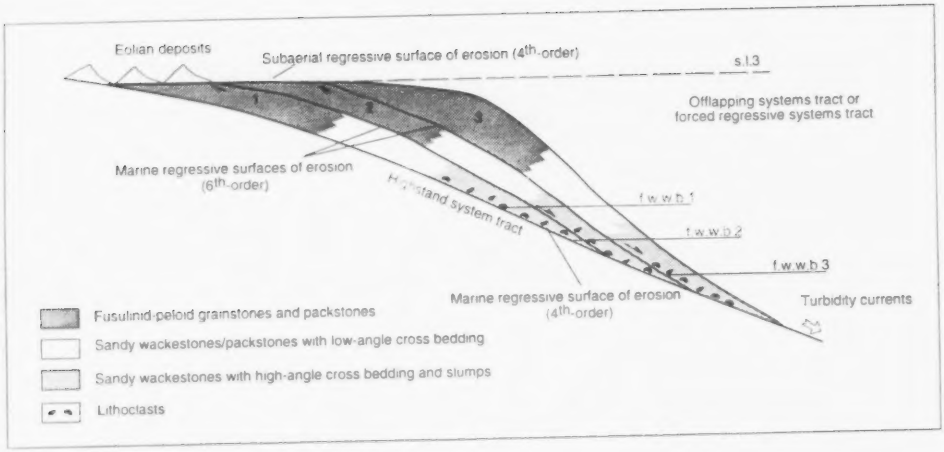

Figure 3.10: Conceptual depositional model for cycle 17. This offlapping systems tract is composed of sixth-order wedges which offlap and downstep according to sea-level fall. Lowering of fairweather wave base produces submarine erosion of the underlying highstand systems tract. Sediments with high-angle cross-bedding and slumps were probably deposited on unstable slopes affected by storms at the toe of the wedges. Fusulinid packstones and grainstones were deposited on the lower to upper shoreface.

Control Factors on Carbonate Deposition and Cyclicity

The main factors that controlled the facies distribution and cyclicity in the Grayburg Formation probably were water geochemistry, antecedent topography, siliciclastic influx, autocyclicity, subsidence, and eustatic sea-level fluctuations.

Water Geochemistry

During the deposition of the lowstand/transgressive systems tract, upwelling currents probably saturated with respect to calcium carbonate and low in nutrients supported a flourishing sessile biota of sponges, branching bryozoa, encrusting organisms, and banks of fusulinids. Marine cementation played an important role in the lithification of shelf margin sediments and created a hard substrate for colonial organisms (Fig. 2.8). Thick framestones, bindstones, and cemented fusulinid grainstones were observed only in the lowstand/transgressive systems tract. When sea level fell to its lowest point during the formation of unconformity A (Fig. 2.7) the volume of the basin was at its minimum and a restriction occurred, causing the waters to become saturated with respect to calcium carbonate. After, sea level slowly began to rise and oceanographic changes in the basin created upwelling currents that mobilized the saturated waters upslope to the shelf margin. Well-developed marine cementation on the slopes of modern shelf-edge reefs (e.g. Land and Loreau, 1970; James et al., 1976; Marshall, 1986) may result from upwelling currents (Schmidt, 1977; Marshall, 1986).

During the succesive highstand systems tract, the shelf margin was dominated by non-cemented fusulinid shoals or bioclastic shoals (Fig. 3.1). The absence of marine cementation in the shelf margin during the highstand, is probably related to a change in water conditions (i.e. turbidity, geochemical properties) and/or a continuous reworking of the sediments due to the lowering of fairweather and storm wave base, that inhibited the formation of relatively stable shoals prone to be cemented (e.g., Tucker and Wright, 1990).

Antecedent Topography

The location of the shelf margin during deposition of the early to late highstand systems tracts was partly controlled by the position of a relict shelf edge. Figure 3.11 shows that the shelf margin during the late stage of the lowstand/transgressive systems tract (maximum of transgression), backstepped from its initial position at well 3713 to a belt restricted between wells 3925-F and 3829. This new shelf margin, dominated by fusulinid banks, developed just basinward of the San Andres shelf break which is considered to be a product of subaerial exposure of the San Andres Formation during a relative, long-term sea-level fall. During the subsequent middle highstand systems tract the shelf margin, composed of skeletal grains, was located on top of older fusulinid shoals, which despite the apparent absence of a marked break in slope still remained an important topographic feature. By the end of the middle highstand systems tract, a strong offlapping and downstepping of the shelf produced during a fourth-order relative sea-level fall, culminated in the formation of a new subaerially exposed shelf break (Fig. 3.11). Finally, during the late highstand systems tract, the new shelf margin (fusulinid dominated) developed just basinward of the relict middle-highstand slope break (well 3713).

The positioning of the shelf margin may be predicted and is generally controlled by relative sea-level fluctuations. This is particularly true when the sea level falls below the shelf margin, exposing the platform and resulting in a significant break in slope. This break in slope then serves as nucleation point for the development of a new shelf margin during the subsequent transgression.

Siliciclastic Influx

On Permian carbonate platforms, periods of relative sea-level fall were normally marked by a siliciclastic influx that bypassed the exposed shelf and were deposited downslope in deep water settings (Sarnthein and Diester Hass, 1977; Fisher and Sarnthein, 1988; Borer and Harris, 1989; Gardner, 1991; Sonnenfeld and Cross, 1993; Kerans et al., 1994). Although not completely shut-down by siliciclastic poisoning, the carbonate shelf

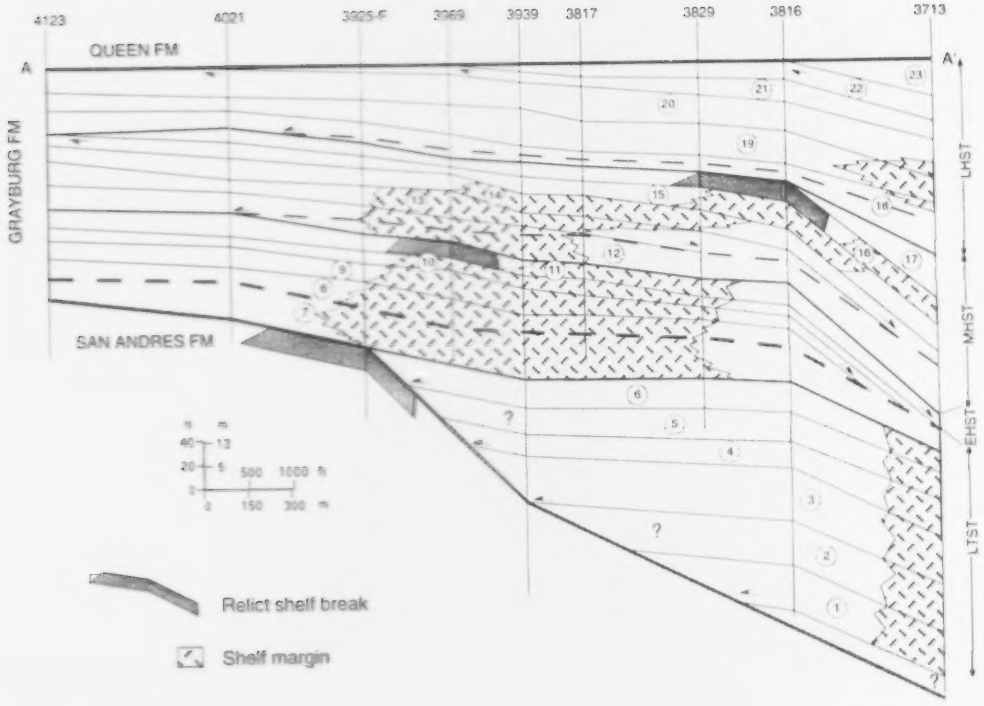

Figure 3.11: Location of relict breaks in slope produced during relative sea-level falls that exposed the carbonate shelf. The cross section shows a geometrical relationship between the position of the shelf margin and the antecedent shelf break.

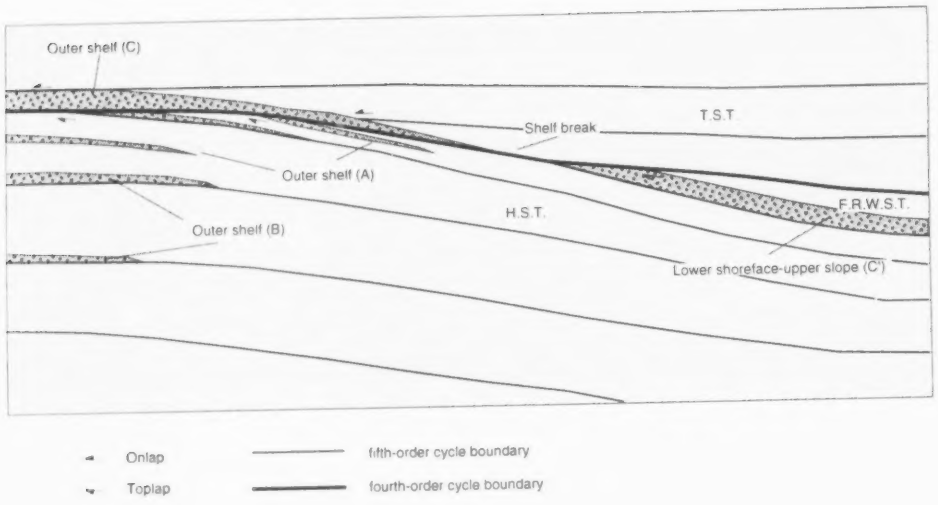

Figure 3.12: Diagramatic distribution of siliciclastic sediments in the Grayburg Formation. A= outer shelf siliciclastics at the top of fifth-order cycles related to sixth-order sea-level fall in the highstand systems tract (H.S.T.). B= outer shelf siliciclastics at the bottom of fifth-order cycles associated with fifth-order sea-level falls (H.S.T.). C and C'= lower-shoreface-upper slope siliciclastics at the bottom of fifth-order cycles associated with fourth-order relative sea-level falls. C represents shallow-water and/or eolian siliciclastics reworked during the deposition of the transgressive systems tract (T.S.T.); C' represents terrigenous sediments that bypassed the shelf and deposited downslope on the forced regressive wedge systems tract (F.R.W.S.T.)

typically became very narrow (e.g., cycle 17, Fig. 3.10). In these mixed carbonate-siliciclastic environments the only allochems observed are fusulinids, peloids, brachiopods, and bryozoa. In modern settings on Barbados, reefs grow despite the periodic influx of large volumes of fine grained siliciclastics (Acker and Stearn, 1990).

Siliciclastic sediments were deposited on two different parts of the shelf: 1) outer-shelf, fine-grained siliciclastics located in the upper (Fig. 3.12; Fig. 3.13A cycle 14) or lower portions of fifth-order cycles (Fig. 3.12; Fig. 3.13A, cycles 18 and 19), and 2) lower shoreface-upper slope, sandy bioclastic wackestones deposited at the base of fifth-order cycles (Fig. 3.12; Fig. 3.13B, cycles 17 and 23). Outer shelf-siliciclastic sediments in the upper part of fifth-order cycles, indicate deposition during sixth-order sea-level falls superimposed on fifth-order regressions (Fig. 3.12). Lower shoreface-upper slope and outer shelf siliciclastic sediments deposited in the lower part of fifth-order cycles are the expression of a fifth- or fourth-order relative sea-level fall depending if they are directly related to a fourth-order cycle boundary or not (Fig. 3.12). In conclusion, the presence of siliciclastic sediments in the Grayburg Formation is an important control in carbonate facies distribution and contribute in the identification of bounding discontinuities of different orders (e.g., cycle and sequence boundaries).

Autocyclicity

Intrinsic mechanisms such as tidal-flat progradation (Ginsburg, 1971) and storm and wave reworking and distribution of sediments (Osleger, 1991) are commonly invoked as important controls in the formation of peritidal and subtidal cycles respectively.

In the Grayburg Formation, the presence of only scattered cycles deposited in peritidal conditions (i.e. cycle 20E; Fig. 3.8) rules out the tidal-flat progradation as a significant mechanism in the generation of cycles.

On the other hand, subtidal shelf-margin cycles were probably deposited between fairweather and storm wave base. In that situation, wave and storm reworking and distribution acting in concert with eustatic oscillations of sea level (Osleger, 1991) may act

to inhibit sediment aggradation above the zone of maximum carbonate production (< 10 m deep; Schlager, 1981). It should be emphasized, however, that variations in sediment dispersal patterns caused by waves and storms certainly contributed to variability in the cycles but appear to have been subordinate to a more dominant allogenic control on cycle formation (Osleger, 1991). Therefore, it is difficult to prove whether or not a given sedimentary cycle is really caused by allogenic or autogenic mechanisms (Einsele et al., 1991).

Tectonics

Dorobek (1994) suggested that carbonate platfoms may develop in foreland basins during or before major orogenic events of deformation (synorogenic), or over inherited topography from earlier synorogenic stages (post-orogenic). According to Dorobek (1994) the main geodynamic models applicable to foreland basins are non-flexural deformation, flexural deformation, and viscoelastic relaxation.

Previous works on the Central Basin Platform (Hills, 1985; Yang and Dorobek, 1992; Dorobek, 1994) indicated that reactivation of basement structures and fault-bounded uplifts (non-flexural deformation) took place during the late Pennsylvanian to early Permian (Wolfcampian). Seismic lines in the McElroy Field (just south of North McElroy) do not show any evidence of major structural complication produced by reactivation of structures during the Upper Permian (Walker and Harris, 1988). Consequently, non-flexural deformation is excluded as an allogenic mechanism that controlled carbonate cyclicity during deposition of the Grayburg Formation.

Most foreland platforms under a flexural subsidence on the order of 1m/yr during 0.01 to 1 m.y., will drown or be forced to backstep (Dorobek, 1994). This is because the average growth potential of a carbonate platform during the same period of time is estimated to be 0.3 to 1 m/yr (Schlager, 1992), a rate that is exceeded or equalled by the rate of subsidence. Under these conditions, carbonate cycles in the Grayburg Formation with frequencies in the range of 0.01 to 1 m.y. (i.e., sixth- to third-order cycles and

sequences *sensu* Vail et al., 1991), were probably controlled in part, by flexural subsidence when the orogenic wedge was advancing.

During periods when the orogenic wedge is not advancing, an isostatic rebound or relaxation may take place with a subsequent exposure of the platform and a basinward progradation (tectonically forced regression) of the carbonate platform (Devlin et al., 1993; Dorobek, 1994). The lithospheric relaxation is commonly on the order of 1 to 10 m.y. (Dorobek, 1994) which should not directly affect the deposition of high-frequency cycles (sixth- to fourth-order). If viscoelastic relaxation had any influence on the cyclicity of the Grayburg Formation, it was at a depositional sequence level (third-order). The relative long-term sea-level fall and subsequent platform exposure at the end of the highstand systems tract may record an interplay of tectonically forced regression and eustatically forced regression.

In summary, flexural deformation probably affected sedimentation in all orders of cyclicity (sixth- to third-order), and viscoelastic relaxation, if present, was likely involved in the falling stages of the relative third-order sea-level change.

Glacio-Eustatic Sea-Level Oscillations

Based on the recurrence of sixth-order cycles, three types of fifth-order cycles were recognized. The first type is composed of two to three sixth-order cycles (3:1 or 2:1 recurrence ratio; Fig. 3.13A, cycles 10, 11 and 14) and is commonly observed in asymmetric shallowing-upward cycles on the shelf crest. The second is composed of five to six sixth-order cycles (5:1 to 6:1 recurrence ratio; Fig. 3.13A, cycles 9, 12 and 13 and Fig. 3.13B, cycles 16 and 17) and is typically observed in symmetric cycles on the outer shelf, shelf margin, and upper slope. The last type is formed of two to four sixth-order cycles (2:1 to 4:1 recurrence ratio; Fig. 3.13B, cycles 7, 12 and 14) and is only observed in asymmetric deepening-upward cycles on the lower slope. Fifth-order cycles with 8:1 and even 10:1 recurrence ratios are locally observed (Fig. 3.13B, cycles 18 and 20).

Recurrence of 5:1 bundles of meter-scale cycles similar to those in the symmetric, fifth-order cycles of the Grayburg Formation, have been considered evidence for Milankovitch orbital perturbations (e.g., Goldhammer et al., 1987; Goldhammer et al., 1990; Masetti et al., 1991; Goldhammer et al., 1993). Such perturbations are related to variations in glacial ice volume caused by global climate changes (e.g., Goodwin and Anderson, 1985; Goldhammer et al., 1990; Koerschner and Read, 1989; Mitchum and Van Wagoneer, 1991; Osleger and Read, 1991). The presence of polar ice caps during the Permian (Veevers and Powell, 1987) may support a glacio-eustatic driven mechanism for the development of high-frequency cycles in the Grayburg Formation.

If we accept a reasonable margin of error of 50 % in the calculations of cycle frequencies (Schwarzacher, 1993), sixth- and fifth-order cycles in the Grayburg Formation may expand from 12,000 and 57,000 years to 18,000 and 86,000 years respectively. A duration of about 18,000 years for sixth-order cycles is compatible with Milankovitch-precession periods of 16,000 and 19,000 years for pre-Pleistocene times (Berger et al., 1989). A frequency in the range of 86-90 k.y. (18 k.y. x 5 cycles) for fifth-order cycles, roughly coincides with the expected 95-123 k.y. for the short-eccentricity signal (Osleger and Read, 1991). In fifth-order cycles with a ratio greater than the average 5:1 or 6:1 (Fig. 3.13B, cycles 1, 18 and 20), the short-eccentricity signature may have been overprinted by autocyclic processes (i.e., storms), random sea-level fluctuations (cf. Goldhammer et al.,1993), and/or episodic subsidence.

Asymmetric fifth-order cycles deposited on the shelf crest with 2:1 to 3:1 ratios (condensed megacycles *sensu* Goldhammer et al., 1990) prevailed toward the top of fourth-order cycles, where the decrease in accommodation space during the relative fourth-order sea-level fall resulted in periods of prolonged emergence of the top of the platform as sea level fluctuated below the platform level for two or more sixth-order "beats". Fifth-order cycles with a 2:1 to 4:1 recurrence ratio (amalgamated megacycles *sensu* Goldhammer et al., 1990) on the lower slope are interpreted to occur when sixth-order sea-

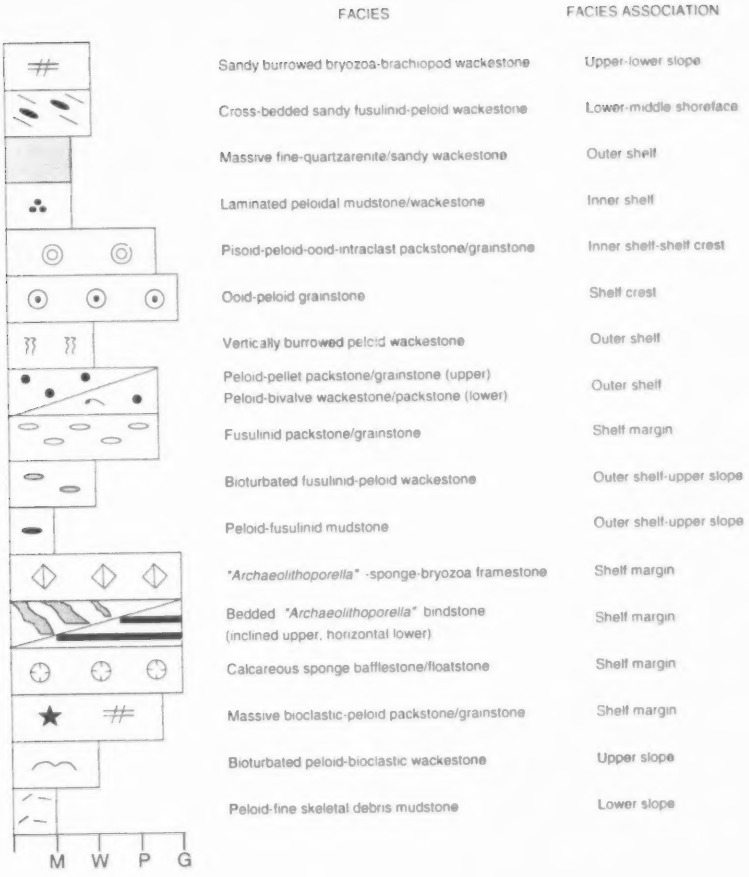

Figure 3.13: Key to depositional facies and interpretation. A) meter-scale description of core NMU-4123 that includes the gamma-ray log, hierarchical system of cyclicity, facies, and percentage of fusulinids and siliciclastics. B) meter-scale description of core NMU-3713 that includes the gamma-ray log, hierarchical system of cyclicity, facies, and percentage of fusulinids and siliciclastics.

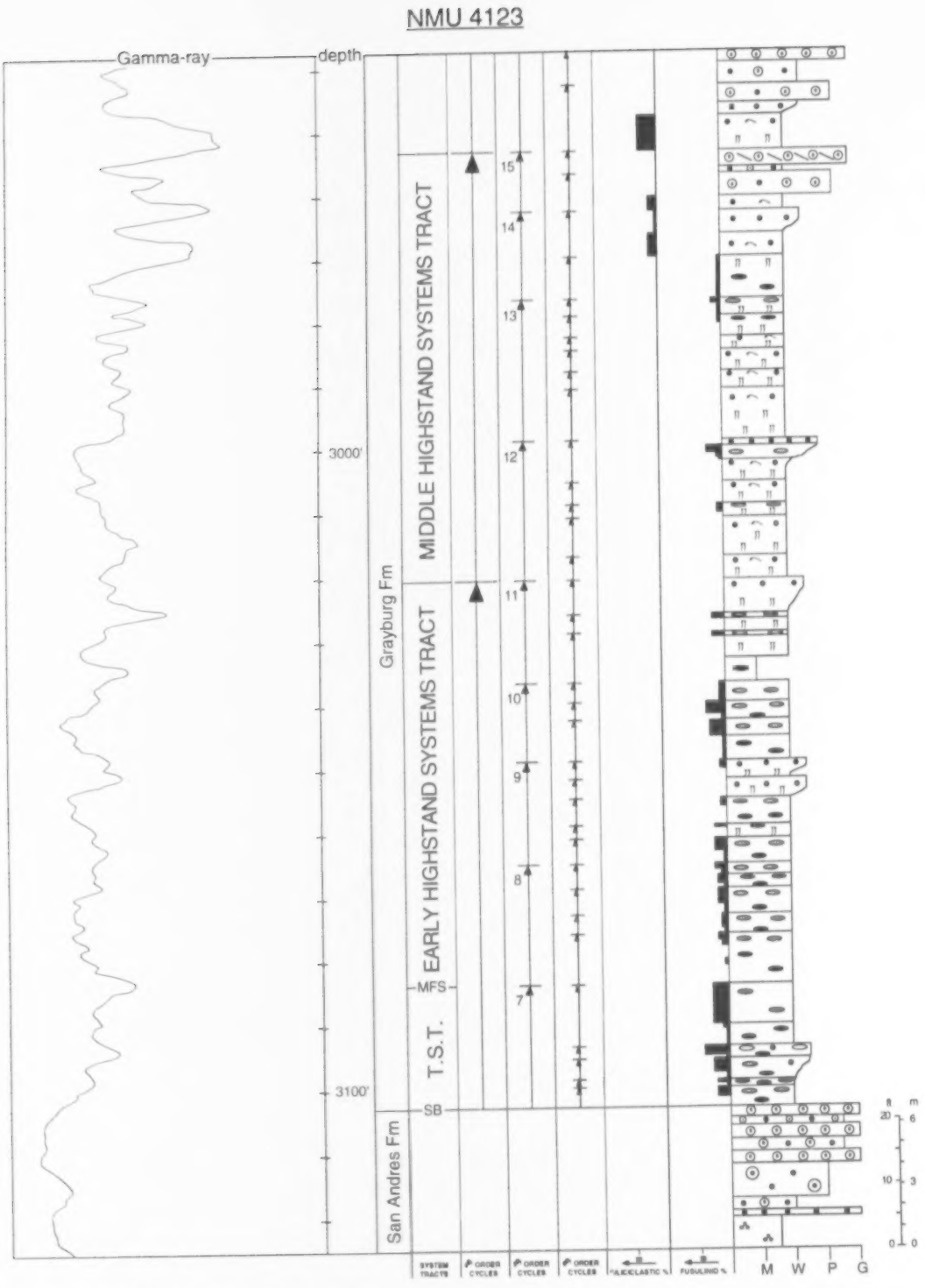

Figure 3.13A: Core NMU-4123 (base to top)

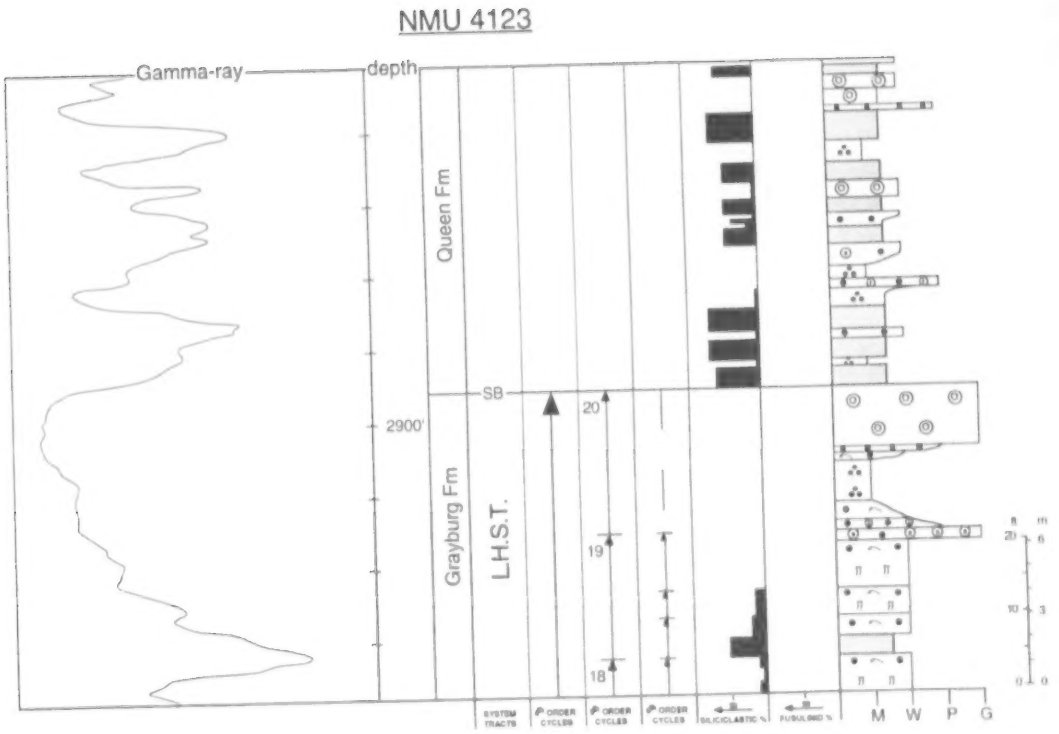

Figure 3.13A: Continued (base to top)

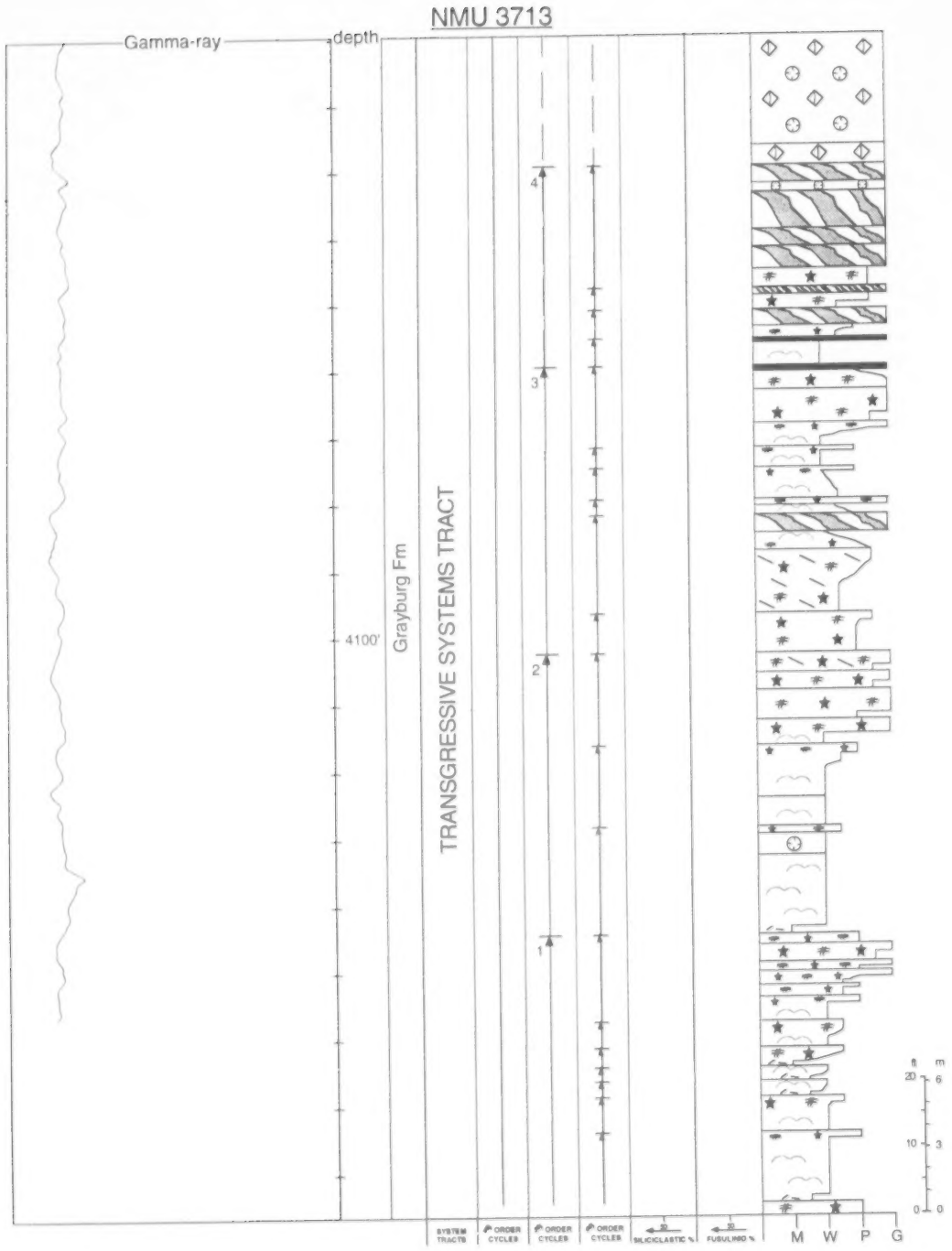

Figure 3.13B: Core NMU-3713 (base to top)

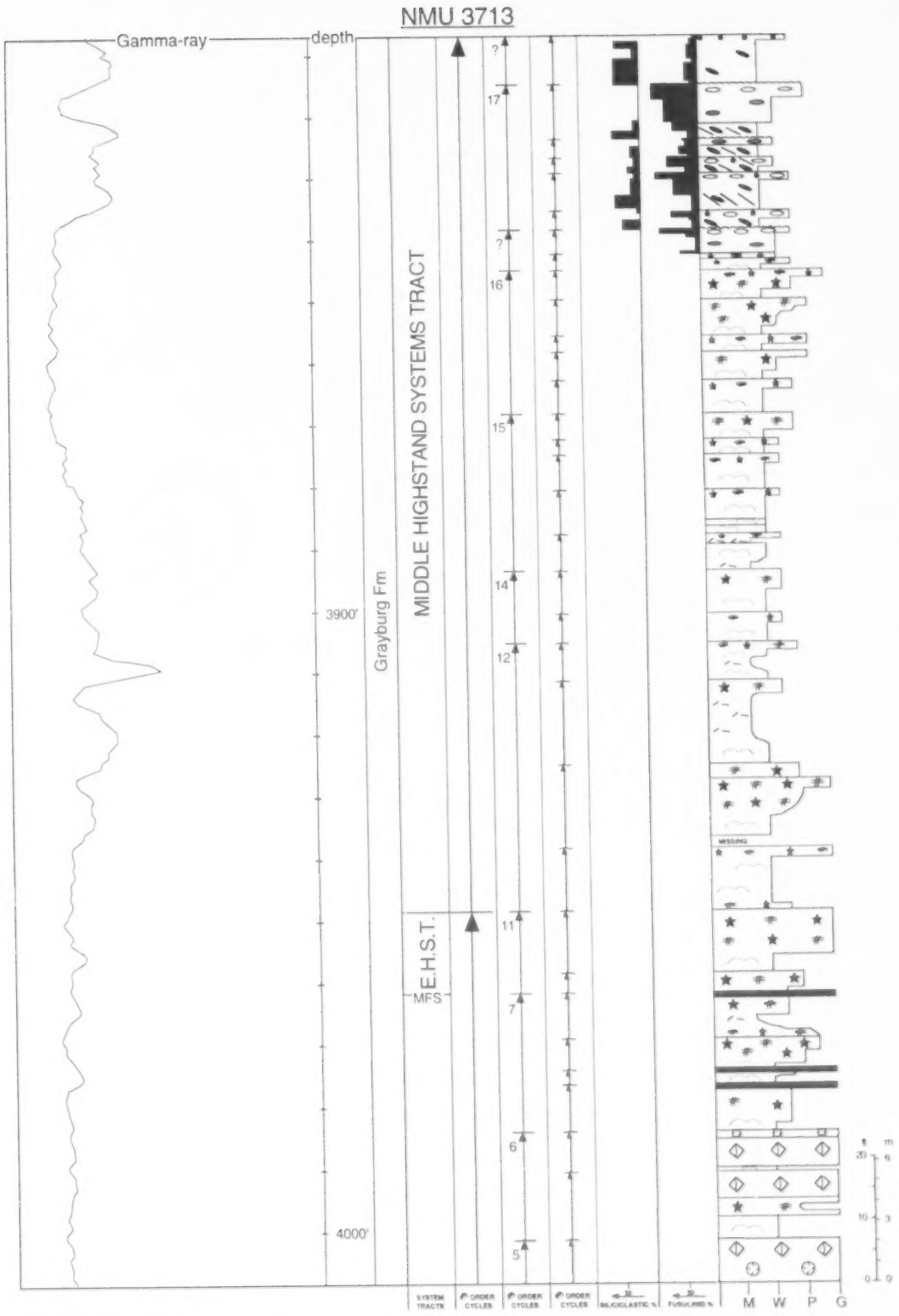

Figure 3.13B: Continued (base to top)

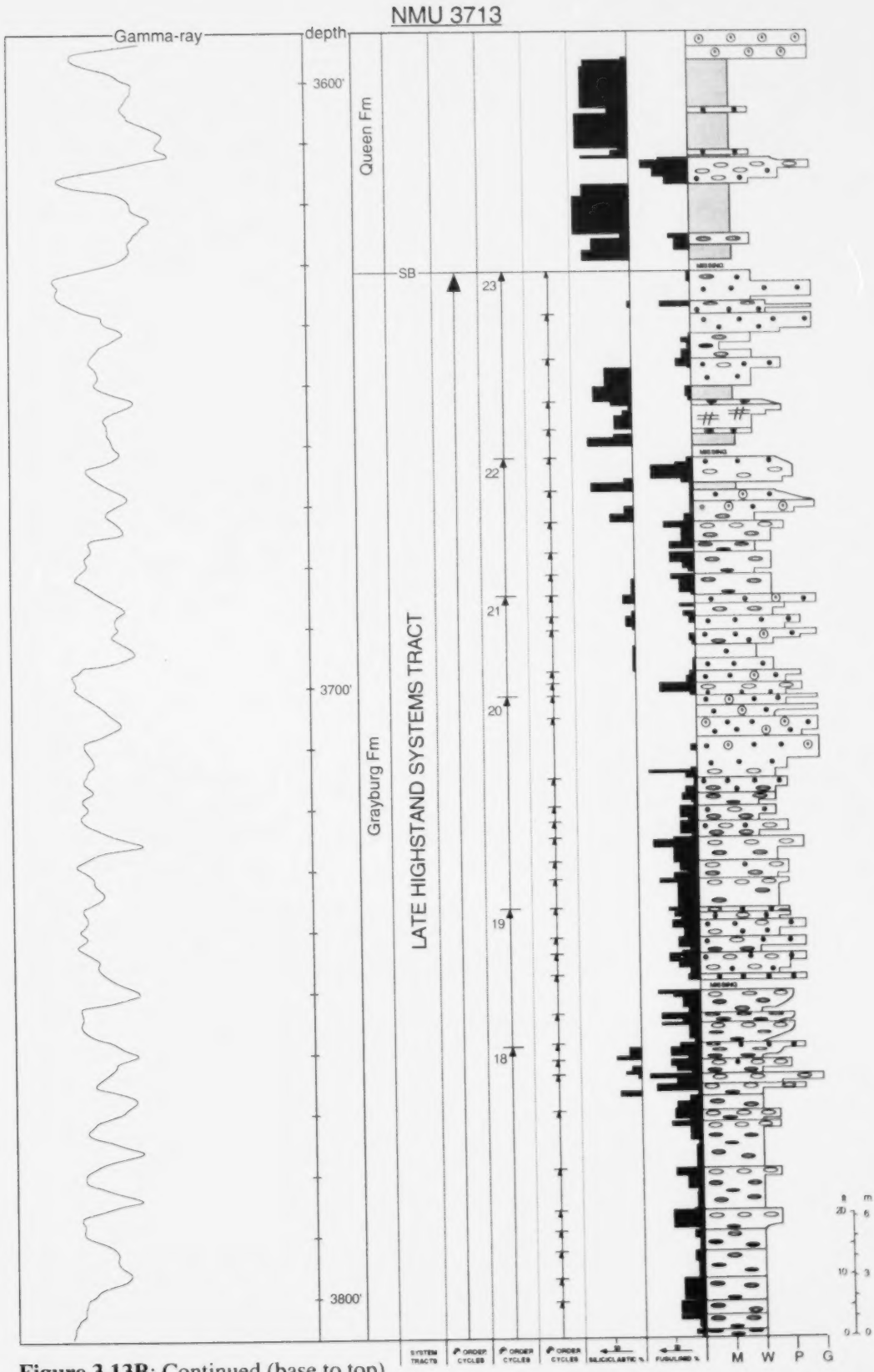

Figure 3.13B: Continued (base to top)

level oscillations happened too far above the sea bottom, leaving no sedimentological record.

Regarding fourth-order cycles, there is a discrepancy between the calculated duration of each cycle in the middle and late highstand systems tracts (516-540 k.y. based on six fifth-order cycles of 86-90 k.y., Fig. 3.1) and the theoretical duration for long-eccentricity Milankovitch oscillations (~400 k.y.). A combination of glacio- and tectono-eustasy may explain this incongruence. If sea level falls as a consequence of long-term eccentricity perturbations at the same time that active convergence is occurring (flexural subsidence), it must fall fast enough to outpace the increase in accommodation produced by subsidence (Dorobek, 1994). This suggests that probably during the regressive part of the long-term eccentricity pulse the eustatic sea-level fall did not completely outpace the increase in accommodation created by flexural deformation, which is indicated by the deposition of "extra" fifth-order cycles. In a situation where cyclicity is mainly controlled by long-term eccentricity (~400 k.y.), a fourth-order cycle is composed of four fifth-order cyles of ~100 k.y. each (cf. Borer and Harris, 1991; Osleger and Read, 1991).

Reservoir Characterization

After the analysis of facies distribution, cycle hierarchy and possible mechanisms that affected the carbonate platform, the cyclostratigraphic template can be tested as a predictive tool in the characterization of North McElroy Field. The main reservoir zones (Fig. 3.14) are associated with the outer shelf (peloid and fusulinid dominated), shelf margin (in particular when bioclastic dominated) and upper slope (bioclastic dominated facies) sequences. In all these cases, the mud-rich facies which have the best reservoir properties, are mainly located at the bottom of fifth-order cycles. Grain-rich facies with a high primary porosity (e.g., ooid-peloid grainstones) lost their reservoir potential because of the early emplacement of sulfate minerals (Longacre, 1990); they now serve as lateral and overlying seals. Dolomitization of the mud-rich facies during the early stages of

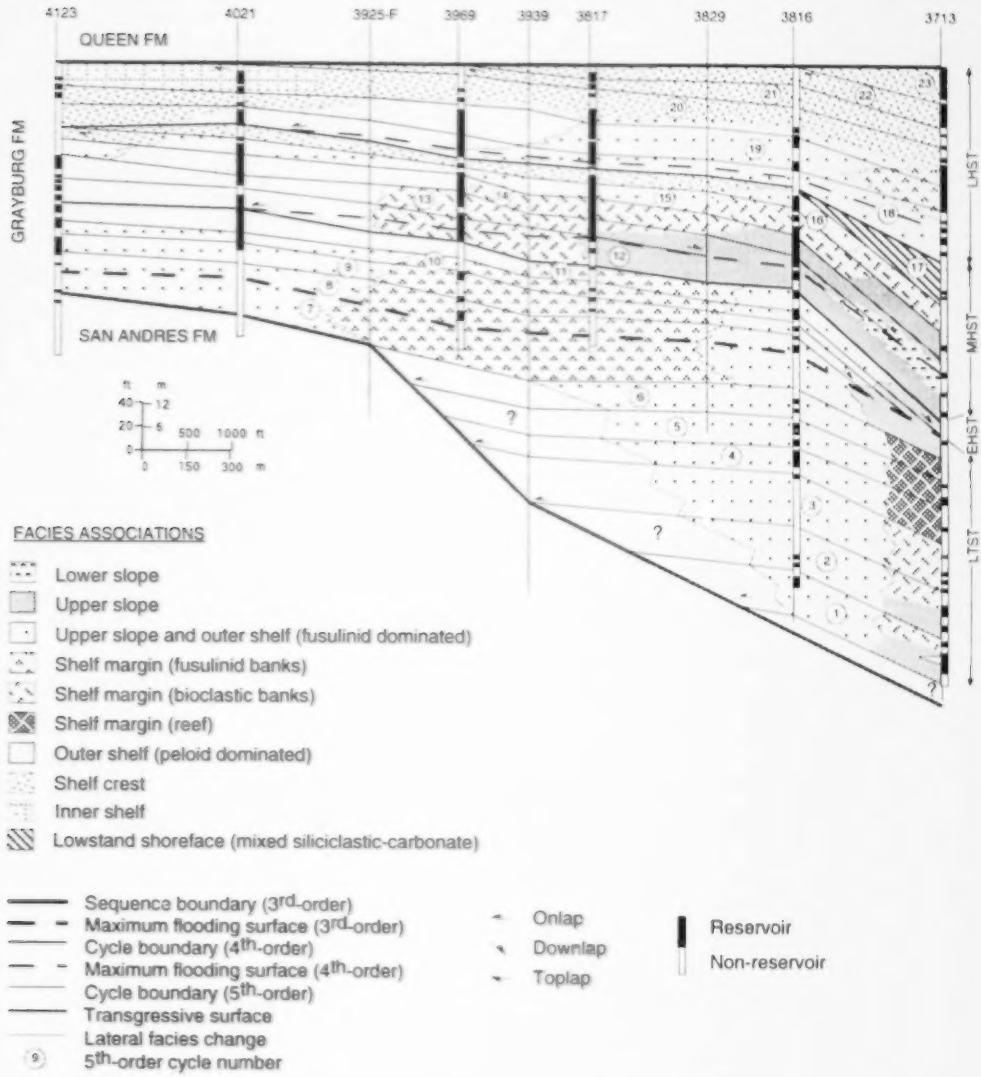

Figure 3.14: Reservoir distribution superimposed on the cyclostratigraphic framework.

diagenesis appears to have caused a reorganization of porosity and permeability enhancement (Longacre, 1990).

At the lowstand/transgressive systems tract only thin and laterally discontinuous reservoirs are present in the shelf margin and outer shelf. Cycle 7, which records the maximum of retrogradation, does not show any reservoir potential. During the subsequent early highstand systems tract reservoir intervals are thin but laterally traceable in most of the fifth-order cycles. Only cycle 11, below the fourth-order cycle boundary, is characterized by a thicker reservoir (Fig. 3.14, between wells 4123 and 4021).

The two main reservoirs zones are part of the middle and late highstand systems tract. The reservoir in the middle highstand systems tract is bounded below by the fourth-order maximum flooding surface (cycle 12) and above by the prograding shelf-crest sediments of cycles 15 and 16 and the forced regressive wedge (cycle 17). In the late highstand systems tract, the reservoir is confined at the bottom by the fourth-order maximum flooding surface and at the top by the shelf crest portions of cycles 18 to 20 (Fig. 3.14). Smaller reservoirs are confined to the mud-rich intervals in cycles 21-23. In both reservoir zones when the transgressive systems tract is thinner than 3 m, the transgressive unit is part of the main reservoir (i.e., cycle 12 at well 3969).

The effects of relative sea-level fluctuations probably controlled the initial distribution of reservoirs. During fourth-order relative sea-level falls, fifth-order cycles were affected by fabric-selective dissolution (leaching of allochems) and early processes of dolomitization that enhanced the reservoir potential of the rocks. Third-order sea-level falls probably overprinted and increased the effects of dissolution and porosity reorganization produced during fourth-order sea-level falls. Fifth- and sixth-order oscillations are probably responsible for the distribution of thinner productive intervals such as in the lowstand/transgressive systems tract where relative long-term sea-level falls (third- to fourth-order) did not have much influence.

Synopsis

1) The Grayburg Formation in the North McElroy field is composed of a single third-order depositional sequence. This depositional sequence is divided into a lowstand/transgressive systems tract and a highstand systems tract that can be traced across the entire field. The internal geometry of the systems tracts is dictated by the vertical succession of higher-frequency cycles (sixth- to fourth-order).

2) All cycles record similar internal characteristics, regardless of the thickness, time duration, and the mechanism that induced the cyclicity of carbonates. Features that in the past were considered exclusive of third-order sequences (e.g. systems tracts, maximum flooding surfaces and sequences boundaries) are now extrapolated to higher-frequency cycles which have all attributes of conventional sequences.

3) Carbonate platform cyclicity and facies distribution in the Grayburg Formation is probably controlled by an interplay of subsidence and eustatic sea-level fluctuations. During relative sea-level falls, siliciclastic sediments bypassed the exposed carbonate shelf and were deposited dowslope in deeper water settings. These siliciclastic pulses not only affected the growth potential and distribution of the carbonate factory, but also are useful in the identification of cycle boundaries of different orders. Relict breaks in slope generated during relative sea-level falls commonly serve as nucleation points for the development of a new shelf margin during the subsequent transgression.

4) The stacking patterns of sixth-order cycles may record rhythmic sedimentation in tune to the precession signal (~20,000 years) modulated by the short eccentricity signal or fifth-order eustasy (~100,000 years). Fourth- and third-order cycles and sequences were probably governed by a more complex combination of long-term eccentricity perturbations, flexural subsidence and viscoelastic relaxation. Non-periodic events, such as storms, episodic subsidence, and random sea-level fluctuations probably contributed to the "noise" evident in all orders of cyclicity.

5) The reservoir distribution was controlled by relative sea-level oscillations. The best pay zones were formed during fourth-order sea-level falls, during which sediments were affected by fabric-selective dissolution and early dolomitization and reorganization of porosity.

4. SUMMARY AND CONCLUSIONS

This thesis is the result of a sedimentological and cyclostratigraphic study of the Grayburg Formation in the North McElroy Field of West Texas. This analysis was divided into two stages: a) analysis and interpretation of depositional facies and facies associations (chapter 2), and b) analysis of lateral and vertical variability of sequences and cycles, as well as the causal mechanisms of cyclicity and facies distribution (chapter 3).

Based on the constituent depositional facies, lateral relationships, packaging patterns and relative position on the shelf, six facies associations were recognized in the Grayburg Formation. In order of decreasing water depth, these facies associations are the slope, shelf margin, outer shelf, shelf crest, inner shelf and shoreface. Each facies association is composed of small-scale, asymmetric shallowing-upward cycles. Locally, the slope facies association is formed of small-scale, deepening and then shallowing-upward cycles. These facies associations are sixth-order cycles (10,000 to 30,000 years) which are the basic units in the current cyclostratigraphic analysis.

According to the internal distribution of sixth-order cycles, fifth-order cycles are deepening-upward asymmetric, shallowing-upward asymmetric, or symmetric fifth-order cycles. They show internal onlapping, dowlapping, toplapping, and maximum flooding surfaces. As fifth-order sea-level oscillations determine the packaging patterns of sixth-order cycles, fourth-order relative sea-level fluctuations control the stacking patterns of fifth-order cycles. Fourth-order cycles, such as the one in the middle highstand systems tract, are formed of fifth-order cycles arranged into a high-frequency transgressive systems tract, highstand systems tract, and a forced regressive wedge systems tract.

The analysis of depositional sequences, systems tracts, and sixth- to fifth-order cycles indicates that regardless of the order, thickness, facies involved, and the responsible mechanisms, all cycles show similar internal characteristics of trangressive-regressive patterns. This observation suggests that a cyclostratigraphic analysis can be approach using the basic concepts of sequence stratigraphy at any level of cyclicity.

Another important observation is the dynamically changing character of depositional models in carbonate platforms, with facies changing in facies associations and facies associations evolving in high-frequency cycles. The traditional concept of a model with a "rigid" facies distribution that simply moves landward or basinward according to relative sea-level fluctuations, works as a conceptual approach for the prediction of the internal geometry observed in sequences and systems tracts, but fails to explain the dynamic change of facies types and proportions within each systems tract. These dynamic changes are mainly the result of sea-level fluctuations, sediment production, variations in water conditions and siliciclastic influx. For example, the analysis of the middle highstand systems tract shows that with a decrease in the accommodation space and an increase of the offlapping angle, a wide outer shelf dominated by vertically burrowed wackestones and peloid packstones is progressively replaced by outer shelf sediments composed of fusulinid wackestones. A plausible explanation for this change in facies is probably related to a reduction in width of the outer shelf during the relative sea-level fall, which altered water conditions that favored the development of one facies over the other .

The concept of a parasequence defined as *a relatively conformable succession of genetically related beds and bedsets bounded by marine-flooding surfaces and their correlative surfaces* (Van Wagoner et al., 1990) still remains the basic tool for correlations in cyclostratigraphy. Nevertheless, the presence of transgressive hemicyles, regressive hemicycles, and internal surfaces of maximum transgression must be acknowledged. In this case, a chronostratigraphic correlation that considers a model with variable cycle symmetries in different parts of the shelf would be different than a correlation of "shallowing-upward cycles" across the entire platform; the same cycle maybe asymmetric, shallowing-upward on the shelf crest with the maximum flooding surface at the bottom, and at the same time is symmetric on the shelf margin where the maximum flooding surface is in the middle of the cycle. Using a correlation of "shallowing-upward cycles" may lead to the erroneous matching of the asymmetric cycle on the shelf crest with only the

regressive portion of the symmetric cycle on the shelf margin. Here arises the importance of a rigorous hierarchical system of bounding surfaces that may, for instance, distinguish the position of the maximum flooding surface and the symmetry of the cycle in a particular section of the shelf.

Carbonate cyclicity in a foreland basin is probably controlled by an interplay of subsidence and eustatically driven mechanisms. Sixth-order cycles were probably generated by precession perturbations (~20,000 years) and modulated by the short eccentricity signal (~100,000 years) during the generation of fifth-order cycles. Non-periodic deposition such as autocyclicity, episodic subsidence and random sea-level fluctuations overprinted this glacioeustatically driven cyclicity. Long-term sea level fluctuations, i.e. fourth- to third-order cycles and sequences, were probably governed by a complex combination of long-term eccentricity perturbations (~400,000 years), flexural subsidence, and viscoelastic relaxation. Therefore the "popular" assumption that carbonate cyclicity is mainly controlled by eustatically driven mechanisms has to be carefully evaluated, in particular in foreland basins were subsidence can easily outpace the growth potential of the carbonate factory.

The application of cyclostratigraphy to reservoir characterization indicates that most of the questions about reservoir distribution may be answered with high-frequency sea-level falls. When carbonate platforms were exposed, facies with original reservoir potential (i.e., grainstones) were plugged by sulfates, whereas sediments with low primary porosity such as wackestones were overprinted by fabric-selective dissolution and dolomitization that enhanced its porosity and permeability.

REFERENCES

Acker, K.L., and Stearn, C.W., 1990, Carbonate-siliciclastic facies transition and reef growth on the northeast coast of Barbados, West Indies: Journal of Sedimentary Petrology, v. 60, p. 18-25.

Aigner, T., 1985, Biofacies as dynamic indicators in nummulite accumulations: Journal of Sedimentary Petrology, v. 55, p. 131-134.

Allen, J.R.L., 1984, Sedimentary Structures Their Character and Physical Basis: Amsterdam, Elsevier, 663 p.

Bebout, D.G., 1991, Interrelationship of platform dolostone and silicic silstone facies-Grayburg Formation (Permian), Central Basin Platform and Ozona Arch, Permian Basin, West Texas, *in* Lomando, A.J., and Harris, P.M., eds., Mixed Carbonate-Siliciclastic Sequences: Tulsa, OK, Society of Economic Paleontologists and Mineralogists Core Workshop 15, p. 429-446.

Bebout, D.G., Lucia, F.J., Hocott, C.R., Fogg, G.E., and Vander Stoep, G.W., 1987, Characterization of the Grayburg reservoir, University Lands Dune field, Crane County, Texas, University of Texas, Bureau of Economic Geology Report of Investigations 168, p. 98.

Bebout, D.G., and Harris, P.M., 1990, Geologic and Engineering Approaches in Evaluation of San Andres/Grayburg Hydrocarbon Reservoir-Permian Basin: Texas, Bureau of Economic Geology, 297 p.

Berger, A.F., Loutre, M.F., and Dehant, F., 1989, Influence of the changing lunar orbit on the astronomical frequencies of Pre-Quaternary insolation patterns: Paleoceanography, v. 4, p. 555-564.

Blanchon, P., 1995, Controls on Reef Development Around Grand Cayman [Ph.D. thesis, in prep.]: Edmonton, University of Alberta.

Borer, J.M., and Harris, P.M., 1989, Depositional facies and cycles in Yates Formation outcrops, Guadalupe Mountains, New Mexico, *in* Harris, P.M., and Grover, G.A., eds., Subsurface and Outcrop Examination of the Capitan Shelf Margin, Northern Delaware Basin: Tulsa, OK, Society of Economic Paleontologists and Mineralogists Core Workshop 13, p. 305-317.

Borer, J.M., and Harris, P.M., 1991, Depositional facies and model for mixed siliciclastics and carbonates of the Yates Formation, Permian Basin, *in* Lomando, A.J., ed., Mixed Carbonate-Siliciclastic Sequences: Tulsa, OK, Society of Economic Paleontologists and Mineralogists Core Workshop 15, p. 1-134.

Brachert, T.C., and Dullo, W.-C., 1990, Correlation of deep sea sediments and forereef carbonates in the Red Sea: an important clue for basin analysis: Marine Geology, v. 92, p. 255-267.

Brachert, T.C., and Dullo, W.-C., 1991, Laminar micrite crusts and associated foreslope processes, Red Sea: Journal of Sedimentary Petrology, v. 61, p. 354-363.

Crame, J.A., 1980, Succession and diversity in the Pleistocene coral reefs of the Kenya Coast: Palaeontology, v. 23, p. 1-37.

Crawford, G.A., 1981, Depositional history and diagenesis of the Goat Seep Dolomite (Permian, Guadalupian), Guadalupe Mountains, west Texas-New Mexico [Ph.D. thesis]: Madison, WI, University of Wisconsin-Madison.

Crawford, G.A., 1989, Goat Seep - precursor to the Capitan, *in* Harris, P.M., and Grover, G.A., eds., Subsurface and Outcrop Examination of the Capitan Shelf Margin, Northern Delaware Basin: Tulsa, OK, Society of Economic Paleontologists and Mineralogists Core Workshop 13, p. 373-378.

Crevello, P., Sarg, J.F., Read, J.F., and Wilson, J.L., 1989, Controls on Carbonate Platform to Basin Development: Tulsa, OK, Society of Economic Paleontologists and Mineralogists, Special Publication 44, 405 p.

Devlin, W.J., Rudolph, K.W., Shaw, C.A., and Ehman, K.D., 1993, The effect of tectonic and eustatic cycles on accommodation and sequence-stratigraphic framework in the Upper Cretaceous foreland basin of southwestern Wyoming, *in* Posamentier, H.W., Summerhayes, C.P., Haq, B.U., and Allen, G.P., eds., Sequence Stratigraphy and Facies Associations, International Association of Sedimentologists Special Publication 18, p. 501-535.

Dunham, R.J., 1962, Classification of carbonate rocks according to their depositional texture, *in* Hamm, W.E., ed., Classification of carbonate rocks, American Association of Petroleum Geologists Memoir 1, p. 108-121.

Einsele, G., Ricken, W., and Seilacher, A., 1991, Cycles and events in stratigraphy- basic concepts and terms, *in* Einsele, G., Ricken, W., and Seilacher, A., eds., Cycles and Events in Stratigraphy: New York, Springer Verlag, p. 1-19.

Elrick, M., and Read, J.F., 1991, Cyclic ramp-to-basin carbonate deposits, Lower Mississippian, Wyoming and Montana: a combined field and computer modeling study: Journal of Sedimentary Petrology, v. 61, p. 1194-1224.

Embry, A., and Klovan, J.E., 1971, A late Devonian reef tract on Northeastern Banks Island, N.W.T.: Bulletin of Canadian Petroleum Geology, v. 9, p. 730-781.

Fischer, A.G., and Sarnthein, M., 1988, Airborne silts and dune-derived sands in the Permian of the Delaware Basin: Journal of Sedimentary Petrology, v. 58, p. 637-643.

Flugel, E., 1982, Microfacies Analysis of Limestones: New York, Springer-Verlag, 633 p.

Font, R.G., 1985, Late Paleozoic structural patterns of the Delaware Basin, west Texas and southeastern New Mexico, *in* Dickerson, P.W., and Muehlberger, W.R., eds., Structure and Tectonics of Trans-Pecos Texas: Midland, TX, West Texas Geological Society Publication 85-81, p. 77-80.

Gardner, M.H., 1992, Sequence stratigraphy of eolian-derived turbidites: deep water sedimentation patterns along an arid carbonate platform and their impact on hydrocarbon recovery in Delaware Mountain Group reservoirs, West Texas, *in* Mruk, D.H., and Curran, B.C., eds., Permian Basin Exploration and production strategies: applications of sequence stratigraphic and reservoir characterization concepts, publication 92-91: Guadalupe Mountains, Texas and New Mexico, West Texas Geological Society, INC, p. 7-11.

Ginsburg, R.N., 1971, Landward movement of carbonate mud: new models for regressive cycles in carbonates (abstract): American Association of Petroleum Geologists Bulletin, v. 55, p. 340.

Goldhammer, R.K., Dunn, P.A., and Hardie, L.A., 1987, High frequency glacio-eustatic sealevel oscillations with Milankovitch characteristics recorded in Middle Triassic platform carbonates in northern Italy: American Journal of Science, v. 287, p. 853-892.

Goldhammer, R.K., Dunn, P.A., and Hardie, L.A., 1990, Depositional cycles, composite sea-level changes, cycle stacking patterns, and the hierarchy of stratigraphic forcing: examples from Alpine Triassic platform carbonates: Geological Society of America Bulletin, v. 102, p. 535-562.

Goldhammer, R.K., Lehmann, P.J., and Dunn, P.A., 1993, Origin of high-frequency platform carbonate cycles and third-order sequences (Lower Ordovician El Paso Gp, west Texas): constraints from outcrop data and stratigraphic modeling: Journal of Sedimentary Petrology, v. 63, p. 318-359.

Goodwin, P.W., and Anderson, E.J., 1985, Punctuated aggradational cycles: a general hypothesis of episodic stratigraphic accumulation: Journal of Geology, v. 93, p. 515-533.

Halley, R.B., Harris, P.M., and Hine, A.C., 1983, Bank margin environments, *in* Scholle, P.A., Bebout, D.G., and Moore, C.H., eds., Carbonate Depositional Environments: Tulsa, OK, American Association of Petroleum Geologists Memoir 33, p. 464-506.

Hardie, L.A., and Shinn, E.A., 1986, Carbonate depositional environments, modern and ancient. Part 3 - Tidal flats: Colorado School of Mines Quarterly, v. 81, p. 1-74.

Harris, P.M., 1983, The Joulters Ooid Shoal, Great Bahama Bank, *in* Peryt, T.M., ed., Coated Grains: Berlin, Springer-Verlag, p. 10.

Harris, P.M., 1984, Cores from a modern carbonate sand body, the Joulters ooid shoal, Great Bahama Bank, Society of Economic Paleontologists and Mineralogists Core Workshop 5, p. 429-464.

Harris, P.M., Dodman, C.A., and Bliefnick, D.M., 1984, Permian (Guadalupian) reservoir facies, McElroy Field, west Texas, *in* Harris, P.M., ed., Carbonate Sands - a core workshop: Tulsa, OK, Society of Economic Paleontologists and Mineralogists Core Workshop 5, p. 136-174.

Harris, P.M., and Walker, S.D., 1988, McElroy Field - U.S.A., Texas, Permian Basin: Tulsa, OK, American Association of Petroleum Geologists Atlas of Oil and Gas Fields No. 1, 32 p.

Harris, P.M., and Walker, S.D., 1990, McElroy field: development geology of a dolostone reservoir, Permian Basin, West Texas, *in* Bebout, D.G., and Harris, P.M., eds., Geologic and Engineering Approaches in Evaluation of San Andres/Grayburg Hydrocarbon Reservoirs- Permian Basin: Austin, Texas, Bureau of Economic Geology, p. 275-296.

Harris, P.M., Kerans, C., and Bebout, D.G., 1993, Ancient outcrop and modern examples of platform carbonate cycles- implications for subsurface correlation and understanding reservoir heterogeneity, *in* Loucks, R.G., and Sarg, J.F., eds., Carbonate Sequence Stratigraphy: Recent Developments and Applications: Tulsa, OK, American Association of Petroleum Geologists Memoir 57, p. 475-492.

Hills, J.M., 1984, Sedimentation, tectonism, and hydrocarbon generation in Delaware Basin, west Texas and southeastern New Mexico: American Association of Petroleum Geologists Bulletin, v. 68, p. 250-267.

Hills, J.M., 1985, Structural evolution of the Permian Basin of west Texas and New Mexico, *in* Dickerson, P.W., and Muehlberger, W.R., eds., Structure and tectonics of Trans-Pecos Texas: Midland, TX, West Texas Geological Society Publication 85-81, p. 89-99.

Hine, A.C., 1977, Lily Bank, Bahamas: history of an active oolite sand shoal: Journal of Sedimentary Petrology, v. 47, p. 1554-1581.

Hine, A.C., and Mullins, H.T., 1983, The carbonate shelf-slope break, *in* Stanley, D.J., and Moore, G.T., eds., The Shelf-break: Critical Interface on Continental Margins: Tulsa, OK, Society of Economic Paleontologists and Mineralogists Special Publication 33, p. 169-183.

Horak, R.L., 1985, Trans-Pecos tectonism and its effect on the Permian Basin, *in* Dickerson, P.W., and Muehlberger, W.R., eds., West Texas Geological Society Field Conference: Texas, p. 81-87.

Hovorka, S.D., Nance, H.S., and Kerans, C., 1993, Parasequence geometry as a control on permeability evolution: examples from the San Andres and Grayburg formations in the Guadalupe Mountains, New Mexico, *in* Loucks, R.G., and Sarg, J.F., eds., Carbonate Sequence Stratigraphy: Recent Developments and Applications: Tulsa, OK, American Association of Petroleum Geologists Memoir 57, p. 493-514.

Hunt, D., and Tucker, M.E., 1992, Stranded parasequences and the forced regressive systems tract: Deposition during base-level fall: Sedimentary Geology, v. 81, p. 1-9.

James, N.P., 1984, Reefs, *in* Walker, R., ed., Facies Models, Geoscience Canada, p. 229-257.

James, N.P., Ginsburg, R.N., Marszalek, D.S., and Choquette, P.W., 1976, Facies and fabric specificity of early subsea cements in shallow Belize (British Honduras) Reefs: Journal of Sedimentary Petrology, v. 46, p. 423-544.

Johnson, H.D., 1977, Shallow marine sand bar sequences: an example from the late Precambrian of North Norway: Sedimentology, v. 24, p. 245-270.

Kerans, C., and Nance, H.S., 1991, High frequency cyclicity and regional depositional patterns of the Grayburg Formation, Guadalupe Mountains, New Mexico, *in* Meader-Roberts, S., Candelaria, M.P., and Moore, G.E., eds., Sequence Stratigraphy, Facies, and Reservoir Geometries of the San Andres, Grayburg, and Queen Formations, Guadalupe Mountains, New Mexico and Texas [Annual Field Trip Guidebook]: Midland, TX, Society of Economic Paleontologists and Mineralogists Permian Basin Section Publication 91-32, p. 53-69.

Kerans, C., Fitchen, W.M., Gardner, M.H., Sonnenfeld, M.D., Tinker, S.W., and Wardlaw, B.R., 1992, Styles of sequence development within uppermost Leonardian through Guadalupian strata of the Guadalupe Mountains, Texas and New Mexico, *in* Mruk, D.H., and Curran, B.C., eds., Permian Basin Exploration and Production Strategies: Applications of Sequence Stratigraphic and Reservoirs Characterization Concepts, publication 92-91: Guadalupe Mountains, Texas and New Mexico, West Texas Geological Society, p. 1-6.

Kerans, C., Lucia, J.F., and Senger, R.K., 1994, Integrated characterization of carbonate ramp reservoirs using Permian San Andres Formation outcrop analogs: American Association of Petroleum Geologists Bulletin, v. 78, p. 181-216.

Koerschner, W.F., III, and Read, J.F., 1989, Field and modelling studies of Cambrian carbonate cycles, Virginia Appalachians: Journal of Sedimentary Petrology, v. 59, p. 654-687.

Land, L.S., and Goreau, T.F., 1970, Submarine lithification of Jamaican reefs: Journal of Sedimentary Petrology, v. 40, p. 457-462.

Lindsay, R.F., 1991, Grayburg Formation (Permian-Guadalupian): comparison of reservoir characteristics and sequence stratigraphy in the northwest Central Basin Platform with outcrops in the Guadalupe Mountains, New Mexico, *in* Meader-Roberts, S., Candelaria, M.P., and Moore, G.E., eds., Sequence Stratigraphy, Facies, and Reservoir Geometries of the San Andres, Grayburg, and Queen Formations, Guadalupe Mountains, New Mexico and Texas [Annual Field Trip Guidebook]: Midland, TX, Society of Economic Paleontologists and Mineralogists Permian Basin Section Publication 91-32, p. 111-118.

Lindsay, R.F., Hendrix, D.L., Jones, R.H., Keefer, C.M., Lindsey, D.L., McDonald, S.P., and Rittersbacher, D.J., 1992, Role of sequence stratigraphy in reservoir characterization: an example fron the Grayburg Formation, Permian Basin, *in* Mruk, D.H., and Curran, B.C., eds., Permian Basin Exploration and Production Strategies: Applications of Sequence Stratigraphy and Reservoir Characterization Concepts, Publication 92-91, West Texas Geological Society, p. 19-26.

Longacre, S.A., 1980, Dolomite reservoirs from Permian biomicrites: Soc. Econ. Paleont. Mineral. Core Workshop, v. 1, p. 105-117.

Longacre, S.A., 1983, A subsurface example of a dolomitized middle Guadalupian (Permian) Reef from West Texas, *in* Harris, P.M., ed., Carbonate Buildups - A core workshop: Tulsa, OK, Society of Economic Paleontologists and Mineralogists Core Workshop 4, p. 304-326.

Longacre, S.A., 1986, The Grayburg Formation at North McElroy - a Cinderella reservoir, *in* Bebout, D.G., and Harris, P.M., eds., Hydrocarbon Reservoir Studies, San Andres/Grayburg Formations, Permian Basin: Midland, TX, Society of Economic Paleontologists and Mineralogists Permian Basin Section Publication 86-26, p. 123-126.

Longacre, S.A., 1990, The Grayburg Reservoir, North McElroy Unit, Crane County, Texas, *in* Bebout, D.G., and Harris, P.M., eds., Geologic and Engineering Approaches in Evaluation of San Andres/Grayburg Hydrocarbon Reservoirs-Permian Basin: Austin, Texas, Bureau of Economic Geology, p. 239-273.

Loucks, R.G., and Sarg, J.F., 1993, Carbonate Sequence Stratigraphy: Recent Developments and Applications: Tulsa, OK, American Association of Petroleum Geologists Memoir 57, p. 345.

Marshall, J.F., 1986, Regional distribution of submarine cements within an epicontinental reef system: central Great Barrier Reef, Australia, *in* Schroeder, J.H., and Purser, B.H., eds., Reef Diagenesis: New York, Springer-Verlag, p. 8-26.

Masetti, D., Neri, C., and Bosellini, A., 1991, Deep-water asymmetric cycles and progradation of carbonate platforms governed by high-frequency eustatic oscillations (Triassic of the Dolomites, Italy): Geology, v. 19, p. 336-339.

Mitchum, R.M., and Van Wagoner, J.C., 1991, High-frequency sequences and their stacking patterns: sequence-stratigraphic evidence of high-frequency eustatic cycles: Sedimentary Geology, v. 70, p. 131-160.

Montanez, I.P., and Osleger, D.A., 1993, Parasequence stacking patterns, third-order accommodation events, and sequence stratigraphy of Middle to Upper Cambrian platform carbonates, Bonanza King Formation, Southern Great Basin, *in* Loucks, R.G., and Sarg, J.F., eds., Carbonate Sequence Stratigraphy: Recent Developments and Applications: Tulsa, OK, American Association of Petroleum Geologists Memoir 57, p. 305-326.

Osleger, D., 1991, Subtidal carbonate cycles: implications for allocyclic vs. autocyclic controls: Geology, v. 19, p. 917-920.

Osleger, D.A., and Read, J.F., 1991, Relation of eustasy to stacking patterns of meter-scale carbonate cycles, Late Cambrian, U. S. A.: Journal of Sedimentary Petrology, v. 61, p. 1225-1252.

Plint, A.G., 1988, Sharp-based shoreface sequences and "offshore bars" in the Cardium Formation of Alberta: their relationship to relative changes in sea level, *in* Wilgus, C.K., Hastings, B.S., Kendall, C., G,St.G., Posamentier, H.W., Ross, C.A., and Van Wagoner, J.C., eds., Sea-Level Changes- An Integrated Approach: Tulsa, OK, Society of Economic Paleontologists and Mineralogists Special Publication 42, p. 357-370.

Pomar, L., 1993, High-resolution sequence stratigraphy in prograding Miocene carbonates: application to seismic interpretation, *in* Loucks, R.G., and Sarg, J.F., eds., Carbonate Sequence Stratigraphy: Recent Developments and Applications: Tulsa, OK, American Association of Petroleum Geologists Memoir 57, p. 389-407.

Pomar, L., and Ward, W.C., 1994, Response of a late Miocene Mediterranean reef platform to high-frequency eustasy: Geology, v. 22, p. 131-134.

Posamentier, H.W., Allen, G.P., James, D.P., and Tesson, M., 1992, Forced regressions in a sequence stratigraphic framework: concepts, examples, and exploration significance: American Association of Petroleum Geologists Bulletin, v. 76, p. 1687-1709.

Purser, B.H., and Evans, G., 1973, Regional sedimentation along the Trucial Coast, SE Persian Gulf, *in* Purser, B.H., ed., The Persian Gulf: New York, Springer-Verlag, p. 211-231.

Read, J.F., 1985, Carbonate Platform Facies Models: American Association of Petroleum Geologists Bulletin., v. 69, p. 1-21.

Ross, C.A., 1983, Late Paleozoic foraminifera as depth indicators: American Association of Petroleum Geologists Bulletin (abstract), v. 67, p. 542.

Ross, C.A., and Ross, J.R.P., 1987, Late Paleozoic sea levels and depositional sequences, *in* Ross, C.A., and Haman, D., eds., Timing and Depositional History of Eustatic Sequences: Constraints on Seismic Stratigraphy: Washington, D.C., Cushman Foundation for Foraminiferal Research, Special Publication 24, p. 137-149.

Ross, C.A., and Ross, J.R.P., 1988, Late Paleozoic transgressive-regressive deposition, *in* Wilgus, C.K., Hastings, B.S., Kendall, C.G.S.C., Posamentier, H.W., Ross, C.A., and Van Wagoner, J.C., eds., Sea-Level Changes: An Integrated Approach: Tulsa, OK, Society of Economic Paleontologists and Mineralogists Special Publication 42, p. 227-248.

Sami, T.T., and James, N.P., 1994, Peritidal carbonate growth and cyclicity in an Early Proterozoic foreland basin, Upper Pethei Group, northwest Canada: Journal of Sedimentary Research, v. B64, p. 111-131.

Santisteban, G., and Taberner, C., 1988, Sedimentary models of siliciclastic deposits and coral reefs interrelation, *in* Doyle, L.J., and Roberts, H.H., eds., Carbonate-Clastic Transitions: Amsterdam, Elsevier, p. 35-76.

Sarg, J.F., 1988, Carbonate sequence stratigraphy, *in* Wilgus, C.K., Hastings, B.S., Kendall, C.G.S.C., Posamentier, H.W., Ross, C.A., and Van Wagoner, J.C., eds., Sea-Level Changes: An Integrated Approach: Tulsa, OK, Society of Economic Paleontologists and Mineralogists Special Publication 42, p. 155-182.

Sarg, J.F., and Lehmann, P.J., 1986, Lower-Middle Guadalupian facies and stratigraphy, San Andres/Grayburg formations, Permian basin, Guadalupe Mountains, New Mexico, *in* Moore, G.E., and Wilde, G.L., eds., Lower and Middle Guadalupian Facies, Stratigraphy, and Reservoir Geometries, San Andres/Grayburg Formations, New Mexico and Texas: Midland, TX, Society of Economic Paleontologists and Mineralogists Permian Basin Section publication 86-25, p. 1-8.

Sarnthein, M., and Diester Haas, L., 1977, Eolian-sand turbidites: Journal of Sedimentary Petrology, v. 47, p. 868-890.

Schlager, W., 1981, The paradox of drowned reefs and carbonate platforms: Geological Society of American Bulletin, v. 92, p. 197-211.

Schlager, W., 1992, Sedimentology and sequence stratigraphy of reefs and carbonate platforms: Tulsa, OK, American Association of Petroleum Geologists Continuing Education Course Note Series 34, 71 p.

Schmidt, V., 1977, Inorganic and organic reef growth and subsequent diagenesis in the Permian Capitan Reef Complex, Guadalupe Mountains, Texas and New Mexico, *in* Hileman, M.E., and Mazzulo, S.J., eds., Upper Guadalupian Facies, Permian Reef Complex, Guadalupe Mountains, New Mexico and West Texas, publication 77-16, Society of Economic Paleontologists and Mineralogists Permian Basin Section, p. 93-131.

Schwarzacher, W., 1993, Cyclostratigraphy and the Milankovitch Theory: Amsterdam, Elsevier, 225 p.

Shinn, E.A., 1968, Burrowing in recent lime sediments of Florida and the Bahamas: Journal of Paleontology, v. 42, p. 879-894.

Shinn, E.A., and Lidz, B.H., 1988, Blackened limestone pebbles: fire at subaerial unconformities, *in* James, N.P., and Choquette, P.W., eds., Paleokarst: New York, Springer-Verlag, p. 117-131.

Sonnenfeld, M.D., 1991, High-frequency cyclicity within shelf-margin and slope strata of the upper San Andres sequence, Last Chance Canyon, *in* Meader-Roberts, S., Candelaria, M.P., and Moore, G.E., eds., Sequence Stratigraphy, Facies, and Reservoir Geometries of the San Andres, Grayburg, and Queen Formations, Guadalupe Mountains, New Mexico and Texas [Annual Field Trip Guidebook]: Midland, TX, Society of Economic Paleontologists and Mineralogists Permian Basin Section publication 91-32, p. 11-51.

Sonnefeld, M.D., and Cross, T.A., 1993, Volumetric partitioning and facies differentiation within the Permian Upper San Andres Formation of Last Chance Canyon, Guadalupe Mountains, New Mexico, *in* Loucks, R.G., and Sarg, J.F., eds., CArbonate Sequence Stratigraphy: Recent Developments and Applications: Tulsa, OK, American Association of Petroleum Geologists Memoir 57, p. 435-474.

Strasser, A., 1991, Lagoonal-peritidal sequences in carbonate environments: autocyclic and allocyclic processes, *in* Einsele, G., Ricken, W., and Seilacher, A., eds., Cycles and Events in Stratigraphy: New York, Springer Verlag, p. 709-721.

Tucker, M.E., Wilson, J.L., Crevello, P.D., Sarg, J.R., and Read, J.F., 1990, Carbonate Platforms: Facies, Sequences and Evolution: International Association of Sedimentologists Special Publication 9: Oxford, Blackwell Scientific Publications, 352 p.

Tucker, M.E., and Wright, V.P., 1990, Carbonate Sedimentology: Oxford, Blackwell Scientific Publications, 282 p.

Vail, P.R., Audemard, F., Bowman, S.A., Eisner, P.N., and Perez-Cruz, C., 1991, The stratigraphic signatures of tectonics, eustasy, and sedimentology- an overview, *in* Einsele, G., Ricken, W., and Seilacher, A., eds., Cycles and Events in Stratigraphy: New York, Springer Verlag, p. 611-659.

Van Wagoner, J.C., Mitchum, R.M., Campion, K.M., and Rahmanian, V.D., 1990, Sliciclastic Sequence Stratigraphy in well logs, cores, and outcrops: Tulsa, OK, American Association of Petroleum Geologists Methods in Exploration 7, 55 p.

Veevers, J.J., and Powell, C.M., 1987, Late Paleozoic glacial episodes in Gondwanaland reflected in transgressive-regressive depositional sequences in Euramerica: Geological Society of America Bulletin, v. 98, p. 475-487.

Walker, D.A., Golonka, J., Reid, A., and Thomlinson Reid, S., 1992, Changes in latitude bring about changes in attitude concerning carbonate sedimentation, *in* Mruk, D.H., and Curran, B.C., eds., Permian Basin Exploration and Production Strategies: Applications of Sequence Stratigraphic and Reservoir Characterization Concepts, publication 92-91, West Texas Geological Society, p. 134-136.

Walker, K.R., and Alberstadt, L.P., 1975, Ecological succession as an aspect of structure in fossil communities: Paleobiology, v. 1, p. 238-257.

Walker, R.G., 1984, General introduction: facies, facies sequences and facies models, *in* Walker, R.G., ed., Facies Models, Geoscience Canada Reprint Series 1, p. 1-9.

Walker, R.G., 1992, Facies, facies models and modern stratigraphic concepts, *in* Walker, R.G., and James, N.P., eds., Facies Models: Response to Sea Level Change, Geological Association of Canada, p. 1-14.

Wilson, J.L., 1975, Carbonate Facies in Geologic History: New York, Springer Verlag, 471 p.

Wilson, J.L., and Jordan, C., 1983, Middle shelf environment, *in* Scholle, P.A., Bebout, D.G., and Moore, C.H., eds., Carbonate Depositional Environments: Tulsa, OK, American Association of Petroleum Geologists Memoir 33, p. 297-343.

Wright, V.P., 1992, Speculations on the controls on cyclic peritidal carbonates: ice-house versus greenhouse eustatic controls: Sedimentary Geology, v. 76, p. 1-5.

Yang, K.M., and Dorobek, S.L., 1992, Mechanisms for late Paleozoic synorogenic subsidence of the Midland and Delaware Basins, Permian Basin, Texas and New Mexico, *in* Mruk, D.H., and Curran, B.C., eds., Permian Basin Exploration and Production Strategies: Applications of Sequence Stratigraphic and Reservoir Characterization Concepts, Publication 92-91, West Texas Geological Society, p. 45-60.